Indoor/Outdoor Location of Cellular Handsets Based on Received Signal Strength

A Thesis
Presented to
The Academic Faculty

by

Jian Zhu

In Partial Fulfillment
of the Requirements for the Degree
Doctor of Philosophy

School of Electrical and Computer Engineering
Georgia Institute of Technology
August 2006

Indoor/Outdoor Location of Cellular Handsets Based on Received Signal Strength

Approved by:

Professor Gregory Durgin, Advisor
School of Electrical and Computer Engineering
Georgia Institute of Technology

Professor Aaron Lanterman
School of Electrical and Computer Engineering
Georgia Institute of Technology

Professor Ye (Geoffrey) Li
School of Electrical and Computer Engineering
Georgia Institute of Technology

Professor Michael Hunter
School of Civil and Environmental Engineering
Georgia Institute of Technology

Professor Paul Steffes
School of Electrical and Computer Engineering
Georgia Institute of Technology

Date Approved: May 15, 2006

To my loving Dad and Mom,

for their understanding and support through the years.

ACKNOWLEDGEMENTS

I would like to express my gratitude and appreciation to everyone who made thesis possible.

First and foremost, I would like to give my sincerely thanks to my advisor Gregory Durgin for his guidance, support, and encouragement during my PhD studies in these years. I will never forget those many days and nights he spend to revise my paper and report. I've learned not only technology knowledge but also his life altitude which will benefit me in the rest of my life.

I would also express my appreciation to Dr. Ye Geoffrey Li, Dr. Paul G. Steffes, and Dr. Aaron D. Lanterman for being on my proposal committee. Their valuable suggestions and commons have made great contributions to the improvement of my work.

Secondly, I have a long list of generous sponsors and supporters to thanks to.

Thanks to Comarco Wireless Technology for their generous donation of a Comarco LT200 Scanner, which was the workhorse of this experiment. Comarco Inc. memembers Malcolm Levy, Louis Valbuena, and Willem Matins were especially helpful.

Thanks to Joshua Griffin, Chris Durkin, Alenka Zajic, and Albert Lu for many hours in the field helping with the measurement campaign.

Thanks to the Image Lab in the architecture department for their help in obtaining the latest version of campus aerial photographs.

Thank Polaris Wireless Inc. for their technical suggestions and support in this research.

Finally, I give my deepest gratitude and sincerest love to my parents for their love and support through my entire life.

TABLE OF CONTENTS

LIST OF TABLES

LIST OF FIGURES

ACRONYMS

ABBSD - average base station-to-base station separation distance

ARFCN - absolute radio frequency channel number

AGPS - assisted global positioning system

AOA - angle of arrival

BER - bit error rate

BSC - base station controller

CDMA - code division multiple access

CIR - carrier-to-interference ratio

CRLB - Cramer-Rao lower bound

DCCH - dedicated control channel

DMA - distance matrix aggregate

DCM - database correlation method

EOTD - enhanced observed time difference

FCC - federal communications commission

FIM - fisher information matrix

GIS - geographical information systems

GPS - global positioning system

GSM - global system for mobile

MAHO - mobile assisted hand off

MPDP - multi-path delay profile based location

MSC - mobile switching center

NLOS - non-line-of-sight

NMR - network measurement report

PSD - predicted signal database

RSS	-	received signal strength
RSSA	-	received signal strength aggregate
RSSDA	-	received signal strength distance related attenuation
RSSI	-	received signal strength indicator
SINR	-	signal to interference plus noise ratio
TDOA	-	time difference of arrival
TDMA	-	time division multiple access
TA	-	timing advance
TOA	-	time of arrival
WLAN	-	wireless local area network
WCDMA	-	wideband code division multiple access

SUMMARY

This dissertation presents a novel technique for indoor/outdoor location of cellular handsets based on received signal strength (RSS) measurements taken by a cellular handset of the surrounding base stations. The RSS from several base stations is used as a "signature" of a specified location. The RSS at a specified location is a function of the propagation environment from the transmit antenna at the base station to the handset that includes terrain type, building density, foliage, and building materials for indoor environments. To predict and generate RSS maps, propagation and penetration models are built to represent different environments. Furthermore, a set of hybrid location algorithms is developed to improve location accuracy.

This location system, first used in [41], generates the location fix by matching the RSS signature to the predicted received signal strength database. The closest match gives the location estimate. The RSS measurement is reported in the format of network measurement reports (NMRs), which report serving base station information, RSS information from neighbor base stations, and radio environment information.

An accurate predicted received signal strength database is the key in this location method. For the studies in this dissertation, a modified-Hata model is used to generate this predicted signal strength database. To improve the performance of the system, indoor modeling and measurement-based RSS map tuning are investigated as methods of improving accuracy. An initial measurement campaign conducted on the Georgia Tech campus shows that the received signal strength method is sufficiently accurate to satisfy the FCC's E911 location requirements, which require that the cellular service providers locate cell phone users within 100 m error distance 67% of the time and within 300 m error distance 95% of the time. A second measurement campaign conducted in Greenville, SC, extends the experiment environment to a semi-rural area. Finally, a trial in Manhattan, NY, shows that the performance of the RSS method surpasses the FCC's E911 location requirements in a ultra-dense urban area for both indoor and outdoor users.

Several modifications of the location algorithm have been tested in semi-urban and rural areas.

These modifications greatly improve the location performance. Between 13% and 20% more users can be located within 100 m of their actual position.

Accurate indoor penetration models are further refined for dense urban areas by introducing pseudo-transmitters to simulate the wave-guiding effects in urban canyon environments. It not only improves the location performance but also reduces the time and the cost of extensive drive-testing and catch modifications to the coverage when the cellular network undergoes optimization or build out.

RSS location accuracy for different environments is studied as a function of base station separation distance, cell sector density, measurement density, radio propagation environment, and accuracy of measurement. The analytical and experimental results in this thesis serve as a guideline for the accuracy of RSS signature location technology under different conditions.

CHAPTER I

INTRODUCTION

Radiolocation has been gaining more and more attention recently as the U.S. Federal Communications Commission (FCC) seeks to provide 911 dispatchers with additional information on wireless 911 calls [16]. Phase II of the FCC's E911 program requires wireless carriers to provide 100 m accuracy 67% of the time and 300 m accuracy 95% of the time for a network-based solution. For a handset-based solution, the E911 program requires 50 m accuracy 67% of the time and 150 m accuracy 95% of the time.

Accurate geolocation is an important emerging technology for public safety, commercial use, and military applications. In public safety, a geolocation system needs to track the emergency calls, provide the emergency dispatch team accurate location information, and send the team to its task quickly and safely. The system can also be used to track suspects released on bail or prisoners on parole. Commercially, a geolocation system can be used to provide real-time mapping and navigation services to track people with special needs - the elderly and children - or to locate stolen vehicles. Very precise indoor location can also be used to navigate the blind, to locate a remote control, or to find special items in a large room. In military applications, a geolocation system can help troops locate the enemies, provide maps for making attack plans, and navigate troops [38].

Various location methods have been proposed [42], including *time of arrival* (TOA) [23, 7, 6], *time difference of arrival* (TDOA) [18], *enhanced observed time difference* (EOTD), *angle of arrival* (AOA) [35, 22], *assisted global positioning system* (AGPS) [17], *received signal strength distance related attenuation* (RSSDA), *received signal strength signature* (RSS signature) [3, 39, 9], and *multi-path propagation delay profile* (MPDP) [2]. Details of these location techniques are discussed in Section 1.3.

This chapter introduces some basic concepts so that the reader can then follow the development of a handset location in a cellular network as discussed in later chapters.

1.1 Cellular System Structure

A wireless cellular system consists of a fixed network and many mobile stations (handsets). The fixed network includes a gateway to a public switched network, a mobile telephone switching center, and many fixed base stations. The base stations are organized in a cellular structure as shown in Figure 1 [33]. The service area is partitioned into many small regions called "cells." Each cell has at least one base station in the center. All mobile stations (handsets) communicate with a base station. The data stream between the handset and the public telephone network is relayed through the the fixed network.

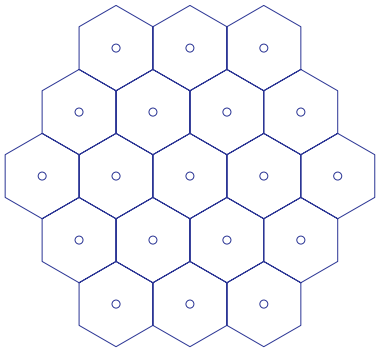

Figure 1: Cellular structure for ideal base station distribution. Each base station is represented by an "o". The hexagons represent ideal cell coverage.

Since wireless frequency resources are limited, a frequency reuse plan is often applied. A radio channel can be simultaneously used at multiple base stations as long as they are far enough apart to avoid interference. If all the S frequency channels are shared by N adjacent cells, each cell may have $k = S/N$ channels. A standard seven-cell frequency reuse plan is shown in Figure 2. To further reduce interference, each base station can use directional antennas and become sectorized. Figure 3 shows a sectored configuration. The cellular structure also brings the benefit of lower transmitting power and increased system capacity.

When a mobile station moves from one base station to another, a handoff is needed to keep continuous communication, especially for an ongoing call crossing a cell boundary. The handoff switches the wireless connection from the current serving base station to another base station with better signal quality. Basically, a handoff decision is based on the signal levels received by the handset through a dedicated control channel transmitted by all base stations. Based on the frequency

reuse plan, each base station is assigned one or more dedicated control channels. Each dedicated control channel has a constant transmitting power. The handset monitors the signal strength of all available dedicated control channels from surrounding base stations and reports to the network via a network measurement report (NMR). A handoff is initialized when the signal strength from a neighbor sector is higher than that from the current serving sector. The scheme of using the signal strength information of a dedicated control channel to make the handoff decision is called *mobile assisted handoff* (MAHO).

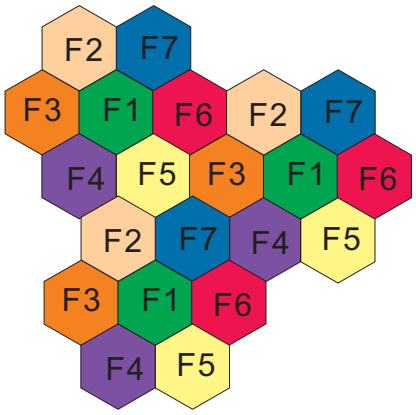

Figure 2: Standard seven-cell frequency reuse pattern.

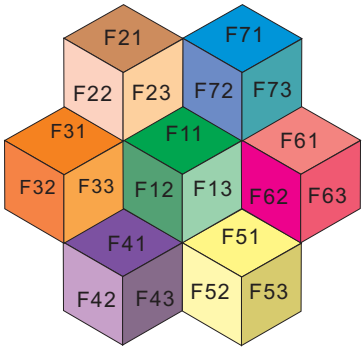

Figure 3: Standard seven-cell frequency reuse pattern with sectors.

1.2 How RSSI-based Radiolocation Works

The operation of the RSSI-based location technique is straightforward. A cellular network area is represented in a computer by a large, two-dimensional raster array with uniform grid spacings of 10 to 50 m. Each raster point in the grid corresponds to a location within the network and contains a

vector of received signal strength indicator (RSSI) values in dBm for all audible base stations. Each RSSI is cross-referenced to a unique cell identification number, as shown in Figure 4. A complete raster array of RSSIs is called a predicted signal database (PSD). Once a PSD has been constructed for a network area, the RSSI-based location engine must compare received signal strength measured by the handset to the PSD vectors. The best match determines the xy-coordinates of the most likely handset location.

This technique is similar to the scheme used to locate wireless local area network (WLAN) modems in a much smaller-scale location problem [27, 28, 29]. The technique has been proposed for use in the cellular network by Yamamoto [41].

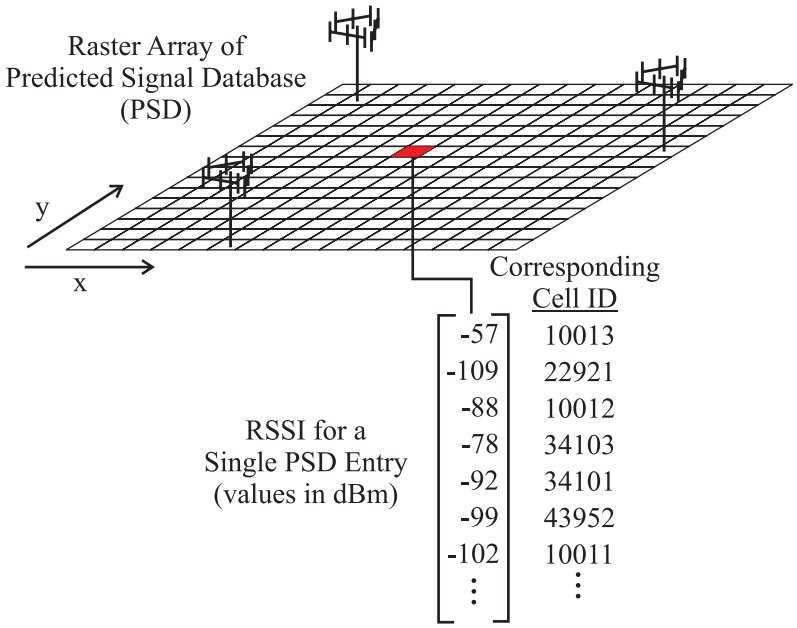

Figure 4: The Predicted Signal Data (PSD) stores a raster database of all RSSI from audible base stations within the network.

Handset RSSI measurements are taken from the user handset's network measurement report (NMR). NMRs are sent from the handset to the base station whenever requested by the mobile switching center (MSC). Each NMR is a list of many RSSIs corresponding to the different radio channels on the network. The exact number of channels depends on handset location, network architecture, and air interface. A typical NMR reports RSSIs from six to twelve unique cells (GSM handsets usually report the six strongest cells, while IS-136 handsets typically report between eight and twelve cells or more. The exact number depends on a preprogrammed neighbor list provided

by the serving cell). Since a handset's location consists of two pieces of information (x and y coordinates), the mapping of six or more RSSI values into this two-dimensional location space results in a significantly over-determined problem; the excess information helps to increase the accuracy and robustness of the RSS location estimate. In normal operation, a single NMR is generated whenever the handset initiates a call or performs a handoff to another cell. By changing just a few settings at the base station's switch, it is possible to request a stream of NMRs during 911 emergency calls. Only one NMR is required to produce a handset location estimate, but a stream of NMRs is quite useful for averaging out residual fading effects at the receiver or tracking a handset in motion. Since the storage of a PSD and the operation of an RSS location engine require only a modest computer terminal, the entire position location system is a remarkably inexpensive and accurate method for E911 and location-based services.

A high-quality PSD is crucial for a successful RSS location solution. The more accurate the PSD leads in, the better the location performance. The best PSD would be generated by measuring signal strength at every possible location in the network. But exhaustive measurement is impractical because of huge labor and time costs. This is particularly true if the RSS solution is extended to the indoor environment. Propagation models can be applied to predict signal strength and thus save cost.

1.3 History of Cellular Location Technology

Position location in the cellular network is not a new problem [24, 10]. Based on the information used in a location method, these methods can be classified into the following categories:

1) angle-based location (AOA),

2) time-based location (TOA, TDOA, EOTD),

3) global positioning system (GPS) based location (GPS, AGPS),

4) received signal strength-based location (RSSDA,RSS signature),

5) multi-path delay profile-based location (MPDP), and

6) hybird-information location [11, 25, 21].

Based on the algorithm in the location methods, these methods can be classified into the following two categories:

1) Triangulation methods are geometry-based algorithms,

2) Signature methods are also called database correlation methods (DCM).

Table 1 gives the relationship between the information and the algorithm used in different location methods.

Table 1: The relationship between the information and the algorithm used in different location methods

Method	Time-based	Angle-based	GPS-based	RSS based	Delay profile based
Triangulation	TOA,TDOA,EOTD	AOA	A-GPS	RSSDA	no
Signature	possible	possible	no	RSS	MPDP

Angle-based solutions use the precise measurement of the direction along the line of maximum signal strength at two or more base stations to triangulate the location of a handset. These techniques require high signal fidelity for super-resolution array processing. Therefore, sophisticated and expensive antenna array hardware is required for each base station.

Time-based solutions measure either the absolute or relative arrival times of several signals, backsolving the location of a handset through triangulation. Time-based solutions require precise synchronization for all base station clocks. Both TDMA and GSM (the most often deployed wireless system in the world) do not include the precise time synchronization of measurement in their original air interface standards. Thus, additional equipment is required for each base station. Because of the new hardware requirements, the deployment of time-based and angle-based schemes would cost at least several million dollars for a metropolitan area like Atlanta. Furthermore, these schemes require a line-of-sight (LOS) link from the base station antenna to the handset in order to work well. In rural areas, these technologies have difficulty reaching enough base stations to perform triangulation; in urban areas, the absence of LOS degrades the performance of this technology [31].

GPS-based solutions are quite accurate when LOS conditions exist between the handset and at least three GPS satellites. This “open-sky” condition exists only for some outdoor locations and never occurs for indoor handsets. Another key problem with GPS-based schemes is that the GPS link is designed to work with a signal-to-interference-plus-noise ratio (SINR) only a few dB above

the noise floor. Any loss incurred by an obstruction (tree, terrain, building, indoor environment, in-vehicle environment, etc.) may knock out the radio link in conventional GPS. In addition, the GPS-based solution requires additional hardware and an out-of-band RF chain in a handset. Replacing all existing non-GPS handsets would take many years.

RSS-based solutions use RSS measurements of the forward control channel, transmitted by all base stations to find handsets. In TDMA (IS-136) systems, the mobile station can measure the power of up to 24 neighboring control channels. Unlike voice channels, the forward control channel is transmitted at a constant power and yields a reliable, repeatable measurement. In GSM systems, handsets report the measured powers of the six strongest control channels. In an RSS location scheme, no additional base station hardware is required because RSS measurements are all the information needed from the handset hardware. Furthermore, the RSS signature method does not require the existence of a LOS signal, which makes it an excellent solution for suburban, urban, and indoor environments.

Because most calls are made indoors where no LOS exists, the indoor location problem cannot be avoided for E911 systems. The LOS requirement is crucial for time-based, angle-based, and GPS-based solutions. The RSS signature solution, however, does not require LOS. The aim of this work is to quantify and improve the feasibility of the RSS signature solution in different environments.

1.4 Our Research at Georgia Tech

To improve the accuracy of an indoor location for a mobile handset within a commercial cellular telephone network, we study the RSS signature solution and conclusively show that the RSS signature technique is also accurate for indoor users – a characteristic unique among all currently proposed location techniques. Our experimental results indicate that the RSS signature technique can approach or even surpass the FCC E911 requirements with a majority of indoor users in an urban environment. Since most cellular phone calls are placed from indoor environments, this result has enormous implications for the E911 rollout and public safety.

The performed research results show that the RSS signature technique can satisfy the FCC E911 requirements for both indoor and outdoor handsets in the semi-urban and high-urban environments.

Furthermore, it may be resilient enough for deployment as a stand-alone position-location solution for satisfying the FCC's E911 requirements in most populated areas.

Ultimately, the ideal solution for the United States' E911 problem may be a combination of the handset-based GPS solution and the RSS signature solution. These two technologies seem to complement each other very well. The handset-based GPS solution works in rural, open-sky environments where network-based location solutions tend to degrade because of the low density of base stations. Conversely, GPS fails whenever satellite links become obstructed. This can happen in any environment, but is particularly true in urban and indoor areas – precisely the places that the RSS signature radiolocation works best.

Our research results are quite promising for this late-coming location technology. Each chapter in this thesis presents a unique contribution to the RSS signature location method.

- Chapter II– Theoretical analysis and numerical results for the performance bound of the RSS-based location method are derived and calculated based on a practical cellular system simplification.

- Chapter III– Preliminary research, conducted in Atlanta, GA, shows the first academic indoor/outdoor cellular location experiment that proves the RSS signature location technique is a feasible way to locate cellular handsets for indoor users as well as outdoor users.

- Chapter IV – Extended research in Greenville, SC, provides performance data of the RSS signature method in rural areas and suggests several algorithms to use more network measurement information to improve location accuracy for the RSS method. A building height penetration model is tabulated based on the data from field measurements.

- Chapter V– An extended location trial in Manhattan presents performance data of the RSS signature location technique in a typical dense urban environment and the modified indoor propagation model that greatly improves the indoor location performance.

CHAPTER II

THEORETICAL ANALYSIS OF THE RSS LOCATION METHOD

In this chapter, we address how well the RSS signature location method can perform by showing the theoretical performance derived from the Cramer-Rao lower bound (CRLB). Practical solutions for how to improve the RSS signature location method are then discussed.

2.1 Cramer Rao Lower Bound for the RSS location Method

The Cramer-Rao lower bound is a lower bound on the variance achievable by an unbiased location estimator. It is useful as a guideline to evaluate how well an estimator can locate a radio through measurement. Neal Patwari, Anthony J. Weiss and Amer Catovic [29, 39, 8] derived the CRLB for RSS-based location technologies for several situations. Though the Cramer-Rao bound is for an unbiased estimator, it can also be adapted for biased estimation [20].

The statistical model of random measurement is the only thing needed to calculate the bound. For example, $p(\mathbf{X}|\theta)$ is the likelihood function, where $\mathbf{X}$ is the random measurement and θ is the parameter we need to estimate. The CRLB provides a lower bound on the covariance matrix of the unbiased estimator, $\hat{\theta}$:

$$Cov(\hat{\theta}) \quad \triangleq E[(\hat{\theta}-\theta)(\hat{\theta}-\theta)^T] \geq Cov_{CR}(\theta) \quad \triangleq \mathbf{FIM}^{-1} \tag{1}$$

$$Cov(\hat{\theta}) \quad \geq -E\{\nabla_\theta[\nabla_\theta(\ln p(\mathbf{X}|\theta))]\}^{-1} \tag{2}$$

Where **FIM** stand for Fisher information matrix

The details of the derivation for the inequality above are available on pages 327-328 of [40].

2.1.1 RSS Link Budget and Propagation Model

Because all pure signal strength predictions are based on a simple path loss exponent model (such as the Hata model) [33], the radio link budget used for this type of link is given below:

$$P_R = P_T + G_R + G_T - 10n\log_{10}\left(\frac{d}{1\text{ m}}\right) - 20\log_{10}\left(\frac{4\pi}{\lambda}\right) + C_{\text{dB}} \tag{3}$$

where the terms in Equation 3 are summarized as follows:

P_R - power received by a handset (dBm)

P_T - power transmitted by a sector (dBm)

G_R - estimated measurement equipment antenna gain (dBi)

G_T - estimated sector antenna gain (dBi)

d - separation distance (m)

n - path loss exponent

λ - wavelength of radiation (m)

C_{dB} - constant offset (dB)

The variable C_{dB} in Equation 3 is a constant offset term that accounts for additional gains and losses resulting from antenna height and pattern, RF hardware, frequency offset, or any other consistent, unmodeled effects in the RF chain. The value for C_{dB} is chosen to minimize the standard deviation error between the raw modeling and any drive-test measurements corresponding to the sector.

2.1.2 Formulation of RSS measurement

For the RSS-based location method, the PSD is built from a simple propagation model, as shown in Equation 3. All control channels are predicted in the PSD building phase. In the real-time location phase, another set of measurements is made by the handset. Only M channels are measured and reported via the NMR. RSS measurements from these M channels are used to compare with RSS values in the PSD. The position of the closest match is the location estimate. For a specified location $\mathbf{z} = [x, y]^T$, a measurement on channel i can be expressed as

$$m_i = c + P_i(\mathbf{z}) + e_i \tag{4}$$

where the terms in Equation 4 are listed as follows:

c - a constant offset resulting from the RF properties of equipment

$\mathbf{z}$ - location vector

$P_i(z)$ - averaged power received at location $\mathbf{z}$

e_i - measurement error and propagation variance

The term c represents a location's unrelated attenuation caused by the different RF properties of equipment at both the base station and the mobile station. The term $P_i(z)$ is the predictable part of the received signal strength at location **z**. The term e_i represents the unpredicted signal strength variation introduced by head handset distortion, handset polarization mismatch, small-scale fading, and unmodeled shadowing effects.

Comparing Equation 4 with Equation 3, we have

$$c = P_T + G_R + G_T - 20\log_{10}\left(\frac{4\pi}{\lambda}\right) + C_{\text{dB}} \quad (5)$$

$$P_i(z) = -10n\log_{10}\left(\frac{d}{1\text{ m}}\right) \quad (6)$$

and e_i is the measurement error from model prediction if we assume the model is perfect.

Considering that one handset measures M channels from all surrounding base stations in each NMR, all measurements form a vector:

$$\mathbf{m} = c_{m1}\mathbf{O} + \mathbf{P}(\mathbf{z}) + \mathbf{e} \quad (7)$$

where the vectors have the following format:

$\mathbf{m}$	$\triangleq$	$[m_1, m_2, \cdots, m_M]^T$	:Measurement of channel $1 \cdots M$
c_{m1}	$\triangleq$	$P_T + G_R + G_T - 10n\log_{10}\left(\frac{d}{1\text{ m}}\right) + C_{\text{dB}}$	:Common bias term for all observations
$\mathbf{O}$	$\triangleq$	$[1, 1, \cdots, 1]^T$	:Observation vector, length M
$\mathbf{P}(\mathbf{z})$	$\triangleq$	$[P_1(\mathbf{z}), P_2(\mathbf{z}), \cdots, P_M(\mathbf{z})]^T$	:Predicted RSS
$\mathbf{e}$	$\triangleq$	$[e_1, e_2, \cdots, e_M]^T$	:Random error term

2.1.3 RSS Location Algorithm

In the absolute RSS location algorithm, we assume perfect knowledge of the common bias term of all observations c_{m1}. This bias is removed by subtracting a bias constant from every signal strength reported in the NMR. The implementation of the absolute RSS location algorithm used in the Georgia Tech location test is described in 3.5.2. The location decider for the absolute RSS location algorithm is

$$\mathbf{z} = arg\left(min(\|\mathbf{m} - \mathbf{P}(\mathbf{z}) - c_{m1}\mathbf{O}\|^2)\right) \quad (8)$$

In practice, the common bias term of all observations is unknown and the bias is different from handset to handset. Thus, the unknown bias must be estimated from measurements. This makes the problem a joint estimation problem. To get an analytical result, we use the following method to estimate the unknown bias:

$$\hat{c}_{m1} = (\mathbf{O}^T\mathbf{O})^{-1}\mathbf{O}^T(\mathbf{m} - \mathbf{P}(\mathbf{z})) = \frac{\mathbf{O}^T}{M} \cdot (\mathbf{m} - \mathbf{P}(\mathbf{z})) \tag{9}$$

This approach is equivalent to the relative RSS location algorithm. The practical implementation of the relative RSS location algorithm used in the Georgia Tech location test is described in 3.5.2.

Inserting Equation 9 back into Equation 7 forms an expression of the error term:

$$\begin{aligned} \mathbf{e} &= \mathbf{m} - \mathbf{P}(\mathbf{z}) - \mathbf{O}\frac{\mathbf{O}^T}{M} \cdot (\mathbf{m} - \mathbf{P}(\mathbf{z})) \\ &= \left(\mathbf{I} - \mathbf{O} \cdot \frac{\mathbf{O}^T}{M}\right) \cdot (\mathbf{m} - \mathbf{P}(\mathbf{z})) \\ &= \mathbf{R} \cdot (\mathbf{m} - \mathbf{P}(\mathbf{z})) \qquad (10) \\ \text{where } \mathbf{R} &= \mathbf{I} - \mathbf{O} \cdot \frac{\mathbf{O}^T}{M} \qquad (11) \end{aligned}$$

Therefore, the location decider is

$$\mathbf{z} = arg\left(min(\|\mathbf{R} \cdot (\mathbf{m} - \mathbf{P}(\mathbf{z}))\|^2)\right) \tag{12}$$

2.1.4 Derivation of Cramer Rao Lower Bound

The error vector, **e**, is a normally distributed multivariate random vector with zero mean and a positive definite covariance matrix, $\mathbf{C_e}$. The conditional probability density function of the measurement is given by

$$p(m|\mathbf{z}) = \frac{1}{(2\pi)^{\frac{M}{2}}\|(C_e)\|^{\frac{1}{2}}} \exp\left\{-\frac{1}{2}\mathbf{e}^T(C_e)^{-1}\mathbf{e}\right\} \tag{13}$$

Inserting Equation 10 into Equation 13 yields

$$p(m|\mathbf{z}) = \frac{1}{(2\pi)^{\frac{M}{2}}\|(C_e)\|^{\frac{1}{2}}} \exp\left\{-\frac{1}{2}[\mathbf{R} \cdot (\mathbf{m} - \mathbf{P}(\mathbf{z}))]^T(C_e)^{-1}[\mathbf{R} \cdot (\mathbf{m} - \mathbf{P}(\mathbf{z}))]\right\} \tag{14}$$

The Fisher information matrix is simplified after inserting Equation 14 into Equation 2.

$$\mathbf{FIM} = -\mathbf{E}\begin{bmatrix} \frac{\partial^2 lnp(m|z)}{\partial x^2} & \frac{\partial^2 lnp(m|z)}{\partial x \partial y} \\ \frac{\partial^2 lnp(m|z)}{\partial y \partial x} & \frac{\partial^2 lnp(m|z)}{\partial y^2} \end{bmatrix} = \begin{bmatrix} \mathbf{p_x}^T \mathbf{C}_r \mathbf{p_x} & \mathbf{p_x}^T \mathbf{C}_r \mathbf{p_y} \\ \mathbf{p_y}^T \mathbf{C}_r \mathbf{p_x} & \mathbf{p_y}^T \mathbf{C}_r \mathbf{p_y} \end{bmatrix} \tag{15}$$

$$\text{where } \mathbf{C}_r = \mathbf{R}^T \mathbf{C_e}^{-1} \mathbf{R} \tag{16}$$

$$\mathbf{p_x} = \frac{\partial \mathbf{p(z)}}{\partial x} \tag{17}$$

$$\mathbf{p_y} = \frac{\partial \mathbf{p(z)}}{\partial y} \tag{18}$$

The Cramer-Rao lower bound is given by the inverse of the Fisher matrix:

$$Cov_{cr} = \frac{\begin{bmatrix} \mathbf{p_x}^T \mathbf{C}_r \mathbf{p_x} & -\mathbf{p_x}^T \mathbf{C}_r \mathbf{p_y} \\ -\mathbf{p_y}^T \mathbf{C}_r \mathbf{p_x} & \mathbf{p_y}^T \mathbf{C}_r \mathbf{p_y} \end{bmatrix}}{(\mathbf{p_x}^T \mathbf{C}_r \mathbf{p_x})(\mathbf{p_y}^T \mathbf{C}_r \mathbf{p_y}) - (\mathbf{p_x}^T \mathbf{C}_r \mathbf{p_y})^2} \tag{19}$$

If all errors are independent identically distributed (i.i.d.) such that the covariance matrix $\mathbf{C_e} = \sigma^2(I)$, then Equation 16 becomes

$$\mathbf{C}_r = \mathbf{R}^T(\sigma^2(I))^{-1}\mathbf{R} = \frac{1}{\sigma^2}\mathbf{R}^T\mathbf{R} = \frac{1}{\sigma^2}\mathbf{R} \tag{20}$$

and Equation 15 becomes

$$\mathbf{FIM} = \frac{1}{\sigma^2}\begin{bmatrix} \mathbf{p_x}^T \mathbf{R} \mathbf{p_x} & \mathbf{p_x}^T \mathbf{R} \mathbf{p_y} \\ \mathbf{p_y}^T \mathbf{R} \mathbf{p_x} & \mathbf{p_y}^T \mathbf{R} \mathbf{p_y} \end{bmatrix} \tag{21}$$

The Cramer-Rao lower bound is given by the inverse of the Fisher matrix:

$$Cov_{cr} = \frac{\sigma^2\begin{bmatrix} \mathbf{p_x}^T \mathbf{R} \mathbf{p_x} & -\mathbf{p_x}^T \mathbf{R} \mathbf{p_y} \\ -\mathbf{p_y}^T \mathbf{R} \mathbf{p_x} & \mathbf{p_y}^T \mathbf{R} \mathbf{p_y} \end{bmatrix}}{(\mathbf{p_x}^T \mathbf{R} \mathbf{p_x})(\mathbf{p_y}^T \mathbf{R} \mathbf{p_y}) - (\mathbf{p_x}^T \mathbf{R} \mathbf{p_y})^2} \tag{22}$$

The expressions of $\mathbf{p_x}$ and $\mathbf{p_y}$ are given by inserting Equation 6 into Equation 17 and Equation 18.

$$[\mathbf{p_x}]_i = \frac{\partial\left[-5n\log_{10}(e)\ln\left((x_i - x)^2 + (y_i - y)^2\right)\right]}{\partial x} = 10n\log_{10}(e)\frac{x_i - x}{(x_i - x)^2 + (y_i - y)^2} \tag{23}$$

$$[\mathbf{p_y}]_i = \frac{\partial\left[-5n\log_{10}(e)\ln\left((x_i-x)^2+(y_i-y)^2\right)\right]}{\partial y} = 10n\log_{10}(e)\frac{y_i-y}{(x_i-x)^2+(y_i-y)^2} \tag{24}$$

If we define the location variance of the estimator to be σ_d^2,

$$\sigma_d^2 \triangleq \sigma_x^2 + \sigma_y^2 \tag{25}$$

then the CRLB asserts that

$$\sigma_d^2 \geq tr\{Cov_{cr}\} \tag{26}$$

2.2 Measurement Error Analysis

A lower measurement error leads to a more accurate location estimate. Finding a way to reduce the measurement error will greatly improve location accuracy. In this section, the composition of the measurement error is listed and several methods for reducing the measurement error are discussed.

There are five primary sources of measurement errors:

- Large-scale fading, σ_{LS} – Because the PSD stores the RSSI values in a raster grid with one RSSI vector per bin, it is assumed that the stored RSSI values for each channel are nearly constant across the space of a bin. This is not necessarily true. Buildings and nearby shadowers may cause significant signal fluctuations within a bin – a type of large-scale fading [4]. This error is less prominent for smaller grid spacings and for open areas.

- Small-scale fading, σ_{SS} – In the multi-path environment, the constructive and destructive interference between several multi-path components introduces small-scale fading [14, 37]. This small-scale fading may easily cause the signal strength to change 30 dB in RSSI power with just a few centimeters of movement.

- Head/handset distortion, σ_{HD} – The effect of a human head and hand near the handset antenna will cause spatial distortion in the handset antenna's radiation pattern.

- Antenna polarization distortion, σ_{AP} – The handset antenna is not always vertically polarized. Thus, the antenna's radiation pattern in the horizontal plane will change when the handset points in different directions.

- Handset bias, σ_{HB} – Different types of handsets have different antenna patterns, RF chains, and power level quantizer distortions.

Though there are several sources that may introduce measurement error, there are several ways to reduce these errors. In fact, some measurement errors are lowered by the propagation environment and by the behavior of a cell phone user. The most effective way to reduce measurement error, in practice, is to calibrate the PSD with field measurements. The calibration of a PSD will reduce the prediction error significantly. A well-calibrated PSD can achieve a 3.5 dB reduction in standard deviation of measurement error [12]. This error standard deviation could be 10 dB or higher with pure predictions from a Hata-type model. For the error introduced by large-scale fading, using a smaller bin size is the effective way to reduce the measurement error.

Measurement error caused by small-scale fading is greatly mitigated by the handset. The handset performs time-averaging on all measured RSSI. Small-scale fading could be further reduced by using a sequence of multiple NMRs instead of a single measurement. The movement of the cell phone user also helps to average out part of the small-scale fading.

Measurement error introduced by hand/headset distortion and by the antenna polarization distortion is also likely to be reduced by the user's movement. The multi-path propagation environment helps to mitigate the measurement error caused by the head/handset distortion and the antenna polarization distortion. Because the multi-path propagation environment increases the azimuth spread of the received signal, signals reach a cell phone with different angles of arrival. There are gains from some directions and losses from other directions. The antenna gains of all signals at the handset have an expected value of zero dB because the gain is averaged over the antenna pattern from all angles of arrival.

2.3 Simulation Environment Setup and Numerical Results

An ideal base station configuration is assumed when calculating the CRLB, as shown in Figure 5. All base stations are evenly distributed with a base station separation distance, d. The CRLB is numerically calculated at each dot in the center area of Figure 5. The reported location variance is the linear averaged variance over all location variances calculated.

Because base stations are sectored, several RSS measurements reported in one NMR may come

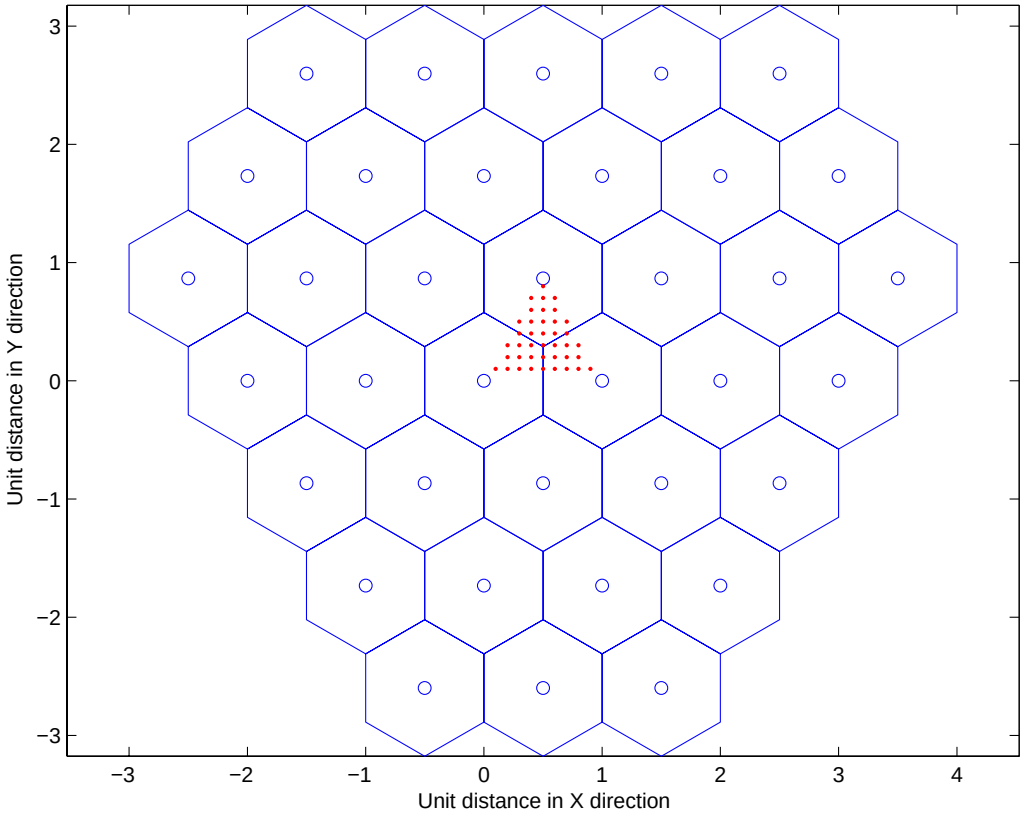

Figure 5: Ideal base station distribution used in calculated CRLB.

from the same base station. For example, if every base station has three sectors, there could be up to three measurements in the NMR from the same base station. In the GSM system, each NMR reports the six strongest neighbors' RSS measurements. Therefore, if there are more than six audible sectors, each NMR may contain measurements from two to six base station locations. This sectoring method introduces correlated measurements. Equation 15 is used in calculating the CRLB in this case. A non-zero correlation coefficient, "MR," is assigned in the correlation matrix for the measurements from the same base station, but different sectors.

A sequence of NMRs rather than just a single NMR could be used in the location engine of RSS location methods. Measurements from the same sector in different NMRs are correlated. When the cellular user is moving, the motion could reduce the correlation between NMRs. The same correlation coefficient MR is used in the correlation matrix for measurements from the same sector, but different NMRs. In other words, MR is also the correlation between measurements from identical sectors in different NMRs.

Table 2: Covariance matrix of 12 measurements from three base stations in two NMRs

	NMR1						NMR2					
	S1[1] B1[2]	S2 B2	S3 B3	S4 B1	S5 B2	S6 B3	S1 B1	S2 B2	S3 B3	S4 B1	S5 B2	S6 B3
S1 B1	1	0	0	MR	0	0	MR	0	0	MR	0	0
S2 B2	0	1	0	0	MR	0	0	MR	0	0	MR	0
S3 B3	0	0	1	0	0	MR	0	0	MR	0	0	MR
S4 B1	MR	0	0	1	0	0	MR	0	0	MR	0	0
S5 B2	0	MR	0	0	1	0	0	MR	0	0	MR	0
S6 B3	0	0	MR	0	0	1	0	0	MR	0	0	MR
S1 B1	MR	0	0	MR	0	0	1	0	0	MR	0	0
S2 B2	0	MR	0	0	MR	0	0	1	0	0	MR	0
S3 B3	0	0	MR	0	0	MR	0	0	1	0	0	MR
S4 B1	MR	0	0	MR	0	0	MR	0	0	1	0	0
S5 B2	0	MR	0	0	MR	0	0	MR	0	0	1	0
S6 B3	0	0	MR	0	0	MR	0	0	MR	0	0	1

[1] S1 means sector 1

[2] B1 means base station 1

For example, Table 2 shows the correlation matrix for two NMRs that report the RSS of six sectors located on three base stations (two sectors are measured from each base station). Because there are 12 measured sectors, the correlation matrix is a 12 by 12 matrix. The diagonal elements of this matrix are all 1s, the entries corresponding to measurements from the same base station have the value of MR, and all others entries are 0s.

The following set of default parameters is used in calculating the numerical results of the CRLB.

$n = 3.3$ - Path loss exponent

$Msigma = 3.5$ - Standard deviation of measurement error

$d = 500(m)$ - Average base station separating distance

$NumOfMeas = 30$ - Number of NMRs

$MR = 0.5$ - Measurement correlation from same base station

$AudibleBas = 3$ - Hearable base stations

We can tell from the CRLB derivation that the accuracy of the RSS location method is related to

1) Measurement error,

2) Number of measurements,

3) Correlation between measurements,

4) Path loss exponent,

5) Geometry distribution of the cellular base stations.

The CRLB is calculated and compared in Figures 6 to 10.

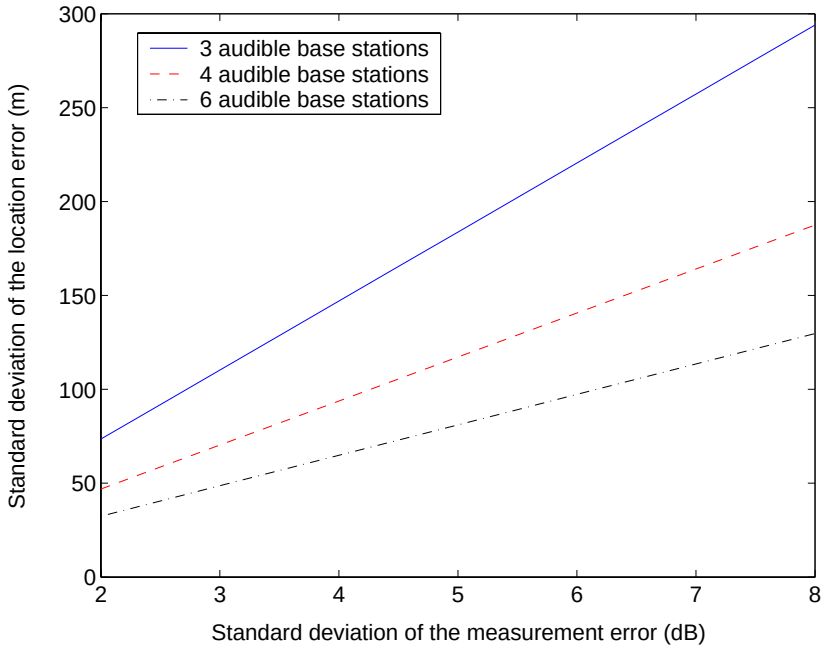

Figure 6: CRLB for different measurement errors (n=3.3 d=500m 30NMRs).

Figure 6 shows how the measurement error affects the location accuracy. A higher standard deviation of measurement error leads to a more inaccurate location estimation. The standard deviation of the measurement error has to be lower than 6.5 dB so that the standard deviation of the location error is lower than 100 m when six base station signals are reported in an NMR. If fewer base station signals can be received, a lower measurement error is required to ensure location accuracy.

Another way to improve location accuracy is to make more measurements. In practice, this means that more NMRs are used in the location estimation. Figure 7 shows the improvement that is achieved by using more NMRs. The location accuracy improves dramatically when the number of NMRs used increases from 1 to 10. Using more than 10 NMRs only helps slightly in improving the location accuracy.

Figure 8 shows that the CRLB is higher if measurements are more correlated because correlated measurements reduce the amount of information included in all the measurements. Figure 9 shows that the location performance improves for a larger path loss exponent because higher path loss

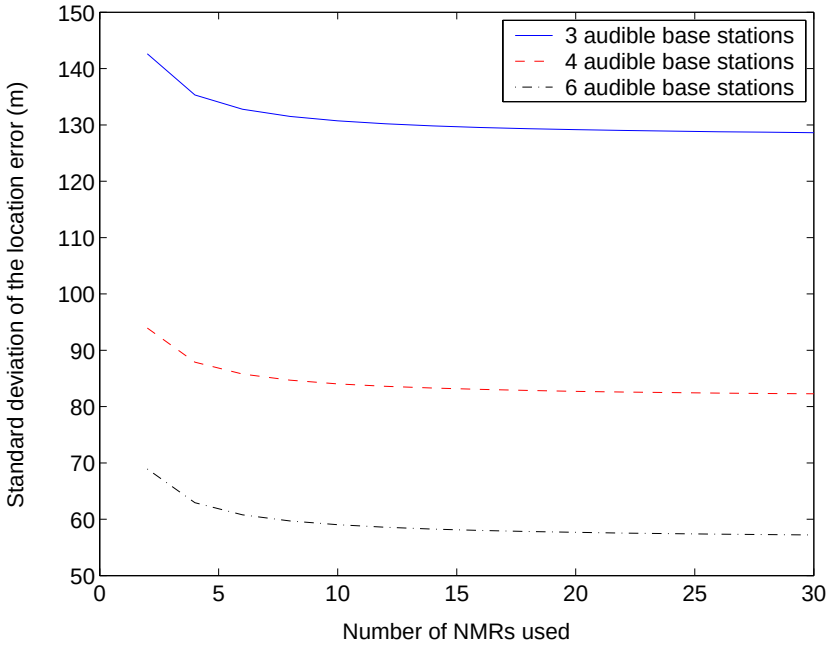

Figure 7: CRLB for different number of NMRs(n=3.3 d=500m σ=3.5).

increases the uniqueness of the RSS signature. Figure 10 shows that the location error increases linearly with the base station separation distance.

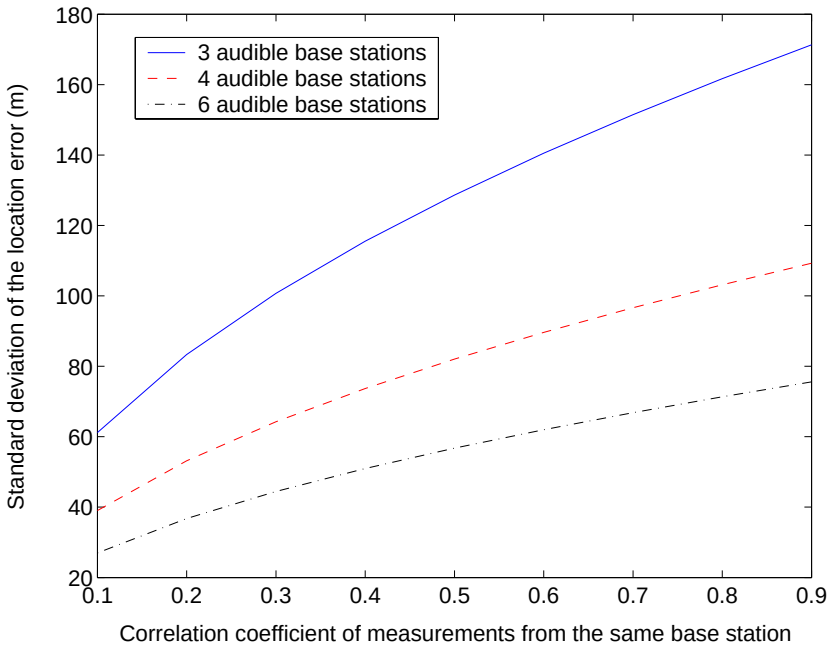

Figure 8: CRLB for different correlation coefficients between measurements from the same base station (n=3.3 d=500m 30NMRs).

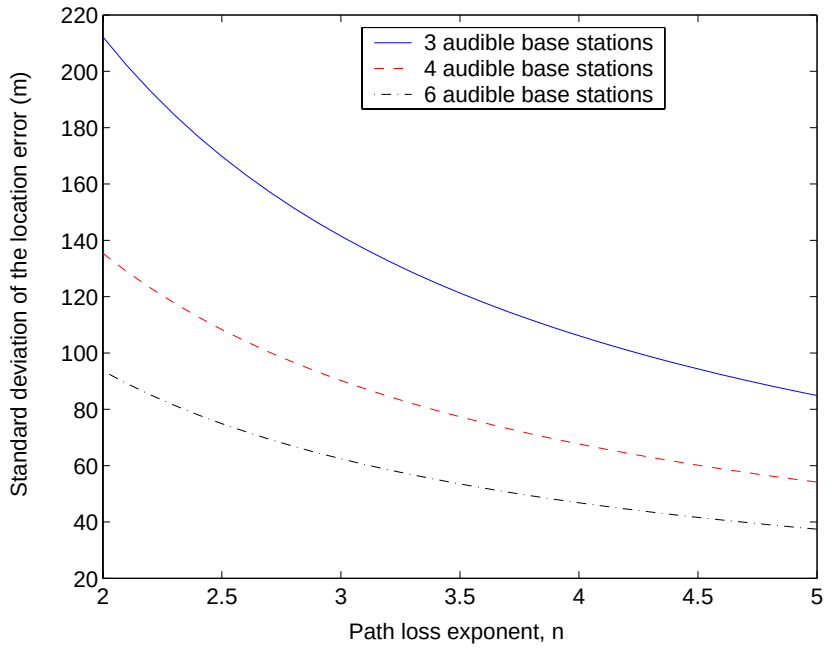

Figure 9: CRLB for different path loss exponents (MR=0.5 d=500m σ=3.5).

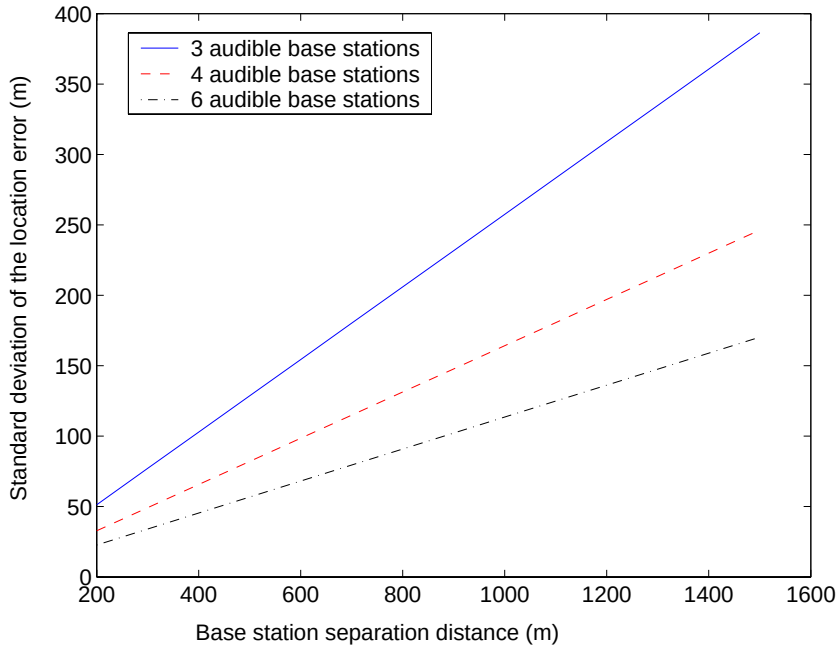

Figure 10: CRLB for different base station separation distances (n=3.3 MR=0.5 d=500m σ=3.5).

In this section, the CRLB of the RSS signature location method is calculated based on the GSM system protocol from a simplified propagation model. An analytical result of the CRLB is presented and numerically calculated for different cases. The numerical results suggest that the RSS signature location method is good for areas with small cell size and high path loss, which are the properties of urban and indoor environments. Furthermore, reducing the measurement error is very important for improving the location accuracy in the RSS signature method.

2.4 Analytical Results and Conclusion

Analytical results show that the RSS signature location method can enhance location-based services by providing better location accuracy in the cellular environment with small cell size and high path loss exponent. Though the location accuracy is still not adequate for some applications that need sub-10-meter location accuracy, the RSS signature technology can be used to achieve the FCC's E911 mandate in some environments where other location technologies fail. Numerical results of the CRLB also suggest that the RSS signature method is not nearly as effective for rural areas where base stations are far from each other. The average base station separation distance should be less than 1000 m for the RSS signature method to achieve the FCC's E911 requirement.

The numerical results discussed in the previous sections are based on a greatly simplified propagation model and a greatly simplified location algorithm. The results provide insight to the relationship between location accuracy and different factors such as the measurement error, the geometric distribution of base stations, the correlation between measurements, the path loss exponent, and the number of measurements. More information could be used in a cellular network to sharpen the location accuracy. For example, a GSM system NMR reports the six neighbor's RSSI, the signal quality of the neighbors, the timing advance for the serving cell, the serving cell identity information, and other radio environment parameters. Adding all this information to the simplified model will make the performance analysis too complex to get an analytical result. Location accuracy from real measurement campaigns in different environments provides the best measure of how well the RSS signature method works. Chapters 3 to 5 document location test details for three different locations, including ultra-dense urban, semi-urban, and urban plus rural environments.

CHAPTER III

PRELIMINARY RESEARCH: ATLANTA, GA

Preliminary received signal strength-based radio location research was conducted in an IS-136 digital system.

To perform the study in a radio location, the Georgia Tech campus has been turned into the world's first indoor/outdoor cellular location laboratory. The ensuing location tests were performed on an 850 MHz cellular network in Midtown Atlanta. The Georgia Tech campus approximates a typical semi-urban or dense suburban area with streets, moderate green space, and many four-to-five story academic and office buildings. Although the potential population density of cellular users was high, there are no skyscrapers or canyons that would be associated with dense urban deployments. A database of RF coverage maps for all nearby serving sectors was created from a combination of propagation modeling and varying degrees of indoor and outdoor measurement calibration using a Comarco IS136 scanner with baseband decoding. Real, pedestrian-style handset measurements were taken with an Ericsson handset connected to an Ericsson TEMs data collection unit.

The results in this study showed that RSS location techniques could satisfy the FCC E911 requirements for outdoor handsets in semi-urban environments. When a majority of the test handset data originated from indoor locations (as it would in real life), the performance degraded somewhat. For example, the error distance between a location estimate and a handset's groundtruth position drops from 100 m or less 68% of the time to 100 m or less 62% of the time. However, a variety of techniques were demonstrated to recover the lost accuracy by modifying the location algorithms, adding indoor calibration measurements, modeling indoor propagation using satellite photogrammetry, and using sequential handset measurements. The most accurate location algorithm was developed by using a sequence of 10 linearly averaged handset measurements and RF maps calibrated with both outdoor and indoor measurements; the error distance for this case was 100 m or less 78% of the time and 300 m or less 98% of the time. This upper limit of performance was well above the FCC E911 requirements.

Several recommendations emerged from this study. Experimental results suggested that RSS-based techniques may be resilient enough for deployment as a stand-alone position-location technology for satisfying the FCC's E911 requirements in most populated areas. There are still several issues about this technology that need to be addressed. First and foremost, it is unclear how much cost and effort are required to maintain the performance in cellular networks that, to one degree or another, are always undergoing build out, optimization, or modification.

Ultimately, the ideal solution for the U.S. E911 problem will be a hybrid combination of handset-based global positioning system (GPS) technology and an RSS-based location system. These two technologies seem to complement each other so well. GPS works in rural, open-sky environments where all network-based location solutions tend to degrade because of the low density of base stations. Conversely, GPS fails whenever satellite links become obstructed. This can happen in any environment, but is particularly common in urban and indoor areas – precisely the places that RSS radio location works best. If public safety is the primary concern, then this long-term tandem of location technologies seems to be the most sensible.

This measurement campaign lasted for four months (March through June) in 2004. All data points were tagged with absolute longitude and latitude coordinates taken from a GPS radio; however, because of the limitations of GPS, many outdoor coordinates and all indoor coordinates had to be painstakingly estimated from geo-referenced maps of campus and manually entered into the database. This is one source of error in the measurements. There are other unique sources of error in measurements that may make the experiment results somewhat pessimistic. For example, there was a seasonal change in the middle of data collections when leaves grew back on the campus trees, changing the propagation characteristics by several dB. Also, one of the large buildings within the test area was demolished in the middle of the measurement campaign. A fairly simple location algorithm is used since the more complicated question of indoor feasibility is our interest rather than location algorithm. There are many other algorithms that have been proposed that could improve the performance.

In the preliminary research, the feasibility of the RSS location method was demonstrated in an IS-136 network at a semi-urban environment loaded with indoor users. The research result from this project was a timely contribution for wireless industry decision making. The research results

removed the uncertainty of model-based simulation results and provided experiment-based numbers in location error statistics and indoor/outdoor discrimination rates for a live cellular network.

3.1 Key Output

This preliminary experiment, which was performed on the Georgia Tech campus, resulted in several key outcomes:

1. This was the first academic experiment to validate the indoor and outdoor performance of RSS location for the North American E911 system in general. Especially, the data collected in this experiment included the effect of indoor environments and the different situations that an active cell phone call would encounter such as head-hand distortion.

2. This study showed that, with regard to FCC-mandated performance statistics, indoor environments showed little degradation of location performance when compared to a system where all handsets were outdoors.

3. Discrimination of outdoor and indoor handsets was possible. With proper algorithms and distribution statistics of indoor/outdoor measurements, the discrimination rate can reach up to 92% (see Section 3.5.2).

4. Several suggestions for algorithms that improved the location performance were presented.

3.2 Measurement Plan

All measurements were taken on the Georgia Tech campus, shown within the box in Figure 11. We selected a 700 m $\times$ 500 m region as our experimental test area. In this area 23 buildings were measured, marked by Xs in Figure 11. There are three base stations inside the test area, where eight medium-tier sectors are in use. Another five base stations in the neighborhood also provided coverage for the edge of the test area. The distance between base stations was approximately 400-500 meters. The construction style for most of the buildings is steel and concrete with brick surfaces. Some of the buildings have glass walls. Terrain in this area is hilly, with ground elevation differences of about 10 m from the peak to trough. The roads in this area are mostly two-lane, two-way streets. The average population on a workday is around 15,000 people. This is a typical semi-urban

area, where radio location is problematic for angle-,time-, or GPS-based location technologies.

The measurement campaign lasted for four months; during this time the leaves grew back on the deciduous trees. The seasonal shift changed the wireless propagation environment, which degraded our calibrated predicted signal database (PSD). Thus, the experimental results are thought to be more pessimistic than when using a timely calibrated PSD.

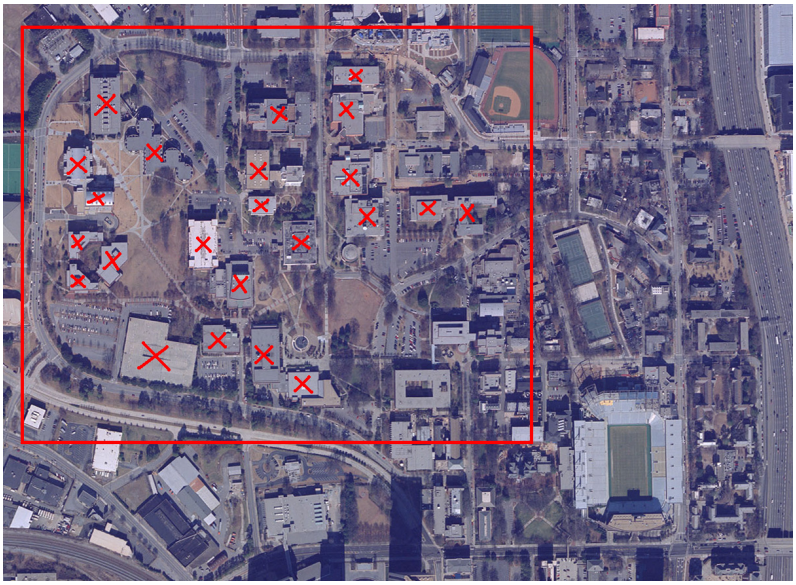

Figure 11: Indoor/Outdoor "location laboratory" at Georgia Tech campus in semi-urban Atlanta, GA.

3.2.1 Setup Overview

Our measurements were performed with two different measurement tools. The data collected by different equipment generated two different databases. PSD calibration data was collected by a Comarco LT200 IS-136 RF scanner with baseband decoding. Handset data was collected by an Ericssion TEMS Light 3.0 unit. To measure as much as possible, drive-test measurements, outdoor walking measurements, and indoor walking measurements were taken. Drive-test measurements provided a fast way to measure across a large outdoor area, while walking measurements filled in the gaps where the drive-test measurements could not access.

Each major campus building within the test area was measured using the following procedure.

1. The measurement system was calibrated before each measurement.

2. Outdoor drive-test measurements were made along the road using the Comarco LT200 unit. Drive-test measurements were kept at the speed of 15-20 km/hr (9-13 miles/hr). The received signal strength of each of the 26 digital control channels was measured.

3. Outdoor walking measurements were made around the building using the Comarco LT200 unit. Walking measurements were taken at the speed of 2-4 km/hr (1-2 miles/hr). The RSS of each of the 26 digital control channels was measured. For details, see Section 3.3.1.

4. Indoor walking measurements were made in all the rooms on the edge of the buildings. If the room was less than 10 m in length, the measurement was taken over a meandering path within the room during a 30-second period. If the length was longer than 10 m, the measurement was performed along a straight line from one end of the room to the other with a constant speed of 2 km/hr.

5. At the end of the day, another hardware calibration was performed to verify the system integrity. This involved repeating measurements at two locations taken earlier in the day to verify system stability.

6. The measurement device was changed from the Comarco unit to the TEMS light 3.0 unit to collect handset testing data. This data were taken through an Ericsson handset that was strapped to the field engineer's head for the most life-like usage. Steps 1-4 were repeated to build up a database of test measurements.

3.2.2 Equipment

Comarco LT200 Unit

The Comarco LT200 is a TDMA 800 and 1900 band scanner. Channel sets collected in our measurement campaign lay in the IS-136 800 MHz band, which were all digital control channels for the network that was measured. The handset used with the scanner is a NOKIA 2160. Figure 12 illustrates the scanner connection. Figure 13 shows how the real scanner system was connected.

Ericssion TEMS Light 3.0 Unit

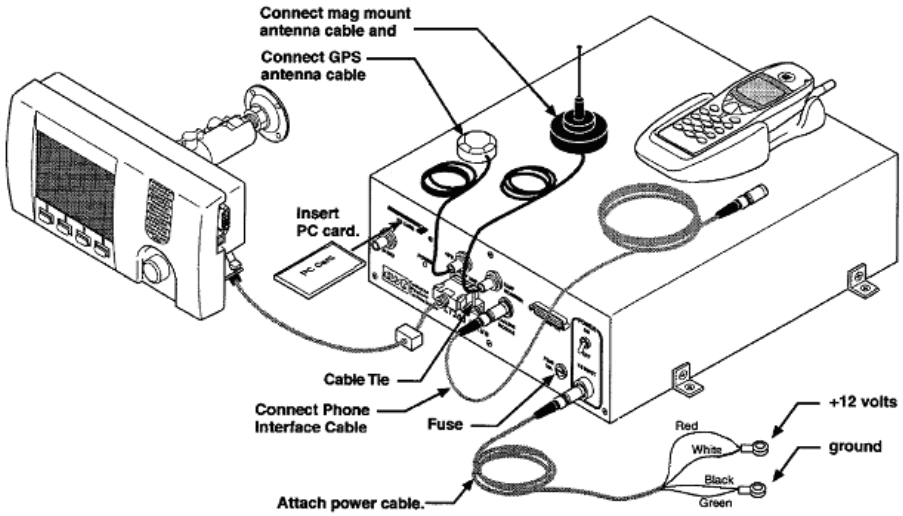

Figure 12: Scanner setup illustration (Comarco LT200 Users Guide[pg162]).

The Ericssion TEMS is a portable device for RF scanning and active call measurement. The hardware components of the TEMS light system include one Ericsson TEMS handset and a FUJITSU STYLISTIC 1000 tablet PC. The total weight of this system is about 4.5 lbs. This unit can scan up to 24 channels simultaneously. The scanning function was used to construct our handset test data. We programmed the 24 channels to correspond with the base stations closest to Georgia Tech.

3.2.3 Calibration

A standard free-space calibration procedure was employed on each day of RF measurement to monitor the integrity and consistency of our equipment. The calibration consisted of spatially averaged power measurements taken on the rooftop of the Van Leer Building at the start and end of each day of RF field measurements. By bracketing each day of field measurement with this calibration procedure, we not only verified the consistency of the RF equipment throughout the day, but could be alerted to any day-to-day biases within either the cellular network or our measurement setup.

The basic calibration procedure for the RSSI measurement system was as follows:

1. Define Calibration Paths: The location of the calibration was on the 5th-floor rooftop of the Van Leer Building on the campus of the Georgia Institute of Technology. Figure 15 shows the layout of the Van Leer Building rooftop. The dashed line marks the calibration routes used in our experiment. Route 1 was a 40.6 m $\times$ 5.5 m box-shaped path whose southwest

Figure 13: Actual Comarco scanner setup.

corner had GPS coordinates of W 84.39747° (longitude) and N 33.77591° (latitude). Route 2 was a straight 39.8 m line running east-west whose western endpoint had GPS coordinates of W 84.39738° (longitude) and N 33.77581° (latitude). Although Georgia Tech is an urban campus, the rooftop of Van Leer places the equipment above most of the trees and smaller buildings that potentially block or distort GPS measurements. Each calibration route was large enough to provide a variety of RSSI measurements within a local area, but small enough not to introduce significant large-scale variations in the average RF power.

2. System Setup: To begin a day of measurements, the RF measurement system was connected on top of the cart according to the block diagram of Figure 12. If a scanner measurement

Figure 14: Actual TEMS unit setup.

was being calibrated, the scanner's cellular antenna was placed on top of the cart in a vertical position. If a handset measurement was being calibrated, the handset was placed on the mounting pole anchored firmly to a stable board with a vertical orientation. The GPS antenna rested on top of the cart, separated from the cellular antenna and the handset by at least 20 cm. The scanner's display unit was also mounted on the stable board that was placed onto the scanner main body for easy movement. Since the scanner's antenna and the GPS antenna have a magnetized base, a metal board was used for mounting.

3. Acquire Data: The equipment was set to measure using either the scanner or the handset. Data were acquired by moving slowly along Route 1. This was repeated along Route 2 so that two unique data sets were taken. Each route was measured in no less than 60 seconds to ensure that sufficient amounts of data were logged.

4. Post-processing: The data were then immediately downloaded to a computer for analysis. The analysis was identical for both scanner and handset data. For every measured control channel measurement, the RSSI values taken around each calibration route were linearly averaged to

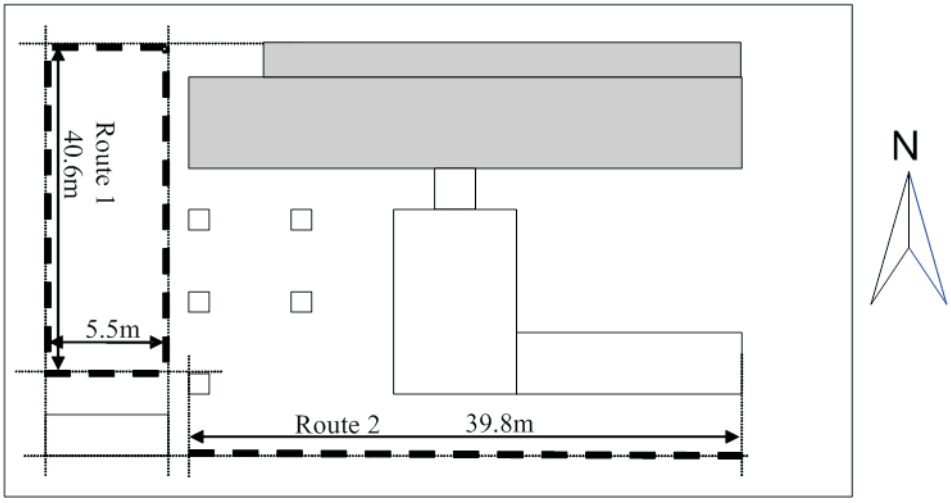

Figure 15: Rooftop calibration route.

produce a single average signal strength measurement in dBm. Four checks were performed at this point of the procedure:

a. Long-Term Consistency Check: the average RSSI values were compared with those taken on previous days. If RSSI values differed from previous measurements by +/- 3 dB, a thorough system check was performed.

b. Short-Term Consistency Check: For an end-of-day calibration, average RSSI values were compared to the start-of-day calibration.

c. GPS Position Check: GPS operation was verified by comparing the readings to previous GPS measurements.

d. Record and Save Average RSSI Values: The average values were dated and recorded for future use. In constructing an RSSI database that uses measurements spanning multiple days, it may be necessary to normalize each day's measurements against the calibrated measurements.

5. Repeat Procedure: The calibration procedure was repeated using the identical procedure at the end of a measurement day.

3.3 Data Collection

Building construction, especially the material and design of the exterior wall, determines the penetration loss of radio waves. To discriminate between indoor and outdoor calls, this penetration loss information is very useful. In this report, we give an analysis of penetration loss for each building. We also present the penetration loss for typical office buildings from a statistical point of view. The buildings in our experiment are mainly steel, concrete, and brick, which are the typical building materials for urban areas.

The sample of measured buildings, summarized in Table 3, represents typical construction practices in our experimental area. The buildings in Table 3 represent typical semi-urban commercial buildings. For several representative buildings, we present some details of construction and site information that provide a better understanding of the test area. These parameters include the following:

Table 3: Building construction summary for Georgia Tech.

Number	Campus buildings in the test area	Construction Material	Stories
075	ARCHITECTURE (WEST)	STEEL/CONCRETE	3
076	ARCHITECTURE (EAST)	STEEL/CONCRETE/BRICK	3
085	VAN LEER (ECE)	STEEL/CONCRETE	5
086	BUNGER-HENRY	STEEL/CONCRETE	4
111	MASON (CE)	STEEL/CONCRETE/BRICK	5
145	SUSTAINABLE EDUCATION	STEEL/CONCRETE	3
081	HOWEY PHYSICS	STEEL/CONCRETE/BRICK	4
095	PETTIT MIRC	STEEL/CONCRETE/BRICK	2
050	COMPUTING (COC)	STEEL/CONCRETE/BRICK	4
066	CHERRY L EMERSON	STEEL/CONCRETE/BRICK	3
114	HOUSTON	STEEL/CONCRETE	2
104	WENN STUDENT CENTER	STEEL/CONCRETE/BRICK	3
123	STUDENT SERVICES	STEEL/CONCRETE	2
103	BOGGS CHEMISTRY	STEEL/CONCRETE	4
124	FERST CENTER THEATER	STEEL/CONCRETE/BRICK	2
135	MRDC	STEEL/CONCRETE	4
055	INSTRUCTIONAL CENTER	STEEL/CONCRETE/BRICK	3
056	WENN STUDENT CENTER	STEEL/CONCRETE/BRICK	3
057	STUDENT SERVICES	STEEL/CONCRETE	2
054	STUDENT CTR DECK	STEEL/CONCRETE	3

1. Construction material,

2. Building type,

3. Size and layout of the building,

4. Type and proximity of the surrounding buildings and trees near the building,

5. Terrain surrounding each building.

3.3.1 Outdoor Measurements

Outdoor measurements were used to calibrate PSD; they were also used to calculate the orientation-dependent penetration loss. The outdoor measurement campaign included two parts. The first part consisted of drive-test measurements, similar to those conducted by wireless service providers to optimize their networks. An RF scanner was placed in a vehicle so that RSSI information could be collected while the field engineer drove through the test area.

The second part of the data collection was walking measurements. Because drive-test measurements were limited to roadways, the RSSI in a field close to a building or a pedestrian path could not be measured by a driving test. The field engineer pushed a handtruck on which the scanner was mounted. The scanner collected data while traveling the designed route. These pedestrian measurements did more than fill in the unmeasured areas of a network for RSSI radiolocation; they also allowed measurements close-in to the test buildings, which allows the calculation of orientation-dependent penetration loss. This is discussed in Section 3.4.1.

3.3.2 Drive-Test Measurement

Wireless service providers maintain their own drive-test measurement RSSI database for the purpose of optimizing their network. Their measurements are performed by their field engineering team. Recalibrating this database with fresh drive-test measurements must be performed from time to time to ensure that the system is working properly. Though this procedure costs manpower, it is a vital function for every carrier.

In our experiment, the goal for drive-test measurements is to calibrate our database of new RF maps for RSS location. By using this PSD, which is calibrated by drive-test measurements only, the location performance of an RSS location algorithm can be simulated. This simulation will also provide a baseline comparison of performance for more complicated PSDs that include indoor modeling.

A Comarco LT200 RF scannner was used in the drive-test measurements. The vehicle was a sedan with the scanner antenna and GPS antenna placed on the rooftop, separated by 0.4 m. The collection vehicle moved at a speed of 20-25 kph. The measurement route is shown in Figure 16.

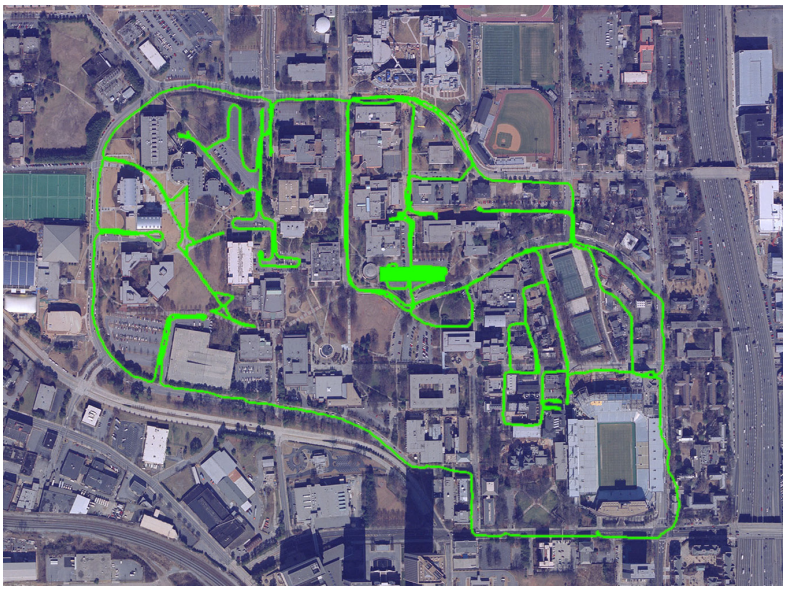

Figure 16: Driving route for outdoor drive-test measurement.

3.3.3 Walking Outdoor Measurement

A good outdoor walking measurement requires collecting the RSS data along the outside wall where a drive-test measurement cannot reach. The goal of the walking measurement is to provide the RSS data for penetration model calculations and to provide the most accurately calibrated PSD. To calculate the penetration loss, the signal strength at both sides of the building's outside wall is needed. The outdoor walking measurement result is used to generate an accurate PSD. Though this PSD is not practical in widespread commericial deployment of an RSS location system, it provides an upper limit of accuracy for these location methods.

After the PSD was calibrated, the handset data were collected using this same walking outdoor measurement. This collection procedure resembles a common cell phone user chatting with others while walking. Figure 17 and Figure 18 show typical outdoor walking measurements.

Figure 17: Georgia Tech student researcher Chris Durkin takes an outdoor walking measurement outside the Bunger-Henry Building.

3.3.4 Indoor Measurements

All indoor measurements were taken at walking speeds. By studying both indoor walking measurements and outdoor walking measurements, the orientation-dependent penetration model can be calculated (See Section 3.4.1). The indoor measurement is also used in calibrating the most accurate PSD. Figure 19 and Figure 20 show typical indoor walking measurements. Figure 21 shows that the handset is strapped to the field engineer's head for the most life-like usage.

The procedure for indoor measurement is as follows:

1. Select the building. Find as much indoor area as possible against the outside wall that is accessible to measurement.

2. Select the measurement route for the building such that the route allows measurement on both sides of the exterior building wall.

3. Decide a measurement route in each room that is as straight as possible, parallel to the exterior wall.

4. Mark the route on a map and record the start time of each route.

Figure 18: Georgia Tech student researcher Alenka Zajic takes an outdoor walking measurement outside the student center parking deck.

5. Move along the route at a constant speed. If the route is less than 10 m, move backward and forward several times to make sure the measurement time lasts at least 30 seconds

6. Record the end time of the route.

7. Repeat steps 4-6 for all routes within the same building working around the perimeter as the floor plan permits.

Figure 22 shows the preferred indoor and outdoor measurement route. Figure 23 shows the actual measurement route in the Architecture Building.

Figure 19: Georgia Tech student researcher Joshua Griffin takes an indoor walking measurement inside the Howey Physics Building.

Figure 20: Georgia Tech student researcher Albert Lu takes an indoor walking measurement inside the Architecture (East) Building.

Figure 21: Georgia Tech student researcher Jian Zhu takes a handset walking measurement inside the Van Leer Building.

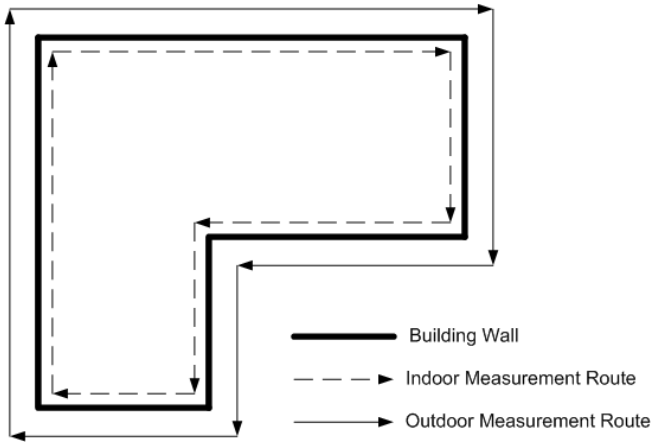

Figure 22: Indoor / outdoor measurement procedure measurement route.

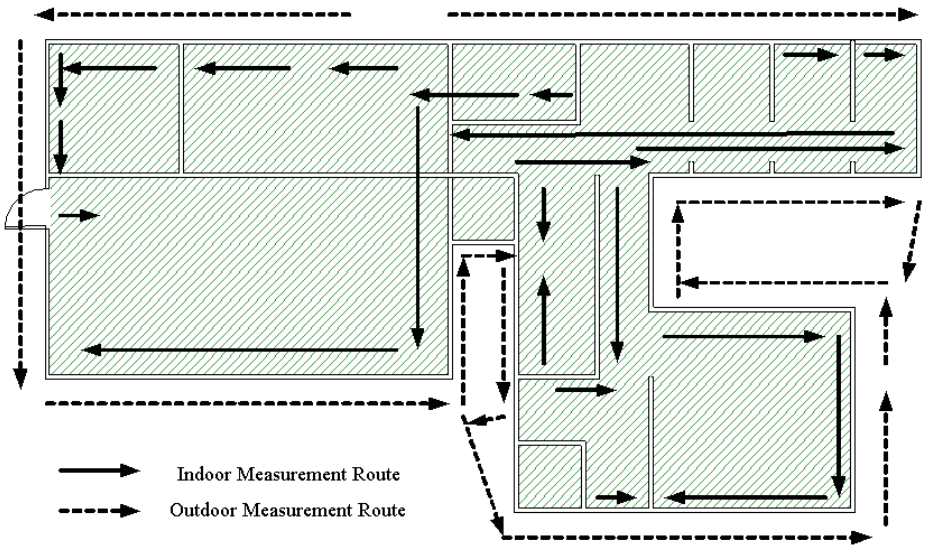

Figure 23: Measurement route record at Architecture Building.

3.3.5 GIS Data

The location experiments in this report use *geographical information systems* (GIS) data to assist in the indoor and outdoor location of users. The principal source of GIS in the study is a high-resolution database of aerial photographs of the city of Atlanta. This GIS image contains photographic pixels with 1 m $\times$ 1 m resolution. The image was constructed in 2002 – nearly one-and-a-half years prior to the measurement campaign.

The aerial photographs were used to construct highly accurate building footprints of the test area on campus. First, the GIS photographs were digitally cropped. By manually associating two outdoor points on the map with their corresponding latitudes and longitudes, as measured by GPS, all pixels on the photograph can be geo-referenced. Using typical imaging software, the buildings in the photographs were manually traced and filled to create a building footprint map. Although this act was performed manually, there are a number of computer algorithms and GIS companies that also provide this type of processing.

The end result of this image processing is a high-resolution binary map that distinguishes (in two-dimensions) coordinates that are indoors and outdoors. Figure 24 shows a sample output of this step. The map is based on recent city photographs; however, several modifications were made in cases of new or demolished buildings. The footprint map is then subsampled to 10 m $\times$ 10 m resolution to match and align with the RF maps used in the experiments. This building footprint map is used for indoor propagation modeling and the location algorithm itself.

3.4 Data Analysis

3.4.1 Angle-Related Penetration Loss

This section presents the methodology for modeling losses for cellular radio waves penetrating buildings.

Basics of Indoor Propagation

The signal strength measured by an indoor wireless handset depends on the propagation characteristics of the building. Regardless of the type of building – office, home, factory, store, etc. – the propagation characteristics of the *outdoor* environment also affect the indoor received signal strength. For that reason, it is usually best to model penetration relative to the path loss immediately

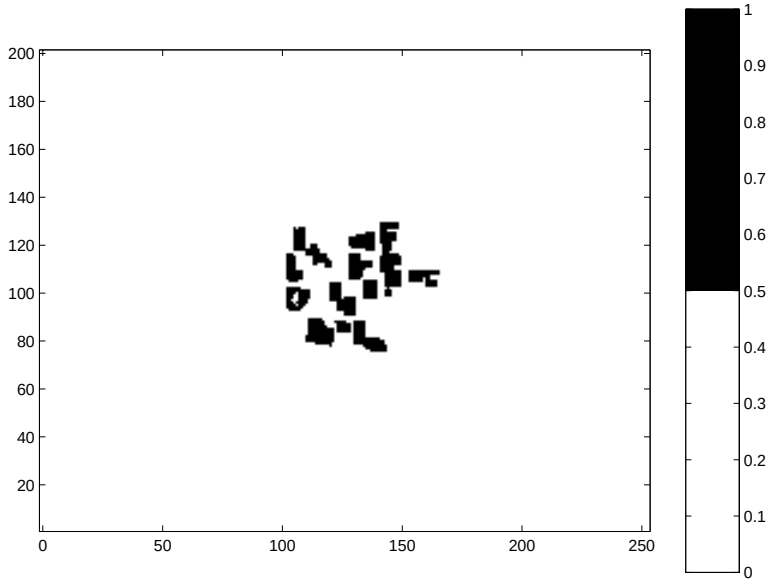

Figure 24: Binary building footprint inside experiment area.

surrounding the building [15].

There are several attributes of indoor propagation that may assist RSS radiolocation if modeled correctly:

- **Initial Loss:** A radio signal in cellular bands experiences an immediate loss upon penetrating a typical building. This value varies from building to building, but it is common to use single-value averages to estimate the loss [1].

- **Orientation Dependence:** Of particular importance to location estimation algorithms is the ability to model the effects of building orientation with respect to the serving base station. A transmitter that illuminates the side of a building directly experiences a different penetration loss than a transmitter that illuminates the side of a building at a grazing angle. Capturing this property in a model is what enables a location engine to discriminate position based on relative signal strengths from different base stations.

- **Layered Loss:** As a rule of thumb, total path loss increases for handsets further inside a building. Indoor walls and partitions screen the propagating waves as they penetrate into the building. This is a higher-order effect that may be too difficult to contribute to the performance of a location engine.

Since it is highly impractical to make measurements of all indoor environments, RSS location must rely on modeling these indoor penetration characteristics to some degree.

Indoor Propagation Issues for RSS Location

We should note that there are three different questions to ask in an indoor radiolocation study, each corresponding to different types of location technology. The first question is *can we discriminate between indoor and outdoor cellular users?* The second question is *can we correctly discern in which building an indoor cellular user is making a call?* The third question is *can we pinpoint the position of an indoor cellular user within a building?* From a technical point of view, these questions are presented in order of increasing difficulty, and each affirmative answer represents a unique location service.

Interestingly, these three questions correspond nicely to the basic indoor propagation characteristics described in Section 3.4.1. It would be valuable in E911 applications to discriminate between an indoor or outdoor cellular user – even if the exact building could not be discerned. This could be done by comparing RSS measurements to the initial or average propagation loss of buildings. Section 3.5.2 presents this analysis for our experiment.

Discerning the exact building of an indoor user is more difficult, and pinpointing users within a building even more so. Success in these two tasks would require an extremely detailed database of indoor and outdoor RF maps. In the absence of exhaustive measurements, *orientation dependence* and *layered loss* are crucial for this type of indoor radiolocation.

Octant Model of Orientation Loss

In our study, we desire to tabulate how penetration loss changes as a function of building incidence with respect to a cellular base station. From physics, we expect normal-incident waves to propagate into a building with less loss than grazing incidence. Thus, if we were to compare received powers in cellular handsets operating on opposite sides of an exterior building wall (one indoors and one outdoors), we would not expect the difference in measured power for each control channel to be the same. Since different control channels originate from different base stations and propagate through a building exterior with dissimilar angles of incidence, the penetration loss will differ for each. If this difference is pronounced, it may be possible to model and exploit this effect in RSS radiolocation.

Average values for building penetration loss for cellular bands are well tabulated [5]. How these losses change as a function of orientation is not well understood. There are a number of physical mechanisms and factors that affect the orientation dependence of penetration loss. Polarization of the incident radio wave, electrical properties of the building exterior, material inhomogeneities, and surface roughness all affect orientation-dependent penetration loss. And although the most powerful radio waves emanate from the direction of the base station, multi-path propagation implies that the arriving angles of many radio waves are dissimilar to the base station bearing angle. From a physics standpoint, calculating orientation-dependent penetration loss is hopeless.

Empirical values for orientation-dependent penetration loss are not nearly so challenging. By studying propagation around and into a variety of typical buildings, representative values can be calculated. One useful way of organizing and tabulating this data is to use the octant model, illustrated in Figure 25. Essentially, incident angles are divided into eight uniformly spaced octants. Unique penetration loss values are calculated and assigned for each octant. Although it may seem crude, the octant model is a useful way to characterize and report orientation-dependent penetration loss. As an added benefit, there are some modeling algorithms that use octant data to model penetration loss [13].

The octant corresponding to a range of incident angles is recorded as an integer value. This integer value ranges from 1 to 5 (not 1 to 8 because of symmetry), as shown in Figure 25. Qualitatively, each octant of incidence corresponds to the following propagation:

1 **Near-Normal Incidence:** The radio wave is arriving at near-normal incidence to the surface of a building. This type of propagation is, on average, the least-lossy mode of radio signal penetration into the building.

2 **Oblique Incidence:** The radio wave arrives at an oblique angle with respect to the building surface (neither perpendicular nor parallel). This type of propagation is lossier than near-normal incidence.

3 **Grazing Incidence:** The radio wave arrives at an incident angle that is nearly parallel to the surface of the building. This type of propagation should be very lossy, unless a significant number of scatterers exist outside the immediate area of the building.

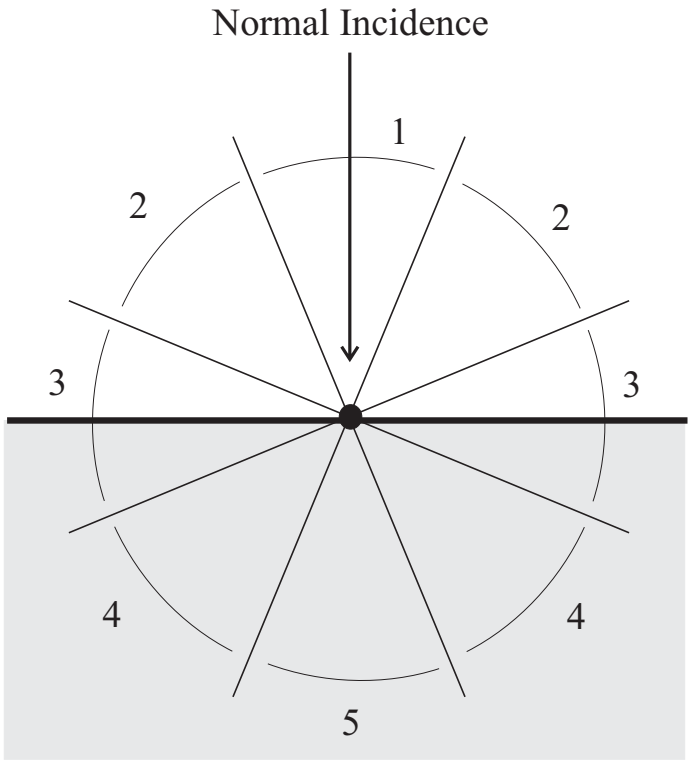

Figure 25: Directions are broken into uniform angle ranges called *octants*. The thick line is the building surface. Above is outdoors, below is indoors.

4 **Oblique Backscatter:** The base station illuminates the surface from an oblique angle on the *opposite* side of the building. The resulting penetration loss should be high.

5 **Near-Normal Backscatter:** The base station illuminates the surface from a direction *opposite* the building surface. The resulting penetration loss should be high, but not necessarily the highest; the surface is nearly normal to much of the back-scattered power [14].

The next section discusses octant model values obtained from our extensive building measurements.

Octant Penetration Values

Table 4: Octant penetration values.

Octant	1	2	3	4	5
Loss (dB)	7.5	8.3	8.9	9.3	9.2

In Table 4, the lowest penetration loss is 7.5 dB and the highest penetration loss is 9.3 dB, a difference of only 1.8 dB. The 850 MHz propagation does not appear to depend on incidence angle as much as the 1900 MHz. This may make the location of an indoor handset within a particular

building nearly impossible.

Building Sample Analysis

In this section, we present an example of penetration loss calculated for one control channel power. The Architecture (east and west) Building is under direct illumination from the Rich Building base station, which is 20 m away to the south. The sector facing the Architecture Building is using digital control channel 792.

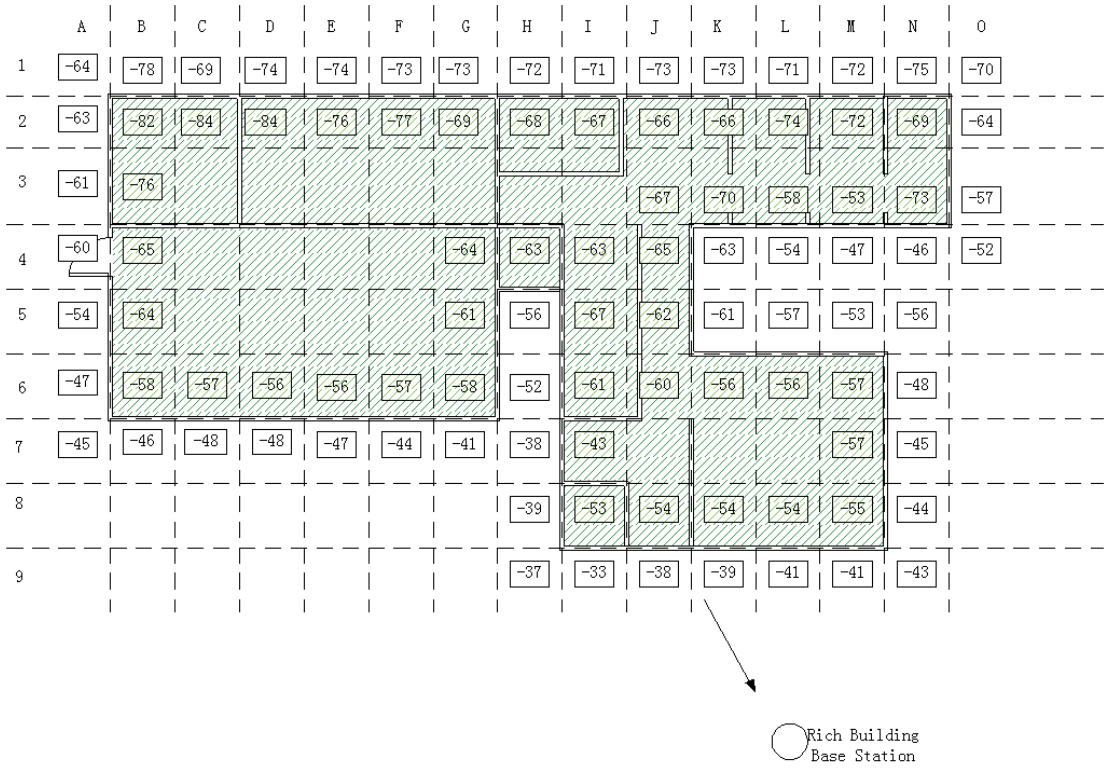

Figure 26: RSS at Architecture Building.

The wall at area H8-N9 is solid red brick. There are no windows. The penetration loss is about 13-18 dB. The wall at area B6-G7 is a metal-framed glass wall; the penetration loss is lower, at 8-13 dB.

The Van Leer Building reflects much of the power into the A1-B7 area. The received signal for the outdoor part of A1-A7 is mainly coming from scattering and reflecting from Van Leer, while the indoor RSS at B1-B7 is mostly due to signals penetrating through wall B6-G7. The area of M6-N8 is similar to A1-B7.

The wall in area A1-O2 is mainly glass and there is no direct illumination; the Delta Tau Delta

building reflects radio waves into this part of the building. The radio waves for the outdoor B1-N1 area are coming from secondary scattering and reflection from the edge of the Architecture, Van Leer, and Delta Tau Delta buildings. The indoor signal for area B2-N2 is a combination of the outdoor waves traveling through the glass wall and the waves propagating through the building.

3.4.2 Handset RSS Distribution

In our experiment, we found that the information used to discriminate between the indoor and outdoor calls is mainly embedded in the absolute value of the RSS. Accurate distributions of RSS from indoor and outdoor callers can be used to calculate whether a call comes from indoors or outdoors.

Indoor RSS Distribution

This section shows the distribution of indoor power measurements taken from the handset data collection. Based on these handset measurements, we calculated the average RSS over the six strongest channels, which we call the *received signal strength aggregate* (RSSA). Because RSSA measured at a handset is affected by several different factors, such as distance, user head effects, penetration loss of different materials, and measurement noise, we can assume the distribution of summation of the six strongest channels is log-normal. Figure 27 and Figure 28 provide good evidence for this assumption. Figure 28 shows that the log-normal assumption is a good model for the distribution of received signal strength for outdoor handsets. In the indoor case, the second peak results from the nonlinearity of the handset RF chain. The handset can only measure signals with strengths higher than -113 dBm. For all the strength levels lower than or close to -113 dBm, the nonlinearity of the handset RF chain will report several dB higher than the actual received signal. This makes all the data points lower than -110 dBm collapse to -110 dBm and form the small second peak. Despite this effect, the major trend of measurement statistics still matches up to the theoretical distribution.

Based on our experiment, the mean of indoor RSSA is -97.8 dB and the standard deviation is 14.1 dB. The statistics from the measurement and the theoretical distributions are shown in Figure 27.

Outdoor RSS Distribution

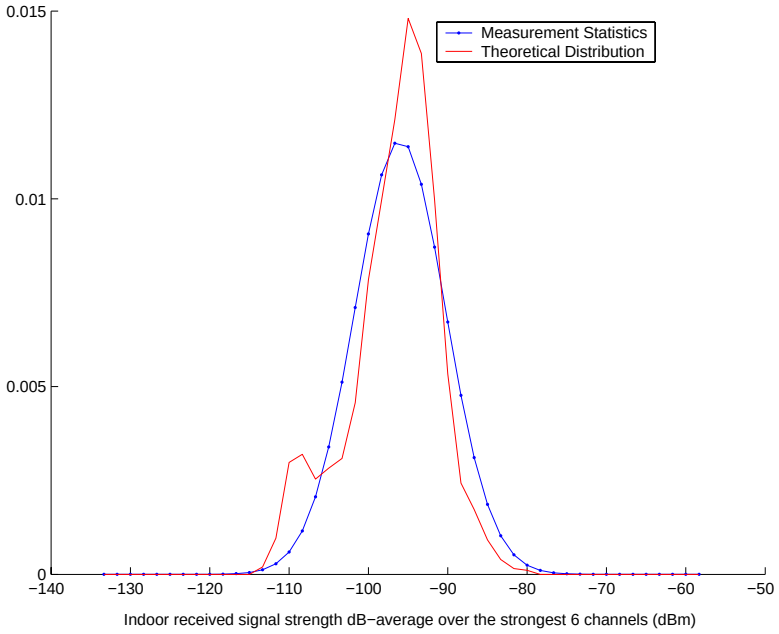

Figure 27: Indoor received signal strength aggregate distribution measured on the Georgia Tech campus.

Based on the handset data, the mean is -85.5 dB and the standard deviation is 9.7 dB. The statistics from the measurement and the theoretical distributions are shown in Figure 28

Indooor/Outdoor Comparison

Figure 29 shows the difference between indoor calls and outdoor calls in side-by-side plots. Interestingly, there is a large standard deviation of indoor RSSA (14.1 dB) compared to outdoor RSSA (9.7 dB). The mean indoor RSSA is 12.3 dB lower than the outdoor RSSA. If gains and losses in the handset RF chain are similar, then it may be possible to discriminate between indoor and outdoor handsets using RSSA.

3.5 Location Performance

3.5.1 Overview of Location Algorithm

This section describes the basic concept of Euclidean distance used to estimate handset location.

Definition of M-Distance—Euclidean Distance

To solve for the location of a handset, we must design an algorithm for matching received signal strength measured by a handset (reported in an NMR) with received signal strength recorded in a PSD. In this experiment, we base our location algorithm on the *Euclidean distance* between a set of

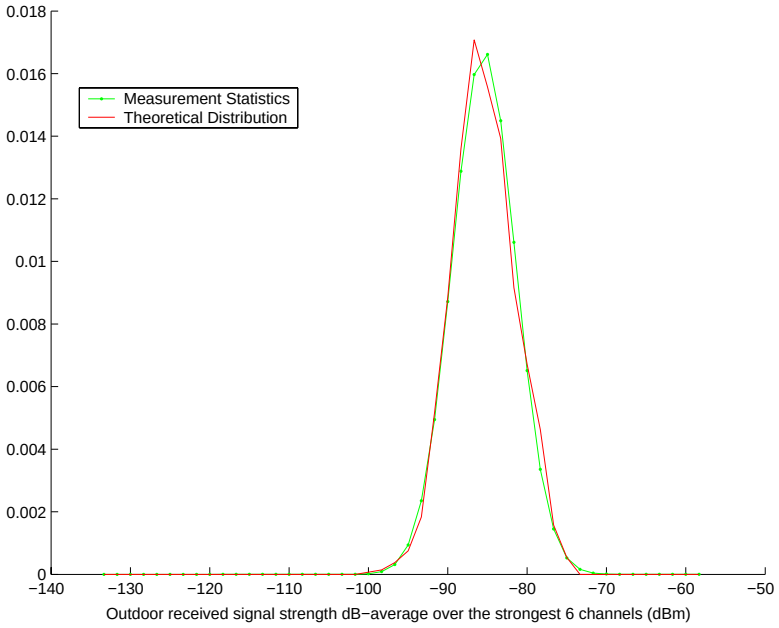

Figure 28: Outdoor received signal strength aggregate distribution measured on the Georgia Tech campus.

measured and recorded signal strengths. We call this the *matching distance*.

Each NMR is like a point in multi-dimensional space. A handset NMR that contains N received signal strength measurements is like a point in N-dimensional space. This is also true for the collection of signal strengths in a PSD. Each physical xy location modeled in the Georgia Tech campus PSDs contains up to 26 received signal strength values, each corresponding to different IS-136 800 MHz control channels. From these values, a location algorithm selects a subset of N values that corresponds to the same control channels present in the NMR. Thus, we need a general formula for calculating the matching distance between two N-length vectors of received signal strength.

If an NMR reports signal strengths from N control channels, then we may represent this measurement as a vector of length N:

$$[Nrss_1\ Nrss_2\ \cdots\ Nrss_N] \tag{27}$$

where $Nrss_i$ is the reported signal strength of the ith control channel. Likewise, we may construct a similar vector for each discrete xy location in a PSD:

$$[Prss_{x,y,1}\ Prss_{x,y,2}\ \cdots\ Prss_{x,y,N}] \tag{28}$$

where $Prss_{x,y,i}$ is the predicted signal strength of the ith control channel at the xy coordinate. The

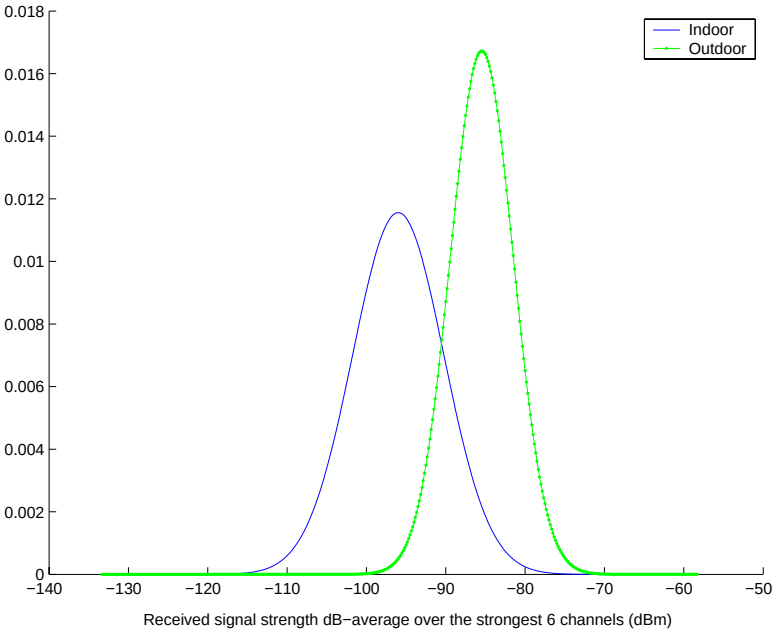

Figure 29: Indoor and outdoor RSSA theoretical distribution.

matching distance M is calculated with the following formula:

$$M_{x,y} = \sqrt{\sum_{i=1}^{N} (Prss_{x,y,i} - Nrss_i)^2} \tag{29}$$

The coordinates xy that yield the lowest matching distance are chosen to be the location estimate.

Metric of Location Performance

To judge the location performance we use the following two standards to measure the accuracy of our system.

- Location Error Statistics
- Indoor/Outdoor Discrimination Rate

Location Error Statistics

The distance in meters between a location estimate and the handset's groundtruth position is the *error distance*. To understand the true performance of any location algorithm, we must study this error distance for many location attempts. The FCC requirements for E911 accuracy place several conditions on the cumulative distribution of error distance. Specifically, the error distance must be less than 100 m 67% of the time and less than 300 m 95% of the time. Thus, for every location

experiment in this study, we calculate and report the percentages of error distance values below 100 m and 300 m.

Indoor/Outdoor Discrimination Rate

For each location estimate, we attempt to discern whether the handset is either indoors or outdoors. We refer to this process as *indoor/outdoor discrimination*. The discrimination *rate* is the percentage of handsets that have been correctly identified as either indoors or outdoors. Indoor/outdoor discrimination is an important piece of information for emergency services.

Dart-Throwing Probability

The reader must keep in mind that discrimination rates may look deceptively successful at first glance. If told that a location algorithm could discriminate between indoor and outdoor users 60% of the time, then one might suppose that this algorithm was somewhat successful. However, one could achieve 50% success simply by flipping a coin. With this in mind, the 60% success rate does not seem nearly as impressive.

To place all reported indoor/outdoor discrimination rates in proper perspective, they must be accompanied by a *dart-throwing probability*. The dart-throwing probability is the success rate for discerning indoor handsets from outdoor handsets by randomly choosing locations on the building footprint map (i.e., "throwing a dart at the map"). Presumably, this is the worst possible method for discriminating the location of handsets.

According to our definition of the discrimination rate, success occurs under two different conditional outcomes of a location experiment: 1) when an indoor handset is detected to be indoors or 2) when an outdoor handset is detected to be outdoors. Furthermore, each of these outcomes must be weighted against the probability of being indoors or outdoors. In mathematical terms, we can write this as

$$\text{Success} = Pr[P = I|M = I]Pr[M = I] + Pr[P = O|M = O]Pr[M = O] \tag{30}$$

$$\text{Error} = Pr[P = O|M = I]Pr[M = I] + Pr[P = I|M = O]Pr[M = O] \tag{31}$$

where M denotes the true (measured) position of the handset and P denotes the predicted position of the handset. The variables M and P both have only two types of outcomes: O for outdoors or I

for indoors. By the conditional probability theorem, we may rewrite these equations as

$$\text{Success} = Pr[P = I \,\&\, M = I] + Pr[P = O \,\&\, M = O] \tag{32}$$

$$\text{Error} = Pr[P = O \,\&\, M = I] + Pr[P = I \,\&\, M = O] \tag{33}$$

In a dart-throwing decision (one made without information), prediction and measurement are independent events and, hence, multiplicative. Thus, the dart-throwing success and failure rates are given by

$$\text{Success} = Pr[P = I]Pr[M = I] + Pr[P = O]Pr[M = O] \tag{34}$$

$$\text{Error} = Pr[P = O]Pr[M = I] + Pr[P = I]Pr[M = O] \tag{35}$$

The calculation for probabilities $Pr[P = I]$ and $Pr[P = 0]$ is based on the fraction of indoor and outdoor geometrical area that exists on a building footprint map, respectively. The calculation for probabilities $Pr[M = I]$ and $Pr[M = 0]$ is based on the fraction of indoor and outdoor groundtruth locations used in the testing.

3.5.2 Performance

In this section we discuss the performance of several different location algorithms. Unless otherwise noted, each NMR is constructed from the eight strongest measured sectors collected from the Ericsson handset.

Absolute RSS Location

The first location algorithm to test is based on absolute signal strength. In the absolute RSS location algorithm, we assume perfect knowledge of the antenna/RF chain bias between the user handset and the scanner used to calibrate the PSD. This bias is removed by subtracting a bias constant from every signal strength reported in the NMR.

$$Nrssc_i = Nrss_i - \text{Bias} \tag{36}$$

where $Nrssc_i$ is the unbiased received signal strength of the *i*th reported control channel. This unbiased set of measurements is then matched to the PSD. The unbiased NMR is used to calculate the matching distance for each raster point, as in Equation 37.

$$M = \sqrt{\sum_{i=1}^{N} (Prss_{x,y,i} - Nrssc_i)^2} \tag{37}$$

The location performance is summarized in Table 5 and Table 6. Without indoor modeling, the experiment shows an abysmal discrimination rate of 32% – statistically equal to the dart-throwing probability. However, when the indoor model is introduced to the PSD, the success rate of in-door/outdoor discrimination jumps to 78%. For a PSD with extensive indoor measurements, this rate improves to 86%. The absolute RSS location algorithm can discern indoor and outdoor handsets admirably with either indoor modeling or measurement.

The error statistics in Table 6 are also promising. In fact, the Level 3 PSD meets the FCC requirements for E911. The Level 1 PSD is sufficiently worse.

Table 5: Discrimination rate of the absolute RSS location algorithm. (Dart-throwing probability of 34%.)

PSD level		Level 1 Outdoor Meas.		Level 2 Indoor Model		Level 3 Indoor/Outdoor Meas.	
		Decision					
		Indoor	Outdoor	Indoor	Outdoor	Indoor	Outdoor
Actual	Indoor	270	2993	2818	454	2837	416
	Outdoor	394	1343	657	1071	270	1477
Correct Rate		32%		78%		86%	

Table 6: Location error statistics of absolute RSS location algorithm.

PSD level		Level 1 Outdoor Meas.	Level 2 Indoor Model	Level 3 Indoor/Outdoor Meas.
Error statistics	<100m	20%	45%	67%
	<300m	60%	90%	95%

Relative RSSI Location

For the relative RSS location algorithm, the measurements in an NMR and the signal strengths in the PSD are normalized before matching. The normalization procedure is described below:

- First, we extract all received signal strength values from the PSD that correspond to the control channels reported in an NMR. This gives us vectors in the form of Equation 28 and Equation 27.

- The mean of each vector in the PSD is calculated in dBm. This mean is subtracted from the vector:

$$Prssr_{x,y,i} = Prss_{x,y,i} - \frac{1}{N}\sum_{j=1}^{N} Prss_{x,y,j} \tag{38}$$

where $Prssr_{x,y,i}$ is the received signal strength of the *i*th control channel at the location coordinates *x* and *y*.

- The mean of the measured NMR vector is subtracted from the measured vector to form a new vector:

$$Nrssr_i = Nrss_i - \frac{1}{N}\sum_{j=1}^{N} Nrss_j \quad (39)$$

where $Nrssr_i$ is the received signal strength reported in the NMR in the *i*th channel.

After normalization, all vectors of received signal strength become independent of any antenna/RF chain bias.

The relative signal vectors from the NMR and PSD are used to calculate the measurement distance for each raster point, as in Equation 40.

$$M(x,y) = \sqrt{\sum_{i=1}^{N}(Prssr_{x,y,i} - Nrssr_i)^2} \quad (40)$$

The smallest measurement distance point (x',y') is the location estimation. Relative RSS algorithms do not require perfect knowledge of the bias of the handset antenna/RF chain, which makes this algorithm more realistic.

The location performance is summarized in Table 7 and Table 8. As Table 7 demonstrates, the relative RSS algorithm cannot discriminate between indoor and outdoor users, regardless of the level of PSD construction. This is not too surprising. Since the bias constant of a handset's RF chain is indistinguishable from the average loss resulting from building penetration, subtracting the mean value gets rid of the most useful piece of information for discerning the position of indoor handsets.

The overall error statistics in Table 8 look promising, however. There seems to be little difference in performance between the three levels of PSD. All three come close to achieving the FCC requirements for E911 in this semi-urban environment.

Hybrid-Method RSS Location

The hybrid-method takes advantage of the robust relative RSS method for locating the handset, but studies the absolute signal value as well to discern indoor/outdoor information. The discrimination algorithm is based on the *received signal strength aggregate* (RSSA) method discussed in

Table 7: Discrimination rate of relative RSS location algorithm. (Dart-throwing probability is 34%)

PSD level		Level 1 Outdoor Meas.		Level 2 Indoor Model		Level 3 Indoor/Outdoor Meas.	
		Decision					
		Indoor	Outdoor	Indoor	Outdoor	Indoor	Outdoor
Actual	Indoor	849	2401	739	2511	1334	1916
	Outdoor	436	1314	417	1333	528	1222
Correct Rate		43%		41%		51%	

Table 8: Location error statistics of relative RSS location algorithm

PSD level		Level 1 Outdoor Meas.	Level 2 Indoor Model	Level 3 Indoor/Outdoor Meas.
Error statistics	<100m	54%	54%	60%
	<300m	94%	94%	95%

Section 3.4.2. After some statistics, we have the knowledge for RSS distribution for the indoor scenario and outdoor scenario, as shown in Figure 29.

By using this information, we can calculate the probability for an active call coming from indoors or outdoors. Refer to Figure 30 for the following discussion.

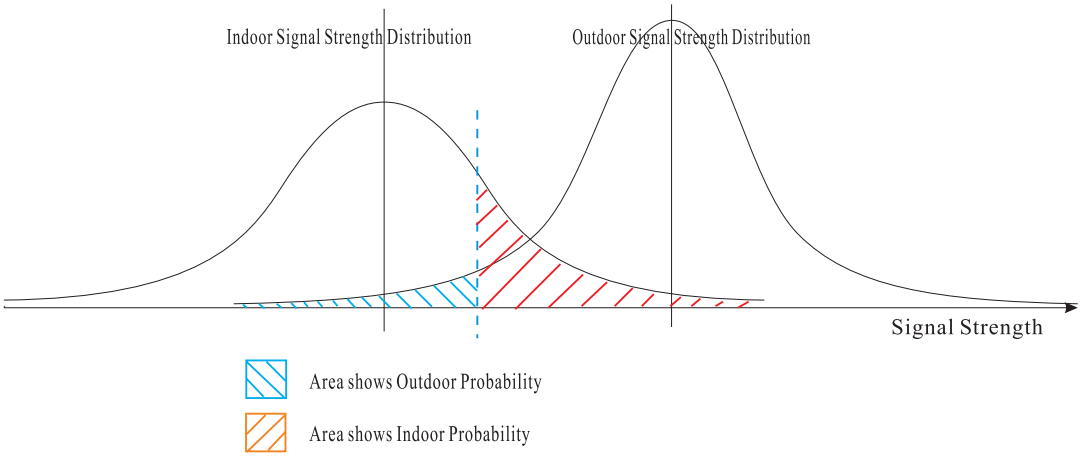

Figure 30: Calculation the probability of indoor call or outdoor call from RSSA.

Let μ_i denote the mean of the sum of the strongest six channels for an indoor handset. Let σ_i denote the standard deviation of this same sum. Let μ_o denote the mean of the sum of the strongest six channels for outdoor handsets. Finally, let σ_o denote the variance of the strongest six channels for outdoor handsets. The distribution of indoor RSSA for the strongest six channels is

$$p(x) = \frac{1}{\sigma_i \sqrt{2\pi}} e^{-(x-\mu_i)^2/(2\sigma_i^2)} \tag{41}$$

The distribution of the outdoor RSS for the strongest six channels is

$$p(x) = \frac{1}{\sigma_o \sqrt{2\pi}} e^{-(x-\mu_o)^2/(2\sigma_o^2)} \tag{42}$$

The probability that the indoor RSSA is greater than a value x is given by

$$P_i(x) = \frac{1}{\sigma_i \sqrt{2\pi}} \int_x^{-\infty} e^{-(x-\mu_i)^2/(2\sigma_i^2)} dx' = \frac{1}{2}[1 - \text{erf}(\frac{x-\mu_i}{\sigma_i \sqrt{2}})] \tag{43}$$

The probability that the outdoor RSSA is less than a value x is given by

$$P_o(x) = \frac{1}{\sigma_o \sqrt{2\pi}} \int_{-\infty}^{x} e^{-(x-\mu_o)^2/(2\sigma_o^2)} dx' = \frac{1}{2}[1 + \text{erf}(\frac{x-\mu_o}{\sigma_o \sqrt{2}})] \tag{44}$$

where erf() is the so-called error function:

$$\text{erf}(z) = \frac{2}{\sqrt{\pi}} \int_0^z e^{-(t)^2} dt' \tag{45}$$

From these equations, we can estimate the probability that a given RSSA is more likely to be indoors or more likely to be outdoors.

The normalization procedure and the location method are exactly the same as in the relative RSS location algorithm.

After the location estimate is made, the RSSA is calculated to decide whether the handset is indoors or outdoors. If the raster point (x,y) is indoors,

$$M_H(x,y) = M(x,y)/P_i(\sum_{i=1}^{N} Nrssr_i) \tag{46}$$

If (x,y) is an outdoor point,

$$M_H(x,y) = M(x,y)/P_o(\sum_{i=1}^{N} Nrssr_i) \tag{47}$$

The point xy with the smallest hybrid measured distance, M_H, is the location estimate.

The location performance is summarized in Table 9 and Table 10. Because the hybrid method uses RSSA instead of PSD information to decide whether a handset is indoors or outdoors, the discrimination rate is the same – 90% – for all three types of PSD. This is quite promising.

The error statistics for this location algorithm are also promising. The Level 1 PSD results in position estimates that are 100 m from groundtruth 56% of the time and 300 m from groundtruth

Table 9: Discrimination rate of hybrid-method RSS location algorithm. (Dart-throwing probability is 34%.)

PSD level		Level 1 Outdoor Meas.		Level 2 Indoor Model		Level 3 Indoor/Outdoor Meas.	
		Decision					
		Indoor	Outdoor	Indoor	Outdoor	Indoor	Outdoor
Actual	Indoor	2895	334	2892	337	2909	320
	Outdoor	167	1604	167	1604	175	1596
Correct Rate		90%		90%		90%	

Table 10: Location error statistics of hybrid-method RSS location algorithm.

PSD level		Level 1 Outdoor Meas.	Level 2 Indoor Model	Level 3 Indoor/Outdoor Meas.
Error statistics	<100m	56%	56%	65%
	<300m	96%	96%	96%

96% of the time. The Level 3 PSD is even closer to the FCC specification. The hybrid-method algorithm seems to have improved both discrimination and error statistics.

Hybrid-Method RSS Location with Averaging

Until now, all location estimates have been performed with single NMRs. However, with several switch modifications at a base station, it is often possible to capture a sequence of consecutive NMRs for position location. The received signal strength in these consecutive NMRs may then be linearly averaged to get rid of any small-scale fading in the handset.

Table 11 and Table 12 show results of a hybrid-method algorithm operating on a linearly averaged set of 10 NMRs. The results are outstanding, as the discrimination rate has climbed to 92% and the error statistics for Level 2 and 3 PSDs satisfy (within statistical error) the FCC safety mandate.

Table 11: Discrimination rate of hybrid-method RSS location algorithm. (Linear averaging of 10 NMRs, dart-throwing probability of 34%.)

PSD level		Level 1 Outdoor Meas.		Level 2 Indoor Model		Level 3 Indoor/Outdoor Meas.	
		Decision					
		Indoor	Outdoor	Indoor	Outdoor	Indoor	Outdoor
Actual	Indoor	637	53	642	48	641	49
	Outdoor	28	282	34	276	44	266
Correct Rate		92%		92%		91%	

Hybrid-Method RSSI Location for Only Six Sectors

The previous algorithm results are based on a total of eight sectors reported in an NMR. This

Table 12: Location error statistics of hybrid-method RSS location algorithm. Linear averaging of 10 NMRs.

PSD level		Level 1 Outdoor Meas.	Level 2 Indoor Model	Level 3 Indoor/Outdoor Meas.
Error statistics	<100m	61%	64%	78%
	<300m	97%	98%	98%

is somewhat below the average number of control channel powers reported in IS-136. GSM, however, is a similar TDMA-style air interface and reports the six strongest sectors. Thus, we repeat the hybrid method analysis for six sectors instead of eight to demonstrate the applicability of the technology for GSM.

Table 13 reports discrimination rates for the single NMR, six-sector case. Each level of PSD has a success rate of 86-87%, which is comparable to the 90% achieved with eight sectors. The error statistics in Table 14 also show similar performance for all three levels of PSD. This performance falls a little short of the US E911 requirements.

Table 15 reports discrimination rates for the case of 10 linearly averaged NMRs with six sectors reporting received signal strength. The values are nearly identical to the single-NMR case in Table 13, suggesting that discrimination performance is unaffected by averaging out small-scale fading. This is not surprising since computing an RSSA in the hybrid method likely averages out fading among the different control channels. The error statistics for the 10-NMR, six-sector case reported in Table 16 are similar to the 10-NMR, eight-sector case in the previous section. This suggests that the strongest six received signals contribute the bulk of accuracy to the overall system performance.

Table 13: Discrimination rate of hybrid-method RSS location algorithm. (Single NMR, 6 sectors, dart-throwing probability of 34%.)

PSD level		Level 1 Outdoor Meas.		Level 2 Indoor Model		Level 3 Indoor/Outdoor Meas.	
		Decision					
		Indoor	Outdoor	Indoor	Outdoor	Indoor	Outdoor
Actual	Indoor	2761	490	2762	489	2813	438
	Outdoor	197	1552	190	1559	220	1520
Correct Rate		86%		86%		87%	

Pure Outdoor Location Performance

To understand how much RSS location degrades for an indoor environment, we also run the RSS location engine with pure outdoor handset data and compare results with the cases above, in

Table 14: Location error statistics of hybrid-method RSS location algorithm. (Single NMR, 6 sectors)

PSD level		Level 1 Outdoor Meas.	Level 2 Indoor Model	Level 3 Indoor/Outdoor Meas.
Error statistics	<100m	52%	53%	57%
	<300m	93%	93%	93%

Table 15: Discrimination rate of hybrid-method RSS location algorithm with averaging. (Linear averaging of 10 NMRs, 6 sectors, dart-throwing probability of 34%.)

PSD level		Level 1 Outdoor Meas.		Level 2 Indoor Model		Level 3 Indoor/Outdoor Meas.	
		Decision					
		Indoor	Outdoor	Indoor	Outdoor	Indoor	Outdoor
Actual	Indoor	610	72	618	64	620	62
	Outdoor	57	261	62	256	67	251
Correct Rate		87%		87%		87%	

which the experimental handset database consists of two-thirds indoor sample points. This pure outdoor location is run under the same conditions as the experiments summarized by Table 15 and Table 16 (linear averaging of 10 NMRs, six sectors of data, Hybrid location method).

Table 17 shows solid indoor/outdoor discrimination performance between 93% and 94%. Table 18 shows that *every level of PSD is capable of meeting the FCC E911 requirements.*

3.6 Conclusions

The results in this preliminary research demonstrate the feasibility of RSS location techniques to meet the FCC's requirements for E911 accuracy. The techniques remain accurate even when the majority of test data is from *indoor* handsets. Since most mobile phone calls are now placed from inside buildings, the inclusion of indoor data in any evaluation of an E911 location system is absolutely necessary. Although the vicissitudes of indoor radio wave propagation degrade the performance slightly, much of the accuracy can be recovered through a number of techniques presented in this report: averaging multiple NMRs, modeling indoor propagation, calibrating RF maps with indoor

Table 16: Location error statistics of hybrid-method RSS location algorithm with averaging. (Linear averaging of 10 NMRs, 6 sectors.)

PSD level		Level 1 Outdoor Meas.	Level 2 Indoor Model	Level 3 Indoor/Outdoor Meas.
Error statistics	<100m	62%	63%	70%
	<300m	96%	96%	96%

Table 17: Discrimination rate of hybrid-method RSS location algorithm. (Linear averaging of 10 NMRs, 6 sectors, pure outdoor.)

PSD level		Level 1 Outdoor Meas.		Level 2 Indoor Model		Level 3 Indoor/Outdoor Meas.	
		Decision					
		Indoor	Outdoor	Indoor	Outdoor	Indoor	Outdoor
Actual	Outdoor	741	4259	807	4193	885	4115
Correct Rate		93%		93%		94%	

Table 18: Location error statistics of hybrid-method RSS location algorithm. (Linear averaging of 10 NMRs, 6 sectors, pure outdoor.)

PSD level		Level 1 Outdoor Meas.	Level 2 Indoor Model	Level 3 Indoor/Outdoor Meas.
Error statistics	<100m	68%	68%	74%
	<300m	97%	97%	97%

measurements, and trying different location algorithms.

Even more interesting is the unique ability of an RSS location engine to discriminate between indoor and outdoor handsets. This could prove to be a very important additional piece of information when dispatching help to the scene of an emergency. The highest success rate for indoor/outdoor discrimination in this experiment was 92%, although this number may be optimistic if there is a wild variability in the RF chains of commercial handsets. The variability of measurement bias in commercial handsets should be investigated further.

Although the results in this preliminary research were developed on a live IS-136 cellular network at 850 MHz, the performance is likely similar to other cellular telephony air interfaces (GSM, CDMA, WCDMA, etc.) and other carrier frequencies. Future work for these techniques should concentrate on accurate propagation modeling and measurement, which enhance location performance regardless of air interface. Propagation modeling will be increasingly important as RSS location systems are deployed. Accurate propagation models reduce the time and cost of extensive drive-testing and also catch modifications to coverage when the cellular network undergoes optimization or build out. Good propagation practice undergirds this entire technology.

CHAPTER IV

EXTENDED RESEARCH: GREENVILLE, SC

Though the preliminary research has proven that the RSS location method is an effective technology in the Georgia Tech campus on an IS-136 digital TDMA network, it is essential to study the performance of an indoor/outdoor RSS-based location engine in other wireless environments. The preliminary research on the Georgia Tech campus had a limited average cell size of 500 m and a relatively small testing area of 2000 m by 2500 m. The limited average cell size puts an upper bound on the egregious errors that could occur in a larger cell. This limited test area removes a lot of ambiguities that would exist in a larger network, especially for a wireless network with more cells and fewer control channels, which introduce a more intensive frequency reuse pattern. The performance of RSS has never been reported in a much larger area with fewer neighbors available. To extend our research to a more general case with more comprehensive results and to provide a general idea about the RSS-based location engine performance, additional indoor/outdoor location research was conducted in Greenville, SC, on a GSM network, the most popular cellular air interface protocol in the world.

The GSM network in Greenville has longer average base station separation distances, around 2000 m. The location performance is expected to drop compared to the Georgia Tech location trial. The results will provider a better idea of how well an RSS-based location engine works for wireless networks with different cell size by interpolating between the Georgia Tech location results and the location results from the Greenville experiments. The results will also examine the performance of the indoor location engine for high-rise buildings.

The results in this extended study show that the RSS location technique itself cannot satisfy the FCC E911 requirements for a cellular network with a cell size as large as 2000 m. The tabulated performance results of the location engine are discussed in detail in Section 4.6.3 using a relative RSS method with a new search-area limiting algorithm, a sequence of 10 network measurement reports, and RF maps calibrated with both outdoor and indoor measurements. The error distance

in this case is less than 100 m 51% of the time and less than 300 m 79% of the time. The location algorithm must be improved to meet FCC E911 requirement for a stand-alone system, but the result shows excellent potential for cellular networks with large munbers of *indoor* callers.

4.1 Key Output

This extended experimental in Greenville, SC, produced several key outcomes

1. Several algorithms using extra information in NMR are suggested. The location test confirms that significant accuracy improvement is achieved.

2. This study reports the GPS signal availability for both indoor and outdoor environments.

3. This study analyzes the vertical coordinate effect on RSS in multi-floor buildings and develops an elevation-dependent propagation model.

4. This study shows that the performance of the current RSS signature location method in rural areas with low cell density is not sufficient to meet FCC E911 mandates. This suggests that a hybrid solution of RSS location and handset-based GPS may work best for public safety applications.

4.2 Measurement Plan

All measurements were taken in Greenville, SC, in the area surrounded by the box in Figure 31. This 7000 m by 9000 m region was selected as the experimental test area. In this large area, nine small test areas (test spots), and over 50 buildings were measured. Nearly 90,000 active call network measurement reports (NMRs) were recorded from the Ericsson TEMs handset.

The distance between base stations in Greenville was approximately 1700-2000 m. Twenty-four macrocells exist in the testing area. Another 24 macrocells exist in the surrounding area. The building construction style varies from steel and concrete with brick surfaces to wood frame and pre-fabricated mobile home units. Terrain in the Greenville area is relatively flat with small hills, but becomes mountainous outside the suburban area.

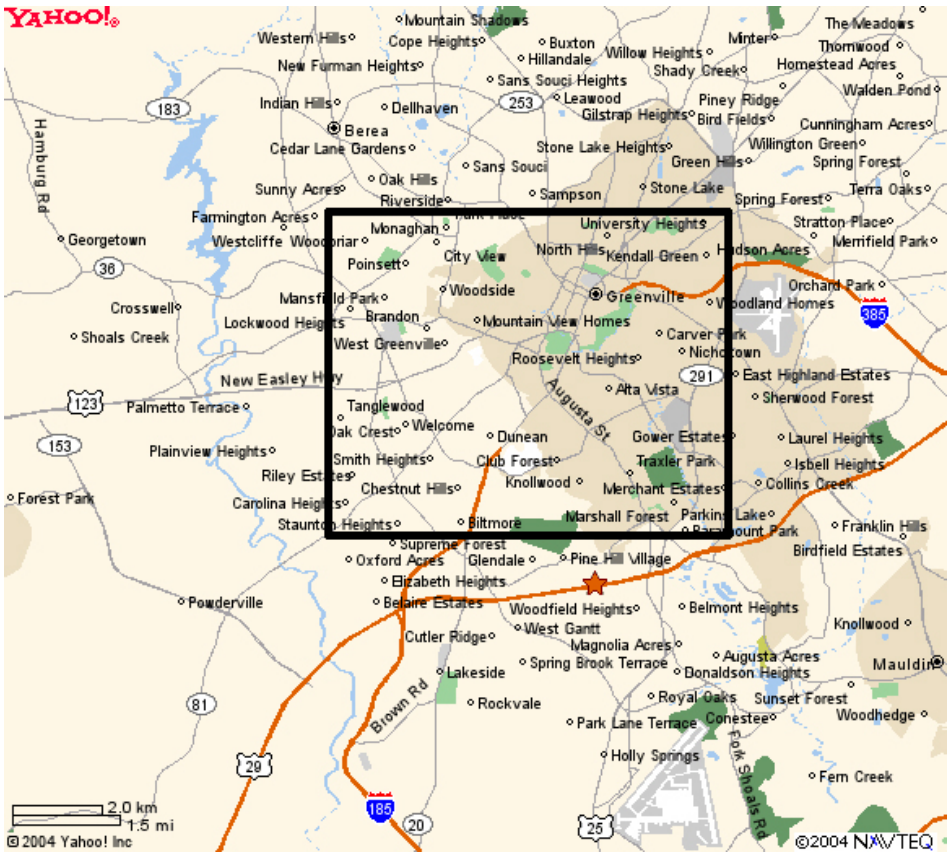

Figure 31: The 7000 m by 9000 m test area in Greenville, SC.

4.2.1 Setup Overview

The measurements were performed with an Ericsson's TEMS measurement unit. The scanner data was collected by running the measurement handset in scanner mode and using an external whip antenna, which has a higher gain than the handset antenna. This antenna was placed on top of the moving car during collections. The scanner data is used to calibrate the predicted signal database (PSD). The handset active call data was collected by the same TEMS unit but with the handset antenna—a short whip connected to the phone instead of the longer drive-test whip antenna.

To measure as much area as possible, drive-test measurements, outdoor walking measurements, and indoor walking measurements were taken. The drive-test measurements were used to construct a calibrated RF map database. These measurements provide a fast way to measure across a large outdoor area. The walking measurements collected active call network measurement reports and filled in regions in the PSD that the drive-testing could not access.

4.2.2 Equipment and Calibration

Ericssion TEMS Unit The Ericssion TEMS is a portable device for RF scanning and active call measurement. The hardware components of the system include one Ericsson TEMS handset, a Garmin GPS V, and a laptop with two serial ports. The total weight of this system is about 7 lbs. The scanning function of this TEMS unit was used to collect data for PSD calibration. We programmed the 30 channels (Absolute Radio Frequency Channel Number 512-526 and 786-800) to correspond with the base stations around the test area in Greenville, SC. The Ericssion TEMS unit also provides the function to record the active call data, which includes network measurement reports (NMRs). This active call function is used to collect NMRs for testing the performance of the RSS location engine.

Calibration Procedure A standard free-space calibration procedure was employed on each day of RF measurement to monitor the integrity and consistency of the test system. The calibration consisted of spatially averaged power measurements taken in an outdoor area without large obstacles in the nearby area. The calibration data was taken at the start and the end of each day. The spatially averaged power measurements were compared to verify the consistency of the RF equipment and to monitor any cellular network change at the calibration area.

For the period Dec 13, 2004 to Dec. 17, 2004, the calibration was performed in front of the parking lot of the Budget Inn at 10 Mills Avenue, Greenville, SC, 29605. For the day of Dec. 23, 2004, the calibration was performed in the parking lot of the shopping mall at 3401 W. Blue Ridge Drive, Greenville, SC, 29611. For the peroid Dec. 29, 2004 to Dec. 31, 2004 the calibration was performed in front of the parking lot of the Valu-Lodge Inn at 107 Duvall Drive, Greenville, SC, 29607.

The basic calibration procedure for the RSSI measurement system was as follows:

1. Define Calibration Paths: The calibration path should be selected in an outdoor open area without any large or mobile obstacles. The surroundings of the selected calibration area should be relatively open and have good vision to the sky in all directions. The path of the calibration is a straight line of length 30 m from start point A to end point B, whatever the orientation. The calibration route is large enough to provide a variety of RSSI measurements

within a local area, but small enough not to introduce significant large-scale variations in the average RF power.

Figure 32: Photograph of TEMS unit setup view.

2. System Setup: To begin a day of measurements, the RF measurement system was connected according to the diagram in Figures 32 and 33. The handset should be held vertically and over the field engineer's head to avoid any head-shoulder shadowing effects. The Garmin V GPS antenna should also be held above the shoulder, set at a vertical orientation, and kept free from obstacles to 80% of the sky. The laptop was held in front of the field engineer's chest in a custom harness.

3. Acquire Data: The equipment is set to measure using the handset. Data is acquired by moving slowly from start point A toward end point B and then returning to point A. This sequence is repeated three times. Movement during calibration is slower than 1.3 miles per hour to ensure that sufficient amounts of data are logged.

4. Post-processing: The data is then immediately downloaded to a computer for analysis. For every dedicated control channel (DCCH) measurement, the RSSI values taken around each calibration route are linearly averaged to produce a single average signal strength measurement in dBm free from small-scale fading effects. Four checks for the DCCH records with

Figure 33: Photograph of TEMS unit connection view.

RSSI values higher than -105 dBm are performed at this point in the procedure:

[a] Long-Term Consistency Check: The average RSSI values are compared with those taken on previous days. If RSSI values differ from previous measurements by +/- 3 dB, a thorough system check is performed.

[b] Short-Term Consistency Check: For an end-of-day calibration, average RSSI values are compared to the start-of-day calibration.

[c] GPS Position Check: GPS operation is verified by comparing the readings to previous GPS measurements.

[d] Record and Save Average RSSI Values: The average values are dated and recorded for future use. In constructing an RSSI database that uses measurements spanning multiple days, it may be necessary to normalize each day's measurements against the calibration measurements.

5. Repeat Procedure: The calibration procedure is repeated using the identical procedure at the end of a measurement day.

6. On-site Check: The following procedure should be performed before taking measurements at any location:

[a] Clock synchronization check: Since the time stamp is the only link between NMRs and the GPS fix program, the synchronization between the TEMS system clock and the laptop system clock should agree, with less than 1 second of difference.

[b] Active call check: Run the script to repeat dialing 611 for customer service to get continuous active call network measurement reports.

[c] Record file size check: Once the system begins recording a file, the record file size should keep increasing. Begin data collection after the recording file size is larger than 18 kB to ensure that the TEMS software is setup correctly.

By going through the calibration procedure, a network frequency optimization was instantly detected on Dec. 17, 2004. DCCHs at testing areas were changed from Absolute Radio Frequency Channel Number (ARFCN) 786-800 to ARFCN 512-526. Section 4.5.1 discusses how this change was accommodated in the experiment without having to re-collect a week's worth of data.

4.3 Data Collection

The Greenville test zone contains a mix of urban, suburban, and rural areas. The measurement campaign lasted for three weeks (Dec. 13,2004 -Dec. 31, 2004). The major sources of error for this analysis include the following: 1) old Geographic Information System (GIS) data, 2) Global Positioning System (GPS) errors in data logging, and 3) compensation for a major frequency plan change that occured in mid-campaign.

4.3.1 Building Construction

Building material and the design of exterior walls determine the penetration loss experienced by radio waves that enter a building. This penetration loss information is very useful in discriminating between indoor and outdoor calls. In the previous Georgia Tech campus experiment, the penetration loss for typical urban office buildings from a statistical point of view was reported to be 12.3 dB [43]. The buildings set in this Greenville experiment are quite different from the Georgia Tech campus buildings, which were mainly steel, concrete, and brick. The building materials at Greenville are mainly brick and concrete in the downtown area and partially modular units and wood in other areas.

4.3.2 Frequency Plan Change

A new complication to the Greenville experiment was the mid-measurement frequency plan change made by the local cellular carrier. Our subsequent compensation for this change demonstrates that real-life network modifications can be considered through data adjustment and software without having to re-collect existing data.

The DCCH channels were changed during the measurement campaign on Dec 17, 2005. This frequency plan change was applied to the entire network. DCCHs originally at ARFCN 786-800 range were moved to ARFCN 512-526 by the carrier, a 55MHz change in carrier frequency in the 1920 MHz band. This network optimization change was limited to the DCCH frequency plan only. No tower transmit powers were reassigned. One drive-test was performed before the frequency plan change on Dec 16, 2004 and another drive-test was performed after the frequency change on Feb 01, 2005.

4.3.3 Drive-Test Measurement

Drive-test measurements were used to calibrate the PSD. The procedure is similar to the drive-test measurements conducted by wireless service providers to optimize their network. The TEMS unit was placed in a vehicle with an external scanner whip antenna mounted on the vehicle rooftop. A GPS antenna was also placed on the rooftop of the vehicle. RSS information from ARFCN 512-526 and ARFCN786-800 was collected in the testing area. Two drive-test measurements were taken in this measurement campaign. The first one occurred before the frequency plan change, the other one after the change.

Figure 34 and Figure 35 show the routes of the drive-test measurements. Data was collected on all highways and major roads within the test area. Only a portion of minor streets were driven, although all streets in the downtown urban section were driven at least once.

Figure 34: Drive-test measurement routes collected on Dec. 16, 2004, in Greenville, SC.

4.3.4 Walking Measurement

Because the drive-test measurements are limited to roadways, the RSS inside a building or on a pedestrian path cannot be measured. Walking measurements become the key for filling in the gaps in the RF maps database (also called PSD). The field engineer must walk and collect data both inside and outside a building while holding the handset in a realistic position to make the RSS have the same propagation features as an active call made by a cellular phone customer. Thus, this active call data contains polarization, body shadowing, and small-scale fading effects.

The outdoor walking measurements collect the RSS and serving cell information in the form of an NMR. Most importantly, the outdoor walking measurements may contain a GPS fix reported from the Garmin GPS V unit with accuracy better than 10 m. These outdoor walking measurements can be used to verify the GPS correction for walking measurements made inside adjacent buildings. All the NMRs collected during the outdoor walking measurement were split into two groups: one group to calibrate the PSD and the other group to test the RSS location. These groups of data are kept separate so that we are not testing the location engine with the same data used to calibrate it, thereby making the results seem overly optimistic.

Figure 35: Drive-test measurement routes collected on Feb. 01, 2005, in Greenville, SC.

Because the outdoor walking measurements are primarily meant to assist indoor GPS corrections and help in penetration loss calculations, they have two requirements: 1) they must be performed under a clear sky condition (if possible) to provide a good satellite channel for the GPS unit to have an accurate location fix and 2) they must follow a pedestrian style walk while the field engineer maintains the posture of a typical cell phone call with handset pressed to head.

Figure 36 and Figure 37 show photographs of typical outdoor walking measurements.

Figure 36: Georgia Tech student research Albert Lu and Jian Zhu take an outdoor walking measurement.

Figure 37: Georgia Tech student research Albert Lu and Jian Zhu take an outdoor walking measurement.

The indoor walking measurements collect NMRs for calls originating indoors. Because there is no open-sky condition, the GPS unit is not providing any location fix during the indoor walking measurement. The GPS fix program "GPSFixerV3.fig" was used to correct the GPS location by converting the selected path on an aerial photograph of the test spot into a GPS location fix. Thus, all of our indoor data is stamped with a precise longitude and latitude.

Figure 38 and Figure 39 show typical outdoor walking measurements.

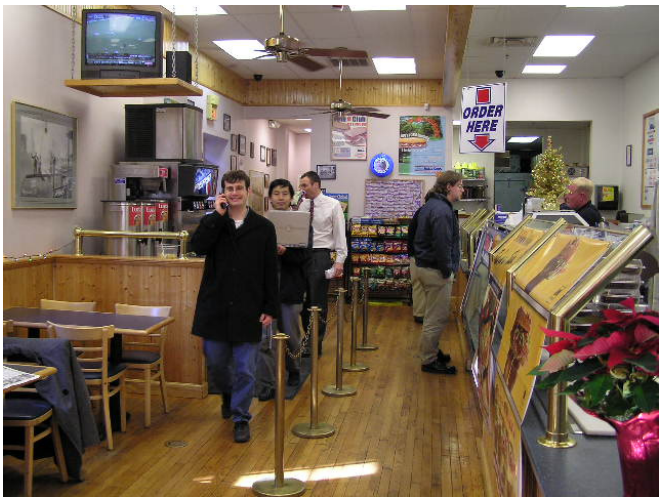

Figure 38: Georgia Tech student research Jian Zhu and Professor Gregory Durgin take a walking measurement in a downtown Greenville eatery.

The following procedure for indoor measurement should be followed to ensure accurate data

Figure 39: Georgia Tech student research Jian Zhu and Professor Gregory Durgin take a walking measurement on the 9th floor of an office building.

collection:

1. Decide a measurement route in each room that covers most of the area, space permitting.
2. Move at a constant speed. If the route is less than 10 m, move backward and forward several times to make sure the measurement time lasts at least 30 seconds.
3. Mark the route on a map in real time at each turn point.
4. Repeat steps 1-3 for all routes within the same building.
5. Walk around the outdoor perimeter and mark down the outdoor route in realtime for GPS correction verification.

4.3.5 GIS Data

The principal source of GIS in the study is a high-resolution database of aerial photographs of the city of Greenville. This GIS image contains photographic pixels with 1 m $\times$ 1 m resolution. The image was constructed in 1994 – nearly 10 years prior to the measurement campaign. Some of the buildings are not on this image and some buildings have been replaced.

Ths source of this GIS data is Terra Server USA at terraserver-usa.com. Small map pieces are downloaded in 200 m by 200 m size and reassembled to form an aerial photograph for the entire test region.

4.4 Data Analysis

4.4.1 Angle-Related Penetration Loss

This section presents the methodology for modeling losses for cellular radio waves of 1920 MHz penetrating buildings.

Building Selection

Nearly 50 buildings were measured for penetration loss. However, some types of buildings are relatively low-loss and may not even be considered truly "indoors." Fast-food restaurants are an excellent example of this building type. They are small, single-roomed structures with transparent glass walls on nearly all sides. The buildings' low penetration loss makes it difficult to identify these locations as indoors. Fortunately, in terms of public safety and E911, there is no advantage to identifying these locations as indoors. Thus, all fast-food type buildings were removed from the data set used to calculate model parameters. The big-window buildings have very low penetration loss, while the raster map of indoor locations cannot distinguish the small building footprints for their different incidence angles. All buildings that are smaller than a raster point were classified as normal incidence by our GIS processing program.

Manual Corrections to Indoor Analysis

Extracting model parameters from Greenville, SC, proved extremely difficult because of some skewing and misalignment in the GIS data. When compared to geo-referenced data, even 1 pixel of misalignment can destroy the accuracy of the analysis because orientation dependence cannot be confidently matched to a measurement. Note that this problem only exists for measurement *analysis* and not penetration loss *prediction*. A slightly skewed GIS map used for predicting penetration loss would not seriously degrade a map or a location algorithm. Because the experimental area is 7 km by 9 km - much larger than the experimental area in the Georgia Tech TDMA experiments - misalignment among indoor measurements, outdoor measurements, and indoor building footprints is more frequent and challenging. This misalignment is fatal when the measured buildings are small because the misalignment may shift the outdoor measurements from one side of the building to the other side. To avoid these serious errors, the corresponding indoor measurement points and outdoor measurement points were manually studied and classified; the incidence angle was manually measured and entered into a database.

Octant Penetration Values

Extensive measurements were performed in Greenville, SC, on the GSM 1920 MHz network. Table 19 reports the octant-dependent penetration loss for the indoor buildings in Greenville, SC. The lowest penetration loss is 15.6 dB and the highest penetration loss is 20.0 dB, a difference of 4.4 dB. Compared to the penetration loss on the 850 MHz TDMA network on the Georgia Tech campus, the 1920 MHz propagation into buildings appears to be lossier and shows a stronger dependence on building incident angle.

Table 19: Octant penetration values.

Octant	1	2	3	4	5
Loss (dB)	16.0	16.9	17.9	20.0	15.6

Octant 5 shows a consistent, anomalous behavior. Previous experiments have shown that, due to backscattering, this penetration loss should drop compared to octant 4. The loss in octant 5, however, drops so significantly that it is less lossy than octant 1. This behavior can be explained by the influence of scatterers around the buildings and the shadowing that occurs outdoors on the back sides of buildings. This behavior indicates a need to modify the simple indoor propagation model to include the effects of the surroundings.

4.4.2 Handset RSS Distribution

Just as in the previous location experiment on the Georgia Tech campus, the information used to discriminate between the indoor and outdoor calls is mainly embedded in the absolute value of the RSS. *Received signal strength aggregate* (RSSA) was used to decide whether a call comes from an indoor or outdoor location.

Indoor RSS Distribution RSSA is defined as the linear average RSS over the six neighbor DCCH channels [43]. The RSSA is assumed to be log-normally distributed. Figure 40 shows the comparison between the theoretical log-normal assumption and the statistical result. The biggest discrepancy between the empirical distribution and the empirical log-normal distribution is the noise floor of the handset RF chain. The handset can only measure signals with strengths higher than -109 dBm, and the linearity for the signal with strengths between -109 to -100 dBm is poor. For the indoor case, the peak at -107 dBm is mainly the result of this noise floor.

Based on our experiment, the mean of indoor RSSA is -96.0 dB and the standard deviation is 7.1 dB. The statistics from the measurement and the theoretical distributions are shown in Figure 40.

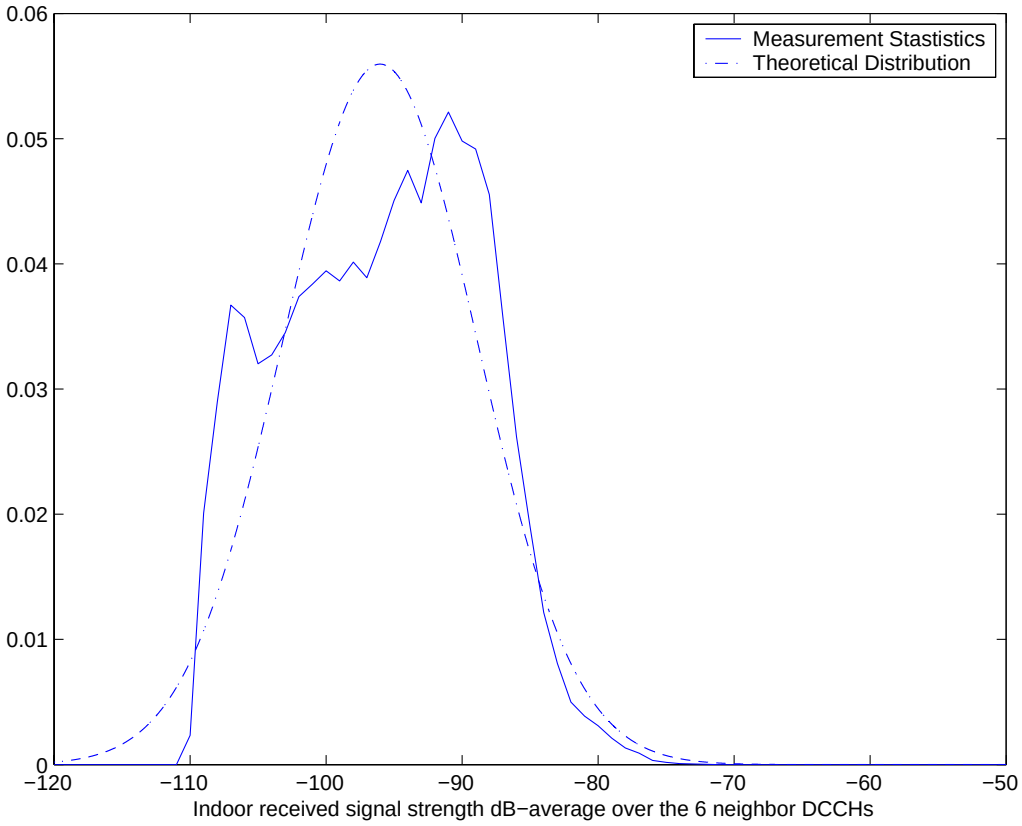

Figure 40: Indoor received signal strength aggregate distribution measured in Greenville, SC.

Outdoor RSS Distribution The local peaks at -101 and -110 dBm are also the results of the noise-induced nonlinearity of the handset RF chain.

Based on the active call data, the mean outdoor RSSA is -86.7 dBm and the standard deviation is 5.6 dB. Figure 41 shows the empirical distribution for outdoor RSSA.

Indooor/Outdoor Comparison Figure 42 shows the difference between indoor calls and outdoor calls in side-by-side plots. Recall that there is a large standard deviation of indoor RSSA (14.1 dB) compared to outdoor RSSA (9.7 dB) in the Georgia Tech campus measurement campaign. The trend of a large standard deviation of indoor RSSA (7.1 dB) compared to outdoor RSSA (5.6 dB) is also observable in the Greenville measurement campaign. The mean indoor RSSA is 9.4 dB lower than the outdoor RSSA, which is a smaller difference than that observed in the Georgia Tech campus

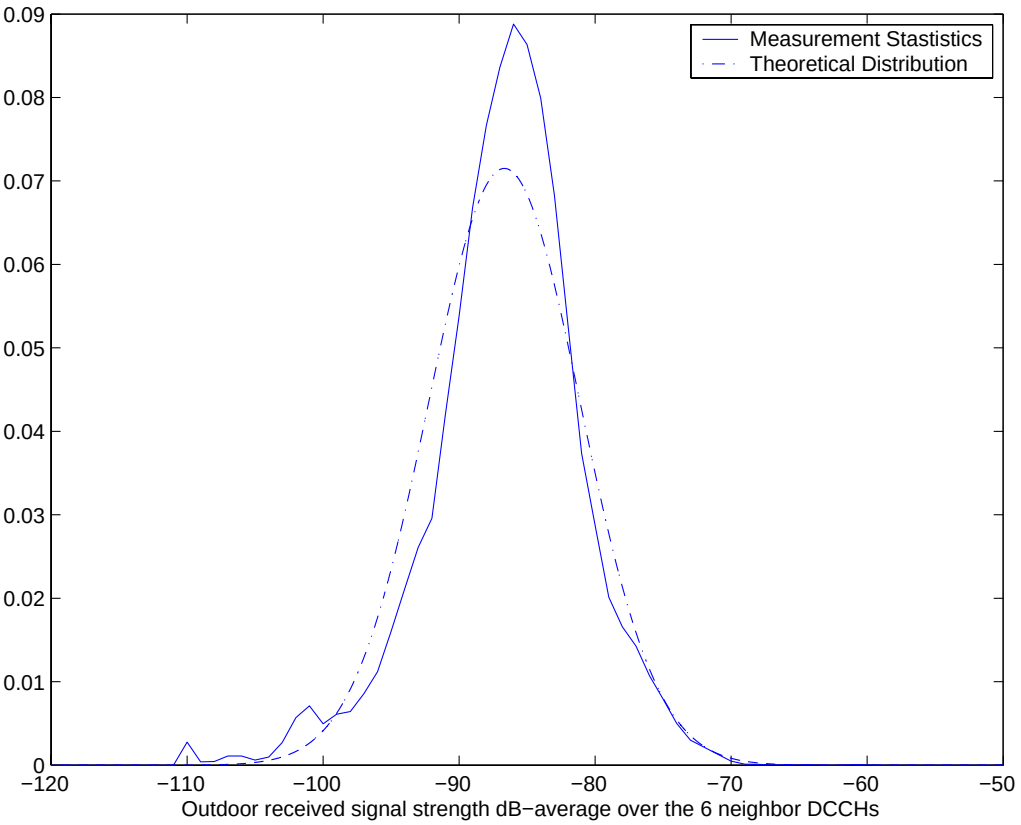

Figure 41: Outdoor received signal strength aggregate distribution measured in Greenville, SC.

campaign (12.3 dB). There are several reasons for the difference. First, the building construction materials are different. Most of the buildings on the Georgia Tech campus are made of brick and concrete. The buildings in the Greenville measurement campaign are made of mixed materials such as modular pieces and wood as well as brick and concrete. Second, the difference between the RF chains of GSM vs. IS-136 handsets may also lead to discrepancies. Third, the carrier frequency was 850 MHz for the Georgia Tech campus measurement and 1920 MHz for the Greenville measurements; this difference is likely large enough to change large-scale path loss characteristics.

4.4.3 Indoor/Outdoor Discrimination Rate

Based on the RSSA theoretical distribution, the threshold (x_{th}=-91.8 dBm) is calculated in Equation 48:

$$\frac{1}{\sqrt{2\pi}\sigma_i} e^{-\frac{(x_{th}-\mu_i)^2}{2\sigma_i^2}} = \frac{1}{\sqrt{2\pi}\sigma_o} e^{-\frac{(x_{th}-\mu_o)^2}{2\sigma_o^2}} \quad (48)$$

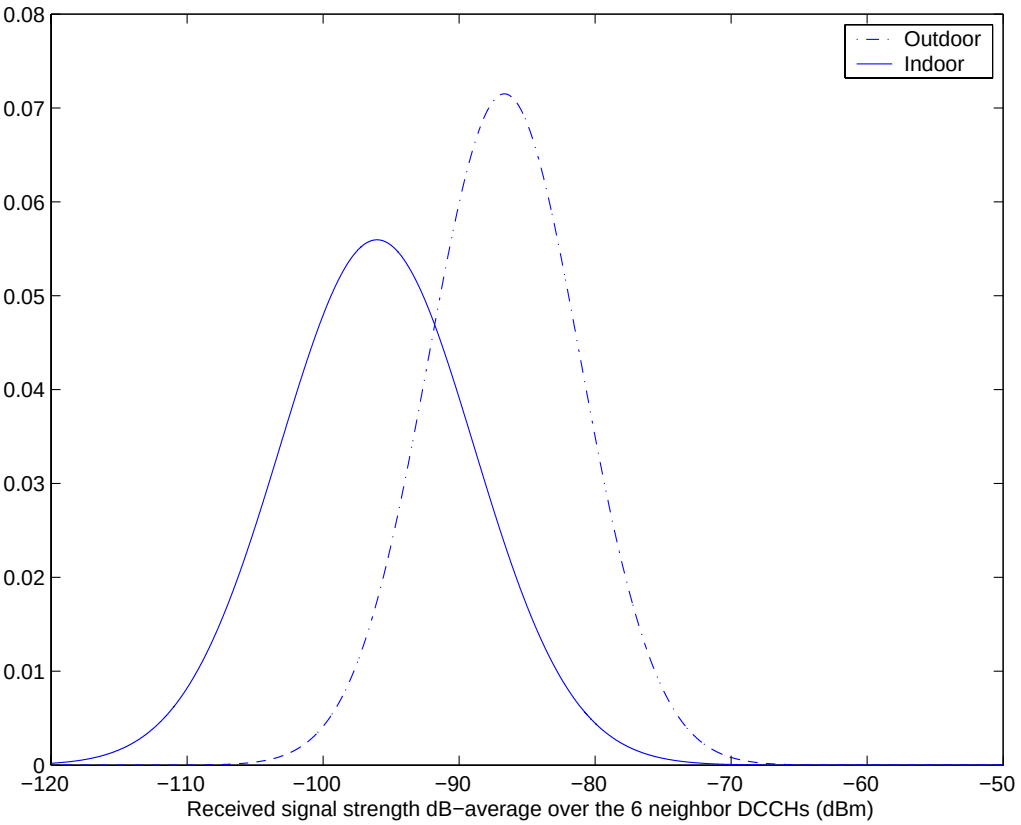

Figure 42: Indoor and outdoor RSSA theoretical distribution.

The decision of indoor/outdoor is made by comparing RSSA with the threshold. If the RSSA is lower than the threshold, the decision is "indoor." Otherwise, the decision is "outdoor."

Table 20 shows that the proposed discrimination method made correct decisions 76% of the time, which is the number of indoor test points that were correctly identified (35.9%) plus the number of outdoor points that were also correctly identified (40.1%).

Table 20: Discrimination rate by using handset RSSA distribution. The number 26,576(35.9%) means there are 26,576 indoor measurements were correctly decided indoors. The number at 12,690 (17.1%) means 12,690 indoor measurements were mistakenly decided outdoors

		Decision		Sub-Total
		Indoor	Outdoor	
Actual	Indoor	26,576 (35.9%)	12,690 (17.1%)	39,266 (53.0%)
	Outdoor	5,140 (6.9%)	29,719 (40.1%)	34,859 (47.0%)
Correct Rate		76%		

4.4.4 GPS Effectiveness

Global Positioning System (GPS) is an accurate location technology that provides location fixes with less than 10 m of two-dimensional error in the best-case scenarios. However, these best-case scenarios require line-of-sights from the GPS receiver to several GPS satellites. Such conditions generally do not exist for indoor cases and are infrequent outdoors when the GPS receiver is close to a building or comparable shadower. This means that conspicuous position errors may exist even if a GPS location fix is reported by the hardware.

A Garmin GPS V device was used in our experiment to provide GPS location information. The Garmin GPS unit updates location fixes every 2 seconds. Because the Garmin GPS V unit cannot always get a GPS fix, the GPS correction program "GpsFixerV3" was written to fill the GPS information.

Our experiment took measurements inside a building as well as the outside perimeter of the building. Among all the outdoor data points, 9.2% of the NMRs do not have a location fix from the Garmin GPS unit. That means that the GPS unit is less than 91% effective outdoors when it is close to a building. As for the indoor cases, the GPS unit is only 10.4% effective. Table 21 and Table 22 show the GPS effective statistics.

Table 21: Garmin V GPS effective statistics based on 60,624 indoor and outdoor measurement records.

	GPS valid	GPS not valid	Sub-total
Indoor	4,069 (6.71%)	35,197 (58.06%)	39,266 (64.77%)
Outdoor	19,394 (31.99%)	1,964 (3.24%)	21,358 (35.23%)
Sub-total	23,490 (38.70%)	37,161 (61.30%)	60,624 (100%)

Table 22: Garmin V GPS effective statistics. Percentages are compared with indoor or outdoor separately.

	GPS valid	GPS not valid	Measurement Count
Indoor	10.36% (4,069)	89.64% (35,197)	39,266(100%)
Outdoor	90.8% (19,394)	9.2% (1,964)	21,358(100%)

During each field measurement, we measured indoor locations first, followed by a measurement of the outdoor perimeter of that building. Considering the satellite acquisition time for GPS, our statistics may be biased toward poor outdoor GPS effectiveness. Considering the "guess" ability of the Garmin V GPS, which uses the last known GPS location when a full satellite fix is unavailable,

our statistics may be biased toward optimistic indoor GPS effectiveness.

Another issue is that the above statistics were measured by a commercial Garmin V unit which is especially designed to acquire and maintain GPS location. It was designed to optimize the GPS estimate from the single-band antenna and RF-chain. This optimized structure does not exist in a GPS-enabled handset. On the other hand, a cellular handset GPS receives synchronization and ephemeris information that the Garmin unit does not have. Thus, Table 21 and Table 22 are only a rough guide to handset-based GPS performance.

4.4.5 RSS in High-rise Building

This section discuss the relationships between RSS and vertical position within a high-rise building. There are only a few high-rise buildings in Greenville and access is limited. We received access to two office buildings that are more than 10 stories in downtown Greenville. One of them has 18 floors and the other one has 12 floors. Active call data was collected in the stairwells of both buildings and on selected floors. Scanner data was also collected in the second stairwell of the 18-floor building.

Figures 43–45 show the relationship between the floor number and the received signal strength aggregate (RSSA). A clear trend of higher RSSA for higher floor level is apparent. In Figure 43, the lowest three floors have similarly low RSSA because of the surrounding buildings and trees. These nearby buildings and trees block the propagation path to the lower floors in the high-rise building. A high increase in RSSA occurs at the 7th floor because of renovations that were being performed at the time. There were no window blinds or furnishings on the 7th floor, which led to much less shielding and obstruction for penetrating radio waves. The same trend is shown in Figure 45, which is taken in the same building but in a different stairwell. Figure 44 does not show the increased loss for the 7th floor, since it was taken in a different building in which the 7th floor was not under renovation.

4.5 Preparing RF Maps

4.5.1 Equivalent Modification on DCCH Change

Network optimization is a routine procedure that every wireless service provider must perform from time to time. During the Greenville measurement campaign, the dedicated control channel (DCCH) frequency plan was changed at the end of the first week (Dec. 17, 2004). The change covered the

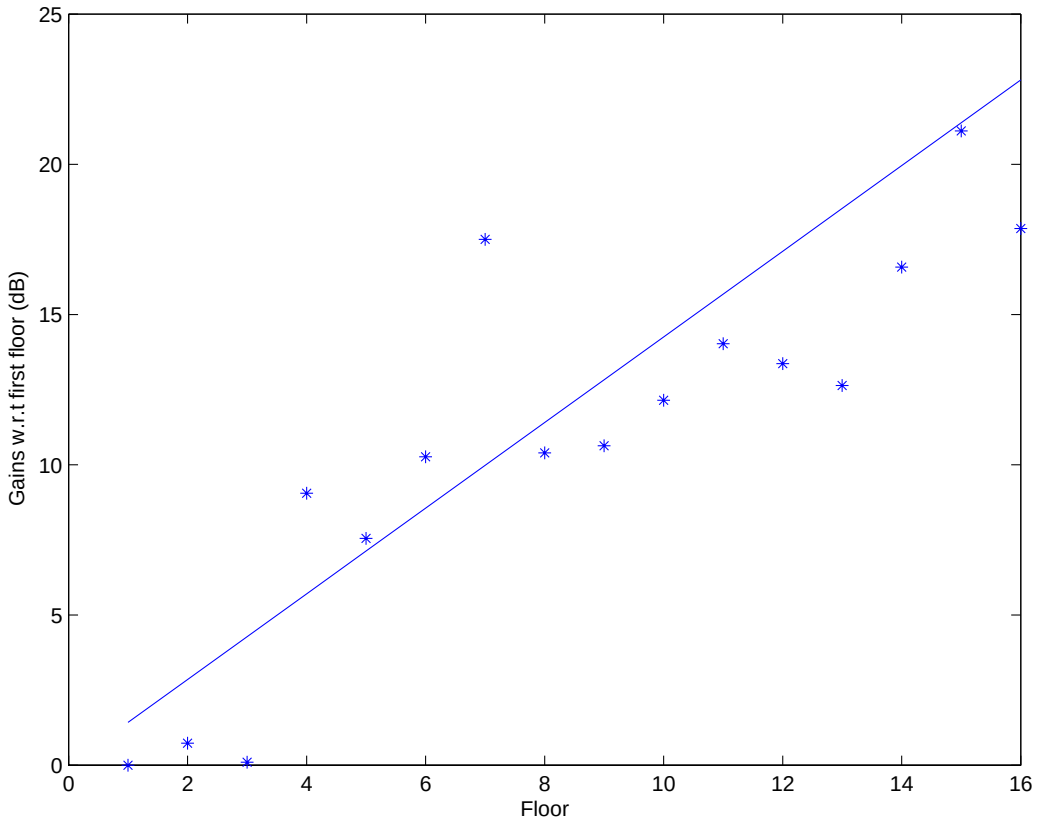

Figure 43: Signal gain vs. floor number, taken from active call data, 6 DCCH channels, slope +1.43 dB/floor.

entire test area. The DCCHs of all cells shifted down from absolute radio frequency channel number (ARFCN) range 786-800 to (ARFCN) range 512-526, a total change of only 55 MHz on the carrier frequency of 1900 MHz. The new ARFCN of the DCCH became the old ARFCN of the DCCH minus 274. Few base stations in the surrounding area had previously used ARFCNs in the range of 512-526 before the frequency plan change. Furthermore, no transmit power was modified for any cell during the measurement campaign. Based on the fact above, one assumption for calibration of the PSD is that the propagation characteristics of ARFCN 786-800 were the same as or very close to the propagation characteristic of ARFCN 512-526. Another assumption is that the carrier-to-interference ratio (CIR) did not change much during this frequency plan update because the entire area has almost the same relative DCCH pattern as before the frequency change.

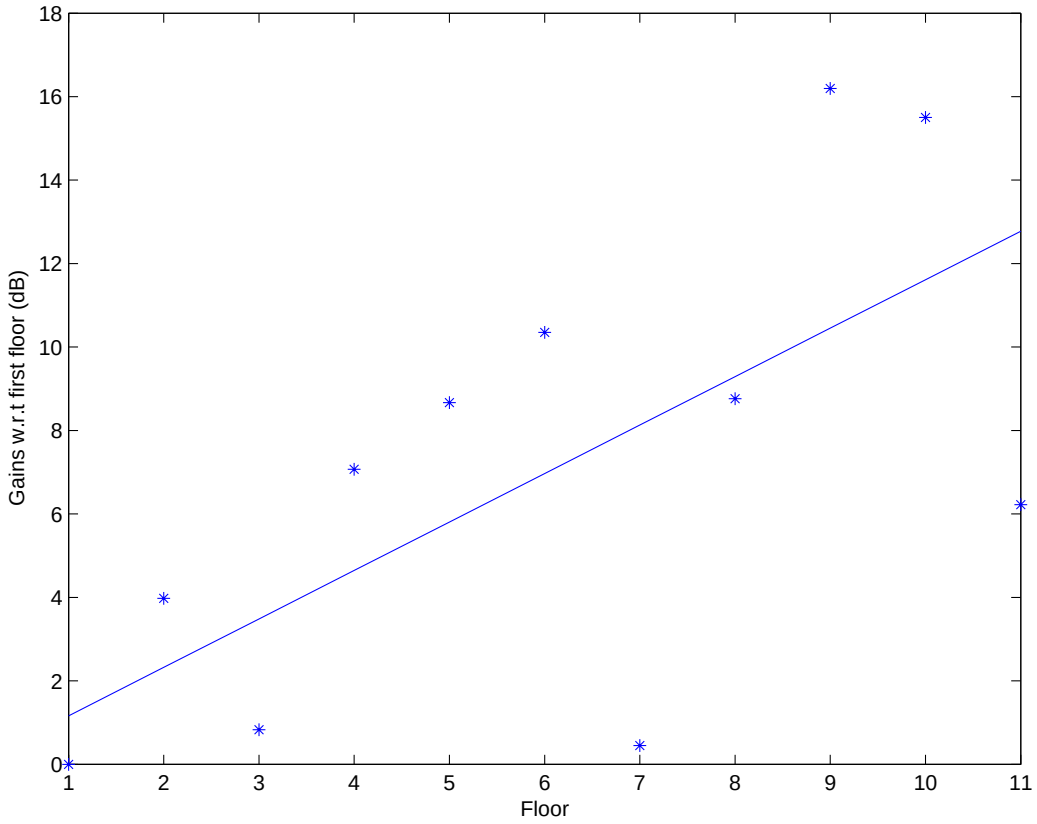

Figure 44: Signal gain vs. floor number, taken from active call data, 6 DCCH channels, slope +1.16 dB/floor.

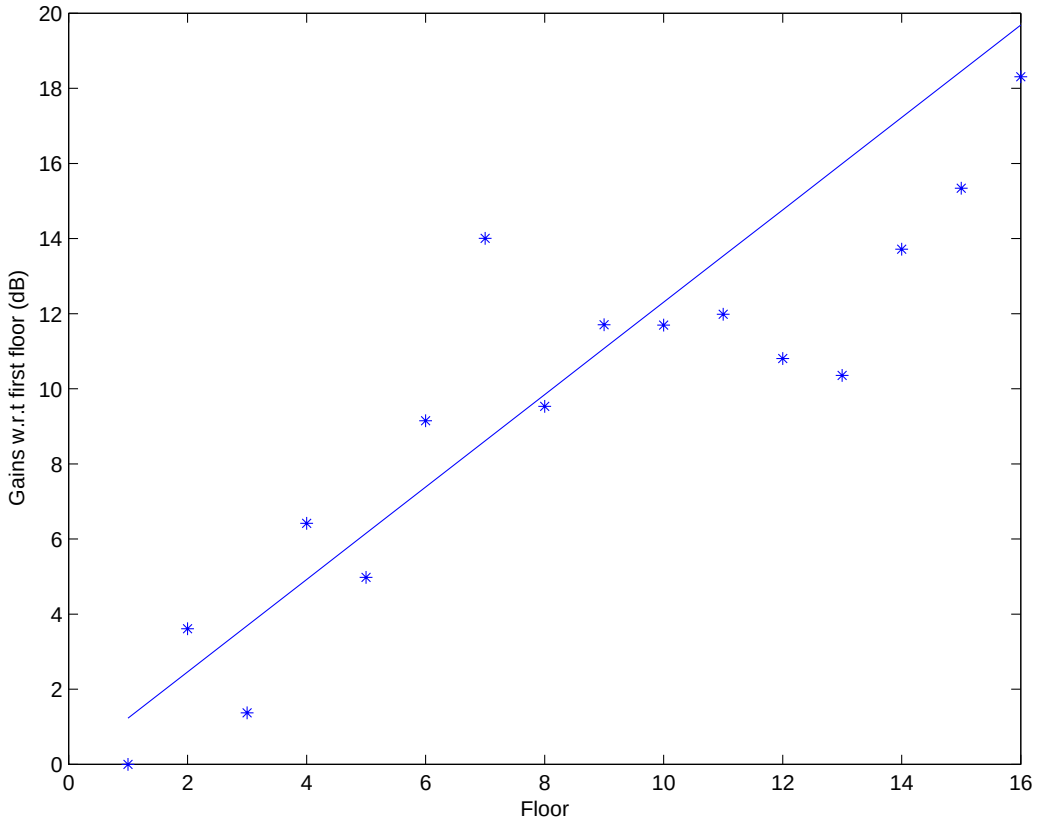

Figure 45: Signal gain vs. floor number, taken from scanner data, 15 DCCH channels slope +1.23 dB/floor.

Figure 46 and Figure 47 compare the DCCH setup in the test area before and after the frequency plan change for DCCH 786 and DCCH 512. Figure 48 and Figure 49 compare the DCCH setup in the test area before and after the frequency plan change for DCCH 787 and DCCH 513. These figures show that the base station distribution of DCCH 786 before the frequency change is the same as the base station distribution of DCCH 512.

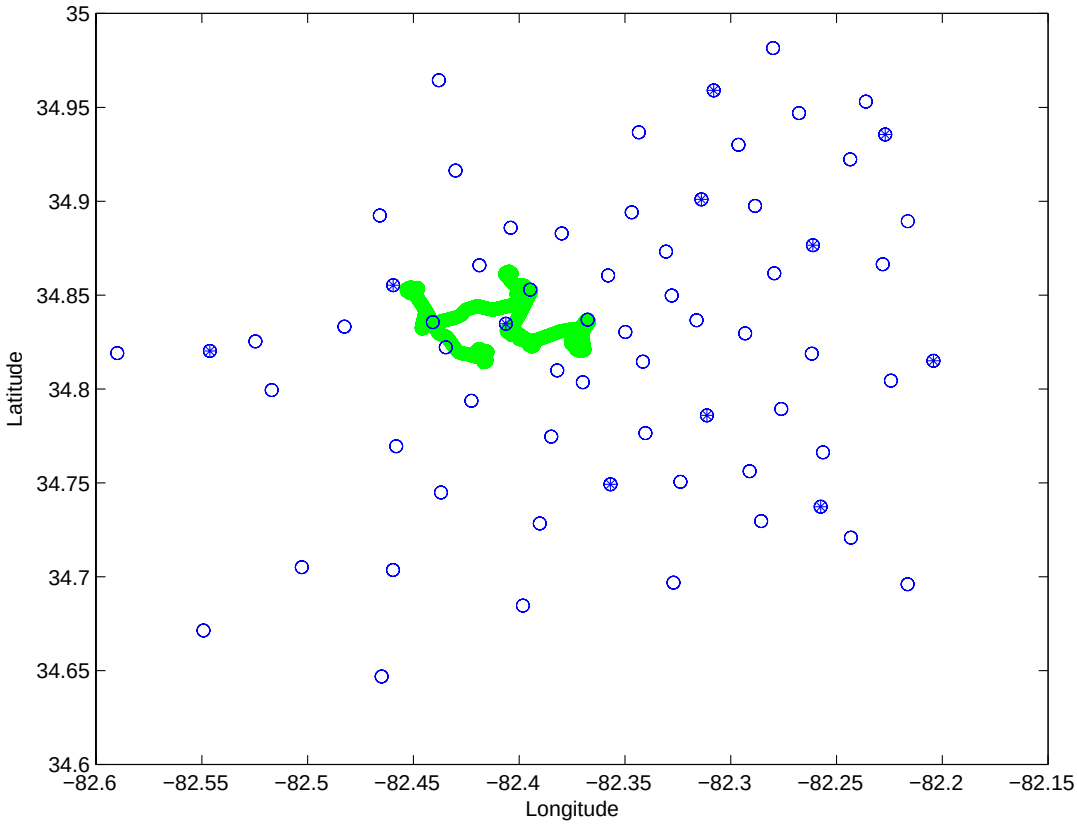

Figure 46: Longitude/Latitude map of base stations (* and O) at Greenville, SC, using DCCH 786 on Dec. 14, 2004. The thick path is a single drive-test route through the test area.

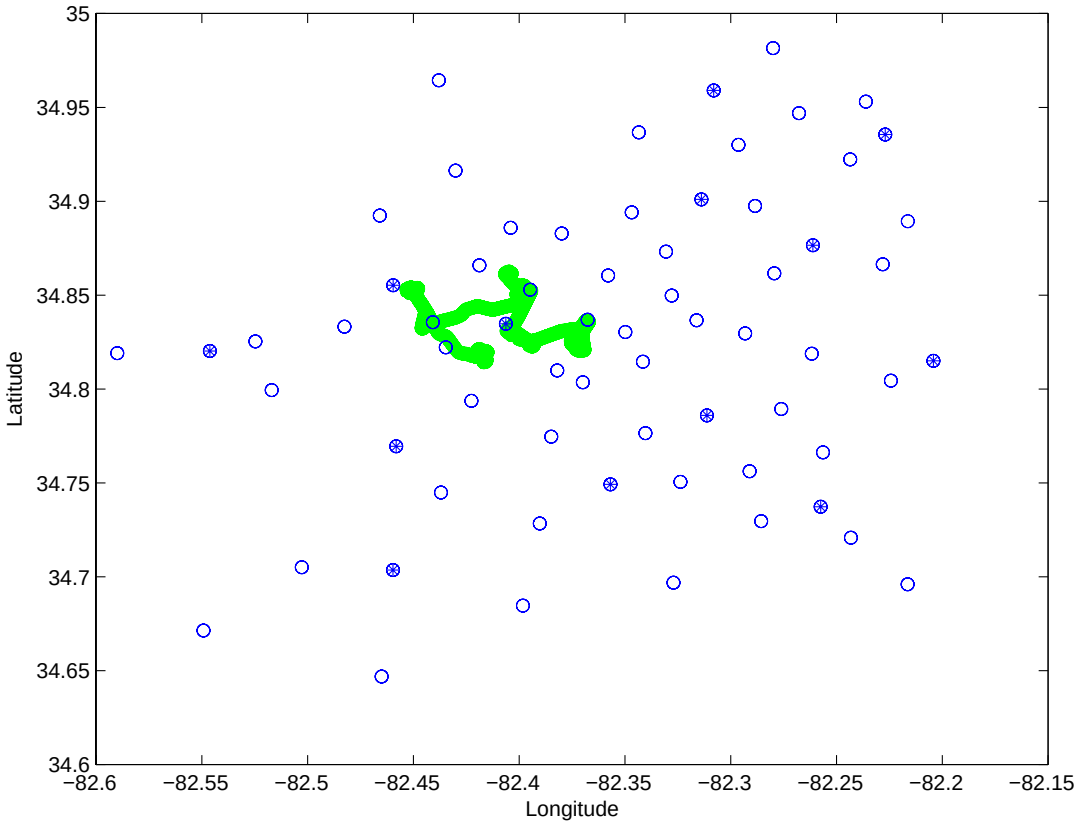

Figure 47: Longitude/Latitude map of base stations (* and O) at Greenville, SC, using DCCH 512 on Dec. 31, 2004.

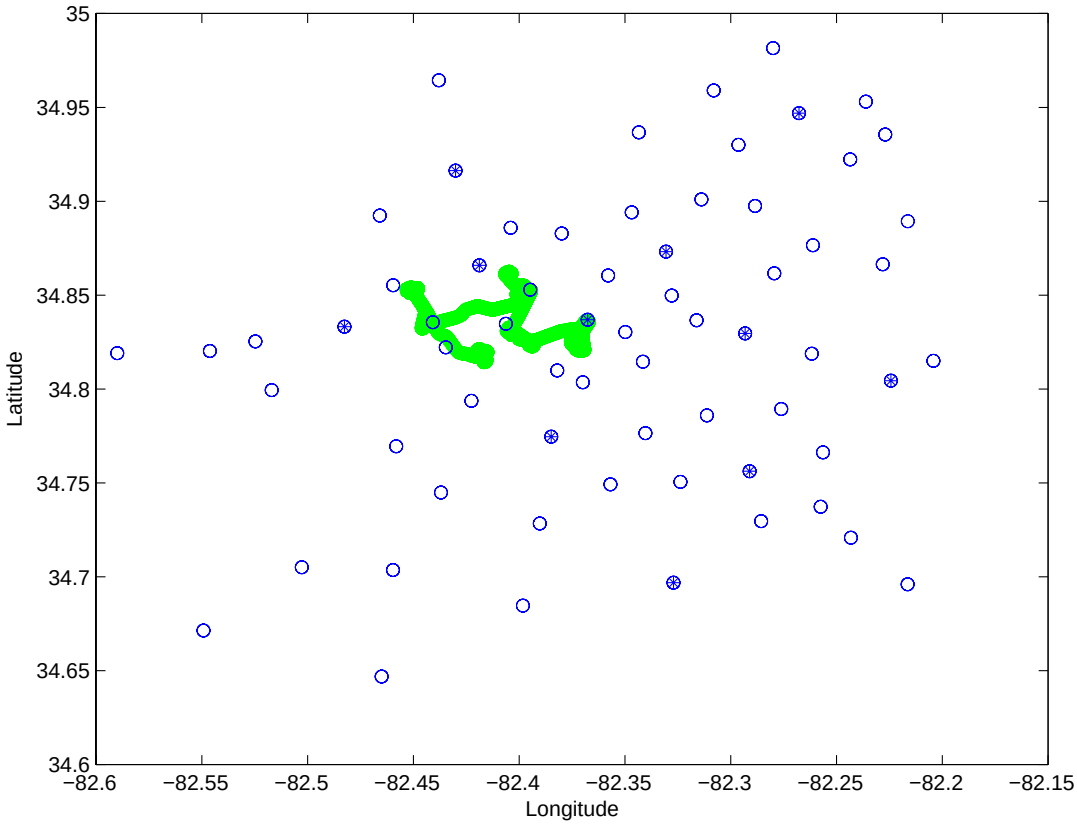

Figure 48: Longitude/Latitude map of base stations (* and O) at Greenville, SC, using DCCH 787 on Dec. 14, 2004.

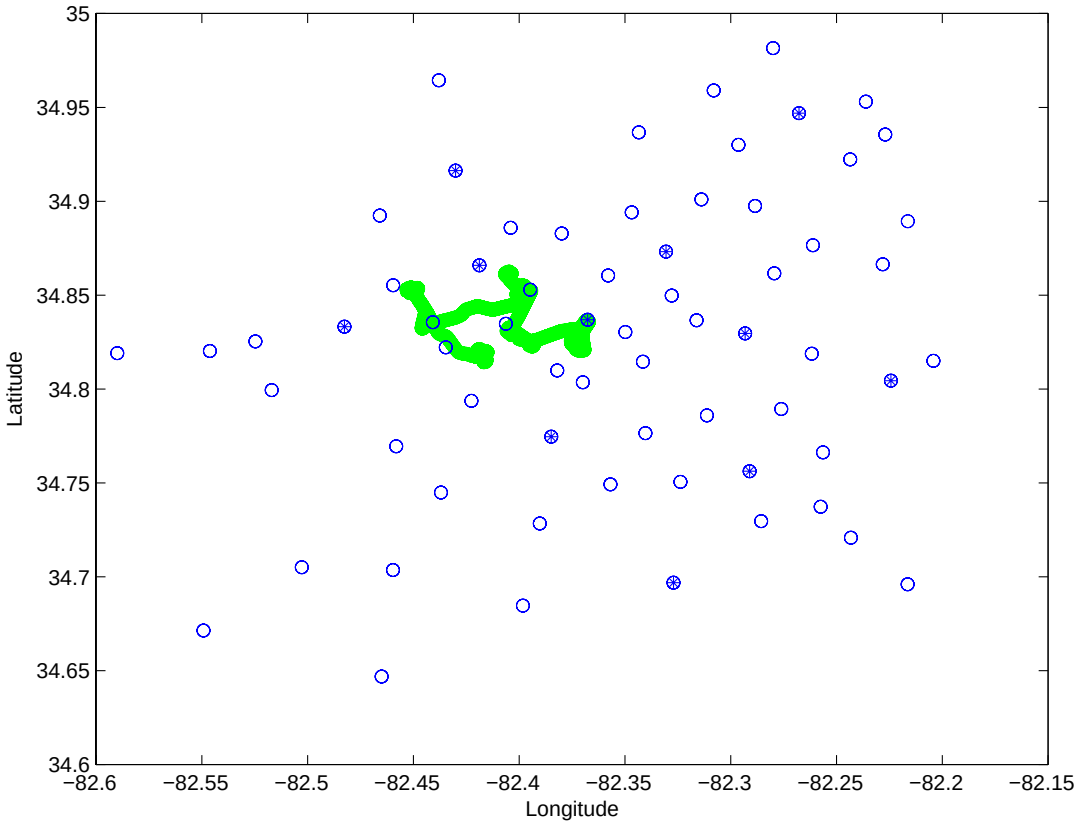

Figure 49: Longitude/Latitude map of base stations (* and O) at Greenville, SC, using DCCH 513 on Dec. 31, 2004.

4.5.2 GPS Manual Correction

The measurement campaign used a Garmin GPS V system to record real-time latitude and longitude for collected data. The unit provides GPS location estimates within 10 m of groundtruth in an open-sky outdoor environment, and sometimes in excess of 25 m under thick cloud, trees, or beside large buildings. In these situations, the GPS often cannot even estimate position because it cannot acquire the minimum three satellites required for triangulation. Most of the time, the GPS signals vanish completely in an indoor environment.

The TEMS program collected data from both the testing handset and the Garmin GPS V unit. Network measurement reports were generated at a rate of two reports per second, which are stamped with system time and all network measurement report data from the handset.

The custom Matlab program GPSFixerV3 is used to correct location information from poor or missing GPS records. As handset measurements are collected, the field engineer clicks on the end-points of the measurement collection path as seen from a geo-referenced satellite photograph (or aerial photo) of the test area loaded on the laptop computer. After clicking, the program GPSFixerV3 adds GPS coordinates to the scanner or active call records by assuming that the measurements are uniformly distributed along the line connecting the two end points.

During the measurement campaign, most of the indoor paths were carefully estimated from the aerial photo. To prevent the marking of a wrong building, outdoor measurement collections were conducted under clear-sky conditions around the building. The indoor GPS locations corrected by GPSFixerV3 were compared with any outdoor GPS locations from the Garmin V unit and aligned with the aerial photo. In this case the error of indoor GPS data should be less than 10 m.

4.5.3 Indoor Calibration

For the indoor calibration of PSDs, we used the active call data collections with the Ericsson TEMS unit. The long list of 74,125 NMRs is grouped into 530 blocks of continuous NMRs taken during the same phone call. Each NMR in a single block is assigned a number showing how many NMRs come after the current NMR in the same block. The active call data is then separated into two groups. The first group contains all odd-numbered NMRs and the second group contains all even-numbered NMRs. The first group is used as indoor calibration data, while the second group is used

as location engine test data. In this case 37,064 NMRs were used to calibrate the indoor PSD and the remaining 37,063 NMRs were used to test location performance. Thus, we ensure that we are not tainting our tests by double counting test data and calibration data.

The active call data was taken with a handset antenna. The GSM NMRs collected from active calls contained received signal strengths (RSS) of six DCCHs from neighbor base stations. The scanner data was collected with a high-gain antenna. The scanner data reports contain all RSSs for all DCCHs. Because scanner data is collected with a different antenna than a handset antenna, the RSSs taken from active calls and scanning data have a dB offset between them. To get rid off the offset, the following operation is used in calibrating the indoor data.

Let $ACRSS_{m,n}$ denote the RSS of the n-th neighbor of the m-th active call record; let $ACDCCH_{m,n}$ denote the corresponding DCCH channels of the m-th active call record; let PSD denote a drive-test calibrated PSD; let the operation $(PSD(DCCH_{m,n}))$ give the RSS of the n-th neighbor DCCH channel of the corresponding m-th NMR at the same longitude and latitude as the location active call NMR was measured. The dB-Offset will be calculated by

$$\text{Offset} = \frac{1}{6}\sum_{i=1}^{6}(ACRSS_{m,i} - PSD(ACDCCH_{m,i})) \tag{49}$$

This offset will be removed from the active call measurements. The corrected RSS value is then blended into the PSD with radius of 1 cell (10 m) to complete the indoor calibration. This RSS map-blending process is described in detail in the first Georgia Tech radiolocation report [43].

4.6 Location Algorithm and Performance

4.6.1 Metric of Location Performance

The distance in meters between a location estimate and the handset's groundtruth position is the *error distance*. For every location experiment in this study, we calculate and report the percentages of error distance values below 100 m and 300 m and the error distances corresponding to the 66.7% and 95% thresholds for cumulative distribution of location error.

4.6.2 Base Line: Relative method, 10 NMR-average

The relative method with RSS averaged over 10 NMR is reported because it was comparable to the location algorithm used in the Georgia Tech campus tests. As the average cell size increased from

500 m in radius to 2000 m in radius, the location performance dropped compared with the original Georgia Tech campus measurements.

We can tell from Table 23 that the location performance drops significantly. The main reason is that we preformed the test in a large area with low cell density, where large errors are possible. Because of the frequency reuse, a location estimate may fall at a point far away from the groundtruth where DCCH configuration and RSS are similar to those measured at original point. For this initial algorithm, the 300 m statistics (39% and 50%) in this Greenville test are even worse than the 100 m statistics (62% and 70%) in Georgia Tech campus test [43]. Because the average cell radius increased from 500 m to nearly 2000 m, the error statistics for this algorithm have increased by the same factor of 4– the 400 m statistic is close to the Georgia Tech campus 100 m statistics.

Because of the large test area, it is almost impossible to produce an indoor mask by hand. An edge detection algorithm in Photoshop software was used to mark out the indoor areas, but misidentification occurred for more than 75% of the entire area. Manual indoor mask correction is required at most locations where we collected active call data. The performance of the location algorithm is almost the same as that using a Level 1 PSD (a PSD calibrated with only outdoor drive-test measurement) in the baseline algorithm. All indoor and pedestrian outdoor collections are omitted from this PSD. Furthermore, there is no attempt to model signal penetration through buildings. This type of RF map database represents the general purpose RSS position location solution proposed in [30],[32]. It is the most practical solution since all measured signal strength data can be collected using standard cellular drive-test procedures. Thus, the data collection is quick and economical.

Table 23: Location error statistics of relative RSS-method. (Linear averaging of 10 NMRs, 6 sectors.)

PSD level		Level 1 Outdoor Meas.	Level 2 Indoor Model	Level 3 Indoor/Outdoor Meas.
Error statistics	<100m	17%	18%	31%
	<300m	39%	39%	50%
Percentage statistics	66.7%	1080 m	980 m	310 m
	95%	5030 m	5030m	5120 m

To improve the performance of the location method, we developed a novel search-area reduction technique, which is discussed in the next section.

4.6.3 Search Area Reduction Based on Linear Regression

Linear regression is a general method for spotting trends in large, complicated data sets. This technique is used here to calculate the relationship between the information recorded in NMRs, the groundtruth of the caller, and the serving base station. This information is *not* limited to only the RSS data in the NMR. By estimating this distance we can improve the position estimate in the RSS-matching portion of the location algorithm.

In a network measurement report, serving sector information and radio environment information such as timing advance, received signal strength, and received signal quality are reported together with neighbor cell DCCH signal strength. Those pieces of information are very useful in reducing the initial search area. By limiting the initial search area, the final location estimate can be calculated much faster and with better accuracy.

Because timing advance (TA) is designed to correct the propagation delay of the wireless radio signal, the timing advance has a direct relationship to the distance from caller to base station. Among all the additional information, TA is the most important information in reducing the search area of a location engine. The TA's value is between 0 and 63 and corresponds to a propagation distance between 0 km to 35 km. Theoretically, one step in TA is about 547 m (35 km/64 TA units). However, through careful data mining, we show that one step of TA change is about 474 m of extra distance from the serving base station. The reason the distance corresponding to one TA step is smaller for the measurement result than the theoretical result is because of NLOS and the multi-path environment. The actual NLOS propagation path is still 547 m. This NLOS path is after reflection, deflection and scattering and not the distance of the straight line from the base station to the handset. The distance calculated from the measurement is based on the shortest distance (straight line distance) between the handset and the base station. Therefore, The distance calculated from measurement is shorter than the theoretical value.

Other information in the NMR also contributes to the search area reduction. The pieces of information tested in this report include TXPOWER, RXLEVFULL, RXQUALFULL, RXLEVSUB, RXQUALSUB, TA, DTXDL, FER, FERSUB, and SQI. These pieces of information are reported in NMRs for the purpose of mobile-assisted handoff (MAHO). A detailed description of these pieces

of information is available in [19, 26, 34]:

- TXPOWER is the transmit power.
- RXLEVFULL is the received signal strength (more specified C1=(RxLev-RxLevAm-MAX((MSTxPwr-MSMaxTxPwr),0))) calculated from continuous transmission.
- RXLEVSUB is the received signal strength (C1) calculated during discontinuous transmission.
- RXQUALFULL is the received signal quality derived from the bit error rate (BER) with continuous transmission from the base station.
- RXQUALSUB is the received signal quality calculated from BER with discontinuous transmission from the base station.
- TA is timing advance.
- DTXDL is the status of the discontinuous transmission down-link.
- FER is the frame error rate of the down-link voice channel with continuous transmission.
- FERSUB is the frame error rate of the down-link voice channel with discontinuous transmission.
- SQI is service quality index, which shows the quality of the current communication status.

Let us assume that all available information in an NMR (timing advance, received signal level, received signal quality, etc.) is linearly related to the separation distance between a base station and a mobile user. Thus, we could relate a set of m distance measurements to a set of m corresponding pieces of NMR info with the following system of equations:

$$\begin{aligned} Ta_{11}c_1 + RxLvl_{12}c_2 + \cdots + RxQual_{1n}c_n &= Dist_1 \\ Ta_{21}c_1 + RxLvl_{22}c_2 + \cdots + RxQual_{2n}c_n &= Dist_2 \\ \dots\dots\dots\dots\dots\dots\dots\dots\dots\dots\dots\dots \\ Ta_{m1}c_1 + RxLvl_{m2}c_2 + \cdots + RxQual_{mn}c_n &= Dist_m \end{aligned} \tag{50}$$

where $xxxx_{mn}$ denotes the nth piece of information from the mth NMR.

The variable c_n represents the correlation between measured data (Ta, TxLvl, RxQual, TxLvlSub, TxQualSub) and the distance from the base station to the caller ($Dist_m$).

This system of equations can be written in matrix format:

$$\begin{bmatrix} Ta_{11} & RxLvl_{12} & \cdots & RxQual_{1n} \\ Ta_{21} & RxLvl_{22} & \cdots & RxQual_{2n} \\ \cdots & \cdots & \cdots & \cdots \\ Ta_{m1} & RxLvl_{m2} & \cdots & RxQual_{mn} \end{bmatrix} \begin{bmatrix} c_1 \\ c_2 \\ \vdots \\ c_n \end{bmatrix} = \begin{bmatrix} Dist_1 \\ Dist_2 \\ \vdots \\ Dist_m \end{bmatrix} \tag{51}$$

Let A denote the matrix of measured data, with each row corresponding to a collection of data during one NMR.

$$A = \begin{bmatrix} Ta_{11} & RxLvl_{12} & \cdots & RxQual_{1n} \\ Ta_{21} & RxLvl_{22} & \cdots & RxQual_{2n} \\ \cdots & \cdots & \cdots & \cdots \\ Ta_{m1} & RxLvl_{m2} & \cdots & RxQual_{mn} \end{bmatrix} \tag{52}$$

Let $\vec{c}$ denote the best possible parameter vector that relates the measurements in A to the distances:

$$\vec{c} = \begin{bmatrix} c_1 \\ c_2 \\ \vdots \\ c_n \end{bmatrix} \tag{53}$$

Let $\vec{d}$ denote the distance vector for each measured point:

$$\vec{d} = \begin{bmatrix} Dist_1 \\ Dist_2 \\ \vdots \\ Dist_m \end{bmatrix} \tag{54}$$

In our data set, we try to find the best values for five of the most important parameters in $\vec{c}$ from 37,063 NMR data points; thus we have many more equations than unknowns in the system represented by Equation 51. This type of system is solved using the *normal equation*:

$$\vec{c} = (A^T A)^{-1} A^T \vec{d} \tag{55}$$

Equation 55 produces a set of parameters $\vec{c}$ that minimizes the mean-square error between the right- and left-hand sides of Equation 51. Once this vector is calculated from the measurement data, it can be used to estimate the handset's distance from the serving base station and generate the distance by using the equation

$$distC = [Ta_1\ RxLvl_2\ \cdots\ RxQual_n]\vec{c} \tag{56}$$

From Equation 56, we can use information in the NMR other than RSS to calculate an approximate distance between user and serving base station. We can then filter the location estimate through a "probabilistic ring" around the serving base station to sharpen our final position estimate.

Figure 50 shows the distribution of the error between the actual distance separating handset and server cell and the calculated distance for 37,062 NMRs analyzed with the regression analysis. On the horizontal axis is the difference between the measured radius and the radius estimated by Equation 56. On the vertical axis is the occurrence of each error, which has been binned into 10 m increments.

In Figure 50, we found that 98% of calculated distances lie within ±600 m of the measured distance and 99% within ±800 m range.

This extra knowledge of predicted distance from the serving base station limits the search area by a ring with a median radius of the calculated distance (*distC*) and with a width of 1200 m (600 m towards inside and outside).

To decide which information is useful we calculate the effectiveness of each kind of information. The effectiveness of one kind of information is calculated as the distance corresponding to one unit change of that information multiplied by the average value of that kind of information.

Table 24 lists the information we found useful in the NMRs. Received signal strength level full, received strength level sub, and service quality index are also considered to be useful information besides timing advance.

The relationship between timing advance and user base station separation distance is obvious because of the constant-velocity propagation of the wireless signal; signals with longer delays have usually traveled farther. The relationship of the received signal strength level sub and service quality index can be explained in this way: the further away the user is from the base station, the lower the

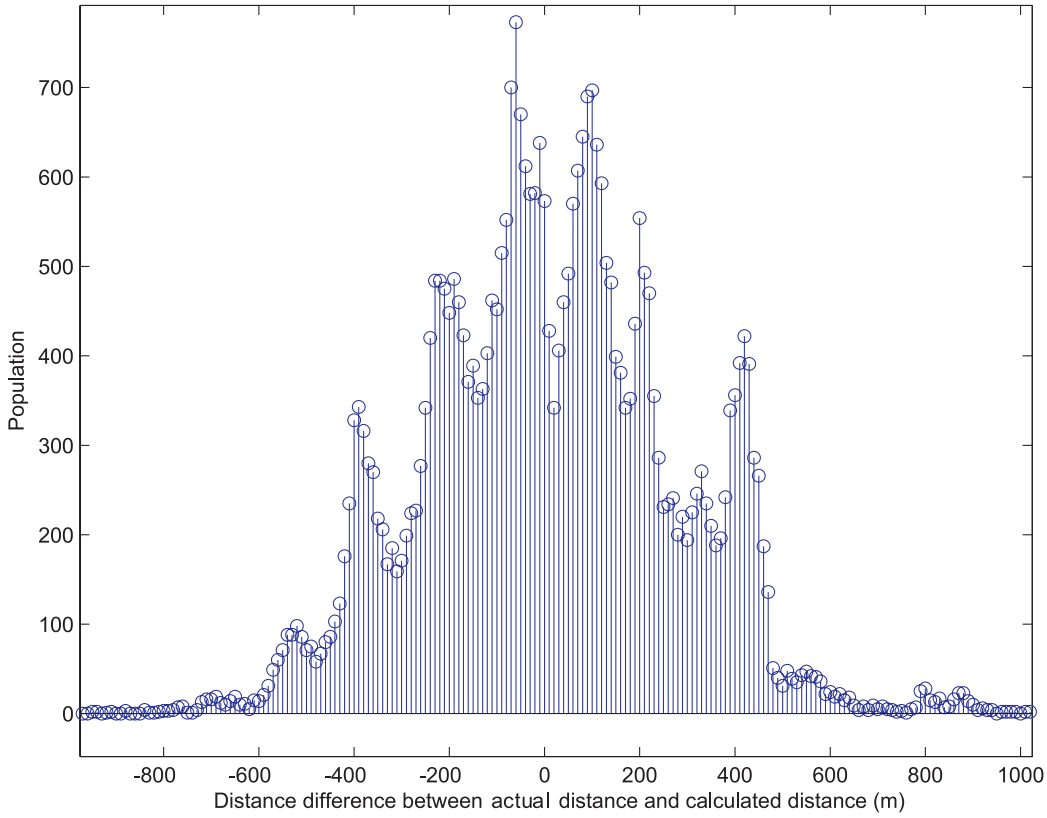

Figure 50: Histogram of base station and user separation distance error between calculated and measured radii. The mean is 13 m and the standard deviation is 289 m.

signal is received and the worse the service quality becomes. That is why the coefficient corresponding to received signal strength level sub and service quality index is a negative number. As for the received signal strength level full, this value is calculated from continuous transmission. To reduce the interference and conserve energy, the power control mechanism lowers the power level during a silence period for both the base station and the handset. This RXLEVFULL is more affected by this power control mechanism, which makes it less correlated with the user base station distance.

Table 24: Coefficient calculated by linear regression method

Timing Advance	474 m/TA step
Received signal strength level full	3.7 m/RXLEV change
Received signal strength level sub	-1.7 m/RXLEVSUB change
Service quality index	-3.8 m /SQI change

The baseline algorithm in Section 4.6.2 searches the entire area for the location estimate based on the RSS of neighbor DCCHs. There is more information available in NMRs such as serving cell information and radio environment information. This extra information can be used to limit the

search area to a ring area surrounding the serving base station, as discussed above. By using this method, location accuracy increases significantly, as shown in Table 25.

In the Level 1 PSD results, position estimates are less than 100 m from groundtruth 26% of the time and 300 m from the groundtruth 62% of the time, which improved the 100 m statistics by 9% and 300 m statistics by 23%. For the Level 3 PSD, The search area reduction brings similar improvements. Position estimates are 100 m from groundtruth 43% of the time and 300 m from the groundtruth 71% of the time, which correspond to increases of 12% and 21%, respectively.

Table 25: Location error statistics of relative RSS-method with limited search area. (Linear averaging of 10 NMRs, 6 sectors.)

PSD level		Level 1 Outdoor Meas.	Level 2 Indoor Model	Level 3 Indoor/Outdoor Meas.
Error statistics	<100m	26%	27%	43%
	<300m	62%	62%	71%
Percentage statistics	66.7%	330 m	320 m	250 m
	95%	1060 m	1060 m	1120 m

Continuous NMR VS. Average NMRs In our baseline algorithm, 10 NMRs are linearly averaged to get one averaged NMR that has less noise and fading than the individual NMRs. This averaged NMR will run through our simple relative RSS location algorithm to get a location estimate. The averaging process limits the availability of NMRs. First of all, it requires 10 continuous NMRs reporting from the same neighbor cells, which is not always possible in a GSM network. Second, the handoff and neighbor list change provides extra information, which is very useful in limiting the search area and improving the location accuracy. Third, the method of averaging is still vulnerable to measurement error and noise.

The improved method uses the search area reduction technique of Subsection 4.6.3. At the same time, continuous NMRs are not just averaged, but are used more effectively by making individual estimates on each NMR and post-processing these results.

In the relative RSSI location algorithm description in Section 6.2.2 of [43], the mean of each vector in the PSD is calculated in dBm. This mean is subtracted from the vector:

$$Prssr_{x,y,i} = Prss_{x,y,i} - \frac{1}{N}\sum_{j=1}^{N} Prss_{x,y,j} \tag{57}$$

where $Prssr_{x,y,i}$ denotes the received signal strength of the *i*th control channel at the location coordinates x, y.

The mean of the measured NMR vector is subtracted from the measured vector to form a new vector:

$$Nrssr_i = Nrss_i - \frac{1}{N}\sum_{j=1}^{N} Nrss_j \tag{58}$$

where $Nrssr_i$ is the received signal strength reported in the NMR in the *i*th channel.

After normalization, all vectors of received signal strength become independent of any antenna/RF chain bias.

The relative signal vectors from the NMR and PSD are used to calculate the measurement distance for each raster point as in Equation 59.

$$M(x,y) = \sqrt{\sum_{i=1}^{N}(Prssr_{x,y,i} - Nrssr_i)^2} \tag{59}$$

This M(x, y) matrix is called distance matrix, which represents the Euclidean distance between the

RSS from the NMR and the RSS in the PSD. The coordinates (x, y) that yield the lowest measurement distance are chosen to be the location estimate.

In our improved algorithm, continuous NMRs are not just averaged and fed into the algorithm described above. Based on the assumption that the distance that the caller moves during a phone call or the period of 10 NMRs is relatively short (compared to the PSD raster point size), a "distance matrix aggregate (DMA)" is used instead of the averaged 10 NMRs. In the distance matrix aggregate method, each NMR will be used to calculate a distance matrix and all the distance matrices will be added together to form a distance matrix aggregate. Each roster point in this distance matrix aggregate is a measurement distance aggregate. The coordinates (x, y) that yield the lowest measurement distance aggregate are chosen to be the location estimate.

The Table 26 reports the performance of using 10 NMRs by calculating the distance matrix aggregate based on the assumption of the user will not move faster than walking speed.

Table 26: Location error statistics for the relative RSS-method with limited search area and distance matrix aggregate. (10 NMRs, 6 sectors.)

PSD level		Level 1 Outdoor Meas.	Level 2 Indoor Model	Level 3 Indoor/Outdoor Meas.
Error statistics	<100m	30%	31%	51%
	<300m	71%	72%	79%
Percentage statistics	66.7%	270 m	260m	180 m
	95%	580 m	580m	530 m

The level 2 PSD location performance shows very slight improvement, which is within the 1% margin of experimental error. There are a number of reasons why the improvement is so small:

1. There are more than 20 fast-food-type buildings that are questionable indoor/outdoor locations. We removed those buildings when extracting model data. They were included, however, as part of the active call test data.

2. More than 20 of the buildings have a footprint smaller than four raster points. Some of them are just one pixel at 10 m resolution mapping. This will disable the advantage of incident-angle dependence, making it impossible to assign the informative propagation model that allows a location engine to fix upon a spot. Very small building footprints also result in inaccurate incident angle calculation. These inaccurate incident angle calculations do not increase the accuracy of the modeled PSD or sometimes make the modeled PSD worse.

3. The incident angles used in model extraction are manually measured and entered into a database. The Level 2 PSD is generated by the program, which calculates the incident angle based on the building footprint by the GIS processing program. This may introduce some calculation differences.

4. The current indoor model does not include information on the building's immediate surroundings, which has been shown in this experiment to play a significant role in the penetration loss.

4.7 Conclusions and Suggestions

Overall, the Greenville, SC, indoor/outdoor position location trials yielded some promising results for cellular carriers that are concerned about FCC E911 compliance in a GSM network loaded with indoor users. The only disappointing set of numbers was the indoor/outdoor discrimination rate, which dropped to 76% compared to a high value of 92% witnessed on the campus of Georgia Tech. This discrepancy is likely due to the more homogeneous building style that made the college campus much more predictable.

Still, the Greenville trial must represent a worst-case scenario for E911 position location: a rural network with low base station density. That the 100 m and 300 m cumulative location error distributions reached 51% and 79%, respectively, in such an environment is a testament to the resiliency of the technique. These numbers could be further improved by honing the location algorithm, incorporating better propagation modeling, and driving minor roads.

The results also suggested the hybridization of GPS-assisted method and RSS signature method as the solution for the handset location problem in cellular networks. The hybrid system will combine the outstanding performance of the GPS system in a rural area and the RSS system in an urban environment.

Suggestions for Improved Indoor Modeling

The current octant penetration model has some valuable insight for radio wave propagation, but there is still room for improvement. The following suggestions for improvement should lead to better performance for RSS location technology:

1. Consider the relationship between the propagation loss and the number of blockages over the propagation path from the base station to the mobile unit.

2. Consider the relationship between the propagation loss and the orientation of small buildings whose indoor footprints are smaller than four raster points.

3. Revise the incident angle calculation function in Matlab.

4. Consider environment-related multi-path effects. Improving these attributes will improve not only the location engine performance, but also the ability to discriminate between indoor and out-door users in a cellular network - which already exhibited a promising performance in Greenville, SC.

CHAPTER V

EXTENDED LOCATION TRIAL: MANHATTAN, NY

The Manhattan area is a very dense urban environment. The multi-path propagation environment introduced by the skyscrapers completely block the GPS signals, which causes conventional triangulation methods to fail. Assisted GPS, angle-of-arrival, and time-of-arrival are not effective solutions for this dense urban environment. However, the RSS signature method has a truly unique advantage in this multi-path propagation environment because the multi-path-induced variations increase the diversity of the signature. The challenge for RSS signature methods in ultra-dense urban environments is to generate an accuracy predicted signal strength database (PSD). This is especially important for areas where no calibration measurements can be made, such as indoor areas and pedestrian passageways.

The Manhattan trial shows how well the RSS signature method can perform in a typical ultra-dense urban environment. Our original octant model does not work in such an ultra-dense urban environment because it is based on an assumption that the major propagation path is over rooftop diffraction. To improve the performance of an RSS signature method in an ultra-dense urban environment, more accurate indoor signal strength prediction is the key. A revised indoor penetration model has been proposed and tested in this Manhattan trial. Encouraging performance improvement showed that 50 m accuracy increased by 11.5% for indoor test trace data. Furthermore, The introduction of a new indoor penetration loss model also helped to improve the location performance for outdoor test points.

The result of the Manhattan trial shows that the RSS signature method is the definitive location solution for dense urban environments. By applying an RSS location engine, a majority of location estimates are less than 50 m from the groundtruth.

5.1 Key Output

The Manhattan location trial proved to be a highly successful experiment with several key outcomes:

1. The experimental results validated the indoor and outdoor performance of the RSS signature location method in an ultra-dense urban environment for FCC E911 systems in both outdoor and indoor areas.

2. A revised indoor penetration loss model for ultra-dense urban environments was presented.

3. This study showed that the revised indoor model greatly improved the overall system performance. The work also suggests a new direction of revising indoor model according to the outdoor propagation environment.

4. The experiment provided more data to predict the accuracy of an RSS signature location method.

5.2 Trial Background

The Manhattan area is famous for its urban canyon environment. The location trial was performed on a live network with radio frequency bellow 1 GHz with help from Polaris Wireless engineers. Polaris Wireless has a patent on RSS signature based location and is extremely interested in extending the RSS signature location method to the indoor environment. In this trial, the new indoor penetration model was used to build PSD for indoor areas. The Polaris location algorithm was used to perform the location match [30, 32]. This Manhattan trial was a good opportunity to test the indoor model and get some insight to further improve the propagation model.

5.3 Measurement Plan

5.3.1 Test Area Selection

All measurement were made inside a 2 $\times$ 2 km center measurement area that was enclosed by a 4 $\times$ 4 km test area in Manhattan, as shown in Figure 5.3.1. There were about 100 cell sectors inside the center measurement area and about 400 in the entire test area. The measurement campaign was performed on an live cellular network. RSS data was measured on forward control channels, which are narrow band and have constant transmit power.

The data for this measurement campaign were collected by Polaris field engineers in Manhattan. The measurement campaign lasted for 1 month. During this period, the network configuration was

Figure 51: RSS location performance test area of ultra-dense urban environment in Manhattan, NY.

frozen. This freeze simplified the process of building the PSD. Therefore, no network configuration update was needed during building the predicted maps.

5.3.2 Setup Overview

For this trial, the data were collected using an Agilent 6474A drive-test equipment connected to a testing handset. A base station controller (BSC) trace for the test mobile was enabled and recorded. Measurement report data were post-processed by Polaris off-line system. The Polaris' off-line system is a set of programs that uses pre-recorded NMRs to simulate real-time activity and provide a location performance report. The predicted signal database was calibrated by the NMRs collected in this process.

5.4 Data Collection

5.4.1 Outdoor Driving Collection

An outdoor drive-test collection for PSD calibration was performed along all streets in the test area. More than 50,000 RSS samples were collected by a commercial scanning receiver and grouped into 10m $\times$ 10m spatial bins. The RSS recorded in a PSD for each bin is a linear average of 3-8 instantaneous power measurements.

Another separate outdoor driving collection was performed at different times to collect 500 trial data for location testing purposes. The second collection was performed in actual cars, emulating the behavior of 911 call situations. Figure 52 shows a sample driving route in the trial area. A total of 10,170 data samples of live handset data were collected for outdoor location testing purposes.

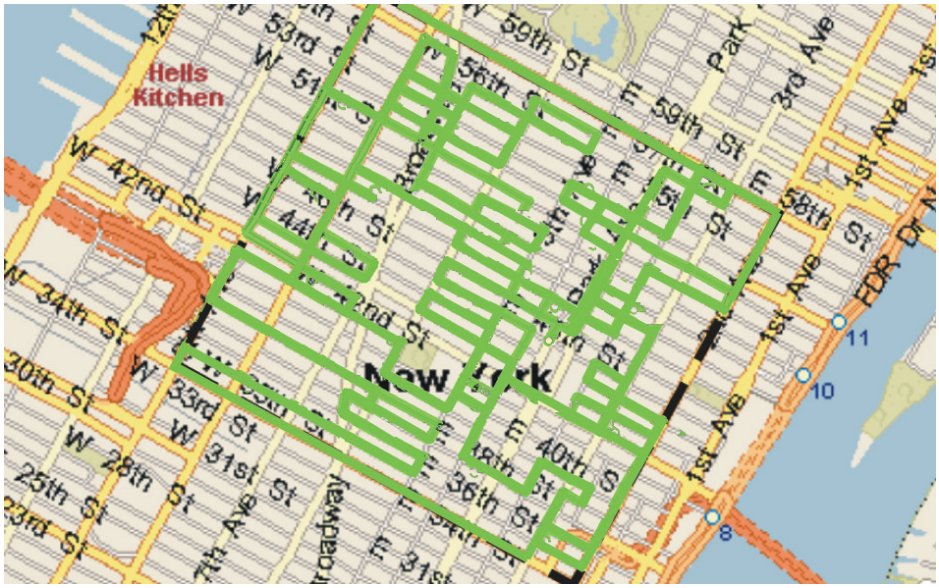

Figure 52: Sample outdoor driving test route in Manhattan, NY.

5.4.2 Indoor Walking Collection

Thorough indoor data collection was performed in three test area buildings to extract indoor penetration loss parameters; this data were used to form a generic penetration loss model. Indoor data samples totaling 2,326 were collected in 21 test area buildings for testing purposes. For this last data measurement, the field engineers simulated actual calling conditions, moving at slow speeds with the measurement handset held by their head.

5.5 Modified Indoor Modeling

Predicting the received signal strength for the indoor environment is critical for building an accurate PSD, especially for areas where no calibration measurement can be made. More accurate RF maps will result in better location estimates.

5.5.1 Original Indoor Modeling

From physics, we expect normal-incidence waves to have less penetration loss than grazing incidence waves. For algorithm simplicity, incident angles are divided into eight uniformly spaced octants, as shown in Figure 25. Unique penetration loss values are calculated and assigned for each octant. Since different control channels originate from different base stations and propagate through a building's exterior wall with dissimilar angles of incidence, the penetration loss for each control channel will vary. This effect is used for indoor signal strength prediction and adds distinctive features to the indoor signal strength that help to distinguish indoor areas from outdoor areas. The original indoor penetration model in [43] assumes that a line-of-sight (LOS) exists or that the major mode of propagation is over-roof diffraction. This assumption simplifies the incidence angle calculation by treating the bearing angle of the base station to the building wall as the principal angle-of-arrival.

5.5.2 Details of Modeling Modification

The LOS assumption of the original penetration model does not hold in the ultra-dense environment of Manhattan, where round-the-street-corner diffraction propagation dominates. A modified indoor penetration model is proposed and implemented in this section. The revised model takes into consideration the urban canyon effect to improve the original LOS penetration loss model. The revised model was used to generate an indoor signal strength prediction for the Manhattan trial.

Manhattan is an ultra-dense urban environment. Most of the buildings are more than 50 stories high. At the street level, there are no LOS paths available for most locations. Because of all the surrounding skyscrapers, the major propagation path to the street level is no longer the over-roof diffraction. The streets become tunnels for propagation. The major non-line-of-sight (NLOS) propagation path is formed by diffraction from the side corner of the buildings or reflection at each intersection. Our original octant model is based on the fact that in most semi-urban and rural areas, the propagation path is the over-rooftop diffraction. Therefore, it does not work for this much more dense urban environment. We need to modify the original octant model by considering street as the major propagation path (wave-guide effect). Diffraction and reflection are the major propagation phenomena in this case. Because tracing each ray in the propagation environment requires extremely

accurate building position and orientation information and also requires tremendous computational power, ray tracing is not an option for practical considerations. We introduce the major/dominant propagation path concept here. The dominant propagation path is the path that contributes the most power to the received signal strength. Based on the dominant propagation path, the concept of a pseudo-transmitter (or called pseudo-base-station) is introduced. For a building without LOS to the real base station, the intersections around that building become the major source of radio wave diffraction and reflection. From the building's perspective, the majority of radio signals come from the intersection in the direction of the real transmitter. We call this intersection the *dominant intersection* or *pseudo-transmitter* for that building. A pseudo-transmitter case is shown in Figure 53.

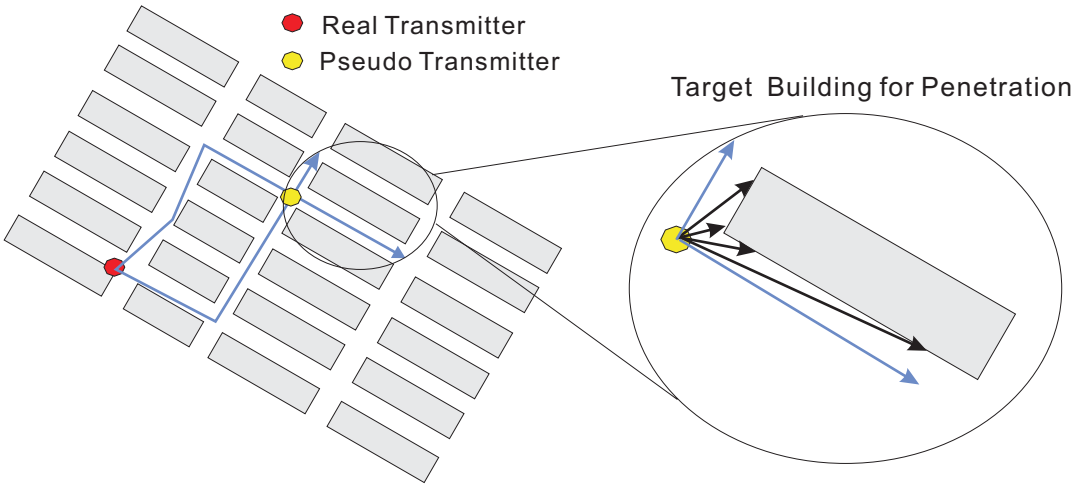

Figure 53: Pseudo-transmitter case in an ultra-dense urban environment.

5.5.3 Improved Octant Number Decider

The octant indoor penetration loss model is based on the direction of incidence of the arriving radio wave. The direction of incidence is calculated from the direction of the building surface and the direction of the major mode of incidence wave. Therefore, extracting building surface orientations from GIS information is a crucial step for indoor modeling.

The original algorithm for calculating octant numbers for building surfaces is applied to a raster database of 30 m to 50 m bin size. A cross-shaped filter with radius of 1 pixel is used to calculate the building face direction, as showed in Figure 54.

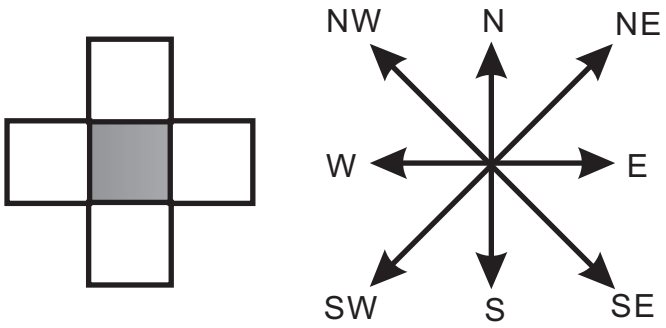

Figure 54: Original building oriental octant number decider with the ability to distinguish eight directions.

The center point of this filter is called the “body,” and the surrounding points are called “arms”. To calculate a building face origination, the body of the filter is placed on the raster point at the building edge. The four arms of the filter are on the neighbor grids. The building face origination decision is the direction that points from the center of all indoor arms to the center of all outdoor arms. The resolution for this cross-shaped filter is 45° and this filter can distinguish eight different directions.

The new direction decider is built under the improved conditions of 10 m bin size, which make finer resolution possible. To improve the octant angle calculator we apply a 3 pixel by 3 pixel rectangular filter. The orientation vector of the central pixel will be calculated based on the status of the surrounding eight pixels. The new filter is shown in Figure 55

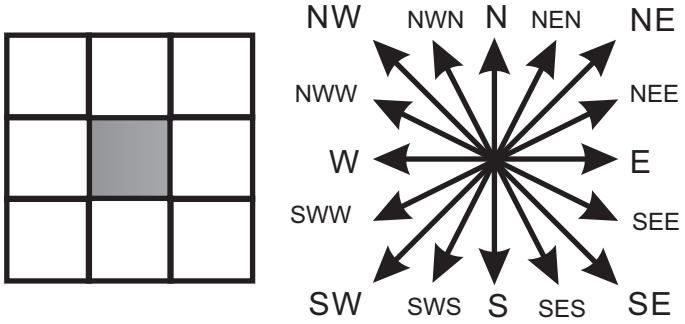

Figure 55: Revised building oriental octant number decider with the ability to distinguish 16 directions.

This new orientation decider also makes building face origination decisions based on the center of the indoor arms and the center of the outdoor arms. It can distinguish 16 different directions. Therefore, the resolution for this new rectangular filter has been improved to 22.5°

5.5.4 Indoor Measurement Examples

Figure 56 and Figure 57 show the scanner measurements of signal strength at the ground floor of the Empire State Building. The indoor area is marked with shadows. Data "0" means that no measurement was collected in that bin.

	1	2	3	4	5	6	7	8	9	10	11	12	13	14	15	16	17
1	0	0	0	0	-80	-82	-85	0	0	0	0	0	0	0	0	0	0
2	0	0	0	0	0	0	-84	-86	0	0	0	0	0	0	0	0	0
3	0	0	0	0	0	0	-100	-100	-84	-85	0	0	0	0	0	0	0
4	0	0	-113	-116	-113	-106	-103	-106	0	-86	-81	-86	0	0	0	0	0
5	0	0	-113	-116	-103	-106	-105	-106	-104	-104	0	-81	-80	-83	0	0	0
6	0	0	-111	-113	-95	-92	-98	-109	-99	-102	-105	-94	-99	-80	-80	-79	0
7	-62	-60	-61	0	-84	-91	-92	-92	-94	-81	-85	-102	-90	0	0	-80	-72
8	0	0	-61	-63	-96	-96	-91	-85	-87	-90	-84	-102	-90	-103	0	0	-76
9	0	0	0	0	-64	-57	-59	0	0	-90	-94	-99	-88	-82	0	-76	0
10	0	0	0	0	0	0	-61	-57	-62	-80	-83	-90	-90	-84	-74	-74	0
11	0	0	0	0	0	0	0	0	-59	-62	0	0	0	0	-72	0	0
12	0	0	0	0	0	0	0	0	0	-56	-57	-52	0	-60	-69	0	0
13	0	0	0	0	0	0	0	0	0	0	0	-51	-54	-56	0	ST	0

Figure 56: Measured signal strength for Channel 18 at Empire State Building. Indoor area is marked by shadows. "ST" stand for pseudo transmitter.

In Figure 56, the pseudo-transmitter is located at the lower right (south-east) corner of the building. The outdoor measurements at column-15 and row-11 and the indoor measurement at column-14 and row-10 show an attenuation of 12 dB. This is a grazing incidence (octant sector 2). Table 27 compares the indoor and outdoor attenuation with the incidence angle for Figure 56.

In Figure 57, the Pseudo-Transmitter is located at the upper left (North-West) corner of the building. Table 28 shows how attenuation changes with incidence angle for the data presented in Figure 57.

Table 27 and Table 28 show the relationship between attenuations and incidence angles. The

Table 27: Compare attenuation and incidence angle.

Indoor			Outdoor			Attenuation	Octant Sector
Column	Row	RSS	Column	Row	RSS		
7	2	-84	7	3	-100	16	4
8	2	-86	8	3	-100	14	4
10	4	-86	10	5	-104	18	4
12	5	-81	12	6	-94	13	4
13	5	-80	13	6	-99	18	4
14	10	-84	15	10	-74	10	1 or 2
10	10	-80	10	11	-62	18	3
7	8	-91	7	9	-59	32	3
6	8	-96	6	9	-57	39	3
5	8	-96	5	9	-64	32	3

attenuation for grazing incidence (octant sector 3) has an averaged value of 25 dB, which is the highest among all types of incidence. The average attenuation for oblique backscatter (octant sector 4) is 16 dB. For oblique incidence (octant sector 2), one sample shows 10 dB attenuation. For near-normal backscatter (octant sector 5), one sample shows 13 dB attenuation. Though the number of samples is limited, the result shows a trend that the penetration loss increases when incidence angle increases and attenuation reaches maximum at near-parallel incidence and backscatter than penetration loss decreases in the backscattering case.

Table 28: Compare attenuation and incidence angle.

Indoor			Outdoor			Attenuation	Octant Sector
Column	Row	RSS	Column	Row	RSS		
7	2	-54	7	3	-69	15	3
8	2	-57	8	3	-74	17	3
10	4	-54	10	5	-87	33	3
12	5	-58	12	6	-77	19	3
13	5	-61	13	6	-81	20	3
14	10	-75	15	10	-88	13	5
10	10	-86	10	11	-99	13	4
7	8	-85	7	9	-101	16	4
6	8	-84	6	9	-111	27	4
5	8	-84	5	9	-93	9	4

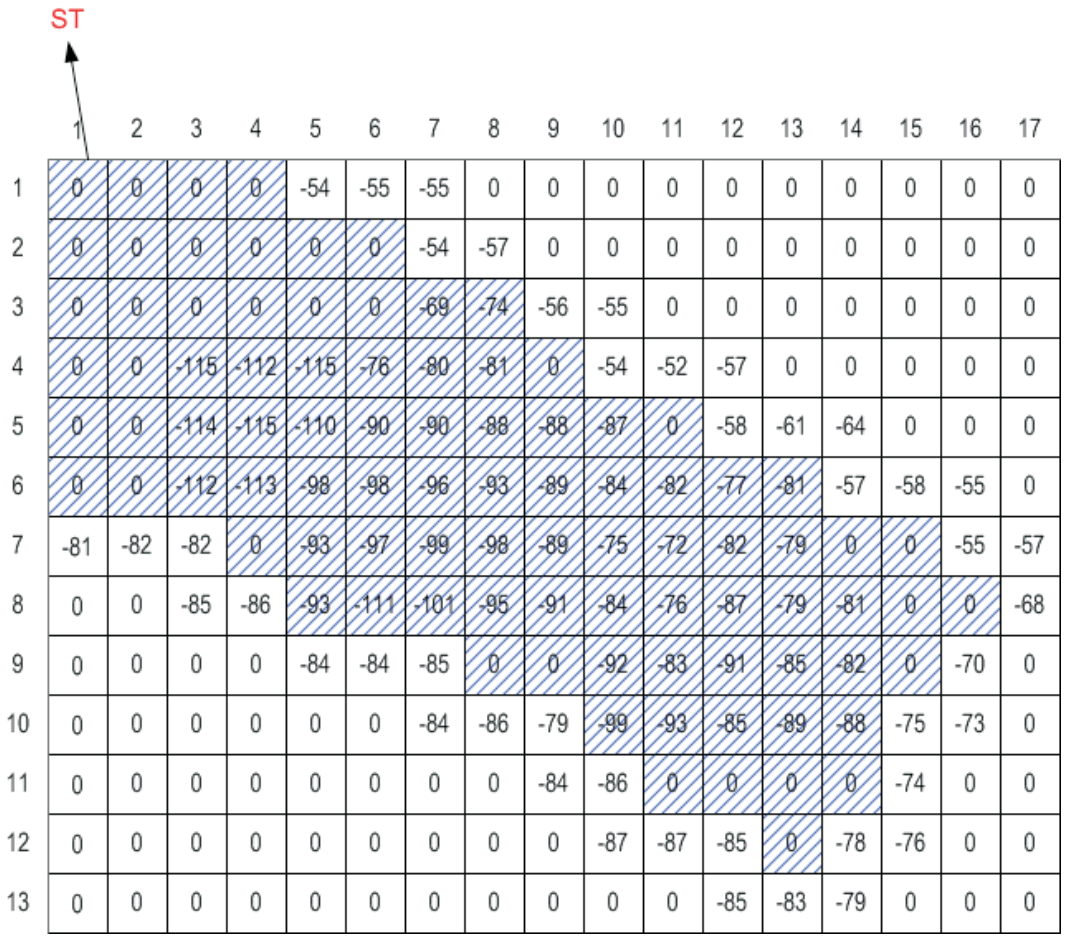

	1	2	3	4	5	6	7	8	9	10	11	12	13	14	15	16	17
1	0	0	0	0	-54	-55	-55	0	0	0	0	0	0	0	0	0	0
2	0	0	0	0	0	0	-54	-57	0	0	0	0	0	0	0	0	0
3	0	0	0	0	0	0	-69	-74	-56	-55	0	0	0	0	0	0	0
4	0	0	-115	-112	-115	-76	-80	-81	0	-54	-52	-57	0	0	0	0	0
5	0	0	-114	-115	-110	-90	-90	-88	-88	-87	0	-58	-61	-64	0	0	0
6	0	0	-112	-113	-98	-98	-96	-93	-89	-84	-82	-77	-81	-57	-58	-55	0
7	-81	-82	-82	0	-93	-97	-99	-98	-89	-75	-72	-82	-79	0	0	-55	-57
8	0	0	-85	-86	-93	-111	-101	-95	-91	-84	-76	-87	-79	-81	0	0	-68
9	0	0	0	0	-84	-84	-85	0	0	-92	-83	-91	-85	-82	0	-70	0
10	0	0	0	0	0	0	-84	-86	-79	-99	-93	-85	-89	-88	-75	-73	0
11	0	0	0	0	0	0	0	0	-84	-86	0	0	0	0	-74	0	0
12	0	0	0	0	0	0	0	0	0	-87	-87	-85	0	-78	-76	0	0
13	0	0	0	0	0	0	0	0	0	0	0	-85	-83	-79	0	0	0

Figure 57: Measured signal strength for Channel 08 at Empire State Building. Indoor area is marked by shadows. “ST” stand for pseudo transmitter.

5.5.5 Octant Model Values

Because the data collected from the indoor walking collection are not sufficient to build a reasonable indoor penetration model, the model parameters are generated based on both the limited data collection from the Manhattan trial and our experience from our previous experiments.

Table 29: Octant penetration values used in the Manhattan trial.

Octant	1	2	3	4	5
Loss values used in simulation(dB)	10	15	20	15	10
Measured and refined loss values (dB)	10.0	10.0	25.0	16.0	13.0

We assume the penetration loss is linearly related to angle of incidence and use the model value in the second row of Table 29 for penetration loss calculation. The lowest penetration loss of 10 dB is assigned for normal incidence and the highest penetration loss of 20 dB is assigned for near-parallel incidence. Grazing incidence is assigned a loss of 15 dB. Because the indoor signal strength at the back side of the building is the result of contributions by not only the signal penetrating through the building outside wall but also the signal propagating through the building, the aggregate signal is stronger than the signal purely from penetrating the back side wall. Therefore, less "penetration loss" is assigned for the backscattering cases.

Model parameters are refined by pure measurement and are listed in the third row of Table 29. Because of limited access to Polaris's commercial engine, the refined model has not been tested yet. The reported location performance is based on the linear incidence-angle related penetration loss model described in the second row of Table 29.

5.6 Steps of applying modified indoor modeling

To apply the modified indoor penetration model, the following extra steps are needed:

- Add Intersection Data

  In an ultra-dense urban environment, streets are the major channels of RF propagation. Line-of-sight conditions do not exist for most of the cases. Instead, street intersections are sources of diffraction. Marking each intersection helps to identify the major diffraction source and is very useful in indoor modeling. An intersection map is a high-resolution geo-referenced raster map that marks intersections in two dimensions. Each intersection is represented by a

logical 1 at the center of the intersection. All other raster points are filled with logical 0's. Intersection information is extracted from digital road data.

- Add Indoor Masks

  Another extremely useful piece of limited-availability GIS data is the indoor mask. An indoor mask is a logical, high-resolution map that describes the footprints of buildings in two dimensions. Logical 1's are placed wherever a geo-referenced raster point would fall within the footprint of the building; logical 0's are placed outside the buildings.

  Since the indoor mask is not a typical piece of information provided by a GIS vendor, its incorporation into the txRSSI database often requires custom programming. For example, an indoor mask is not directly available in Manhattan. However, as more and more GIS information becomes available, especially when the canopy data in the format of digital elevation maps and terrain elevation maps become available, the indoor mask can be purchased or inferred.

- Find Dominant Propagation Corner

  This process identifies the intersection that diffracts the majority of the incident signal. The incidence angle is calculated from the building surface orientation and the direction-of-arrival of the RF signal. The correct dominant propagation corner will provide the information of the RF signal source. The corner in the direction of the base station is assumed to be the dominant corner of the building.

- Apply Indoor Model and Calculate Indoor Signal Strength

  The processes in step 3 have prepared the dominant intersection information for each cell, which will be used to replace the base station location in our original indoor penetration model. By combining the dominant intersection information and building surface orientation information that is derived from the indoor mask, a more accurate incidence angle can be calculated and therefore better indoor penetration loss can be applied to indoor areas.

By performing the steps described above, the modified model for ultra-dense urban environment is applied to the predicted signal database.

5.7 Location Performance

The location algorithm used to compile statistics in this study is described thoroughly in [30]; it uses relative signal strength and takes the movement of the cell phone into consideration, applying a Markov model in the location probability calculation. Six neighbors' info is reported in each network measurement report (NMR). A sequence of 30 NMRs is collected, filtered, and used together to estimate the location of the handset. A serving area reduction algorithm that reduces the search area by using the serving sector's information is also used to further improve location accuracy.

The Polaris Wireless's location algorithm is used to locate the handset for three different sets of NMRs. The first two sets of NMRs are taken outdoors on two different days. The third set of NMRs is taken indoors. Location performance is reported for outdoor measurements calibrated PSD with or without indoor modeling. Location performance is reported by the percentages of calls located within error distance of 50 m, 100 m, 150 m, 300 m, and 500 m. Tables 30-32 compare the location performance of two different levels of PSDs, defined with the standard Georgia Tech conventions: Level 1 contains only outdoor calibration; Level 2 contains outdoor calibration and indoor modeling with modified octant-based penetration loss.

5.7.1 Location Performance for Pure Indoor Trace

Improvement of indoor location accuracy is the ultimate goal for indoor modeling in RSS locations. Calculating the indoor trace location performance is an informative method to verfy the effectiveness of the indoor modeling. Table 30 shows the location performance for indoor handset calls with and without indoor modeling.

Table 30: Location performance for indoor trials in Manhattan; 2,326 indoor test points in 21 buildings.

		Level 1 PSD: Outdoor Measurement Interpolation	Level 2 PSD: Level 1 Plus Indoor modeling
Error Statistics	<50m	25.3%	36.8%
	<100m	75.9%	77.0%
	<150m	92.0%	95.4%
	<300m	98.9%	100%
	<500m	100%	100%

The experiment results show that 12.5% more calls are located within 50 m error distance, and

location accuracies are improved 1.1%, 3.4%, 1.1% for 100 m, 150 m, 300 m error distance, respectively. All calls are located within 300 m from their true location. These results prove that indoor modified modeling increases the location accuracy. Therefore, the modification was successful.

5.7.2 Location Performance for Pure Outdoor Trace

Another interesting effect of applying indoor modeling is that the outdoor location performance was also improved. By applying indoor modeling, the RSS pattern at the indoor area will be different from the outdoor area and closer to the real value. Therefore, mismatching is reduced.

Table 31: Location performance for outdoor trials in Manhattan; 10,170 outdoor test points.

		Level 1 PSD: Outdoor Measurement Interpolation	Level 2 PSD: Level 1 Plus Indoor modeling
Error Statistics	<50m	63.0%	64.0%
	<100m	81.7%	83.9%
	<150m	92.5%	94.1%
	<300m	98.4%	98.4%
	<500m	98.8%	98.8%

Table 31 shows that the modified indoor modeling improves the location accuracy by 1%, 2.2%, 1.6% for 50 m, 100 m, and 150 m statistics, respectively.

5.7.3 Location Performance for Outdoor Trace with Absolute RSS Statistics Information

Because a scanner with super RF properties such as high antenna gain and lower amplifier noise is used to calibrate PSD, and NMRs are measured by a handset that does not have as good RF properties as a scanner, there exists an unknown bias between the scanner measurements and handset measurements. This is the reason that only relative RSS is used in the previous Polaris location algorithm. Polaris researchers improved the algorithm when the distribution of unknown bias was available. Table 32 shows the location performance when the unknown bias has a max-value of -25 dB, a Min-value of -1 dB, an average value of -11.61, and a standard deviation of 3.48 dB. The location performance is further improved and all calls are located within 300 m from the true location. In this enhanced algorithm case, indoor modeling also improves the location performance by 0.6%, 1.6%, 2.8%, and 0.9% for 50 m, 100 m, 150 m, 300 m error distances, respectively.

Table 32: Location performance for the second outdoor trials; 10,170 outdoor test points.

		Level 1 PSD: Outdoor Measurement Interpolation	Level 2 PSD: Level 1 Plus Indoor modeling
Error Statistics	<50m	67.4%	68.0%
	<100m	83.5%	85.1%
	<150m	92.5%	95.3%
	<300m	99.1%	100%
	<500m	100%	100%

5.8 New York Trial Conclusions and Suggestions

This trial demonstrated the effectiveness of RSS-based location performance in ultra-dense urban environments. Sixty-seven percent of the outdoor location estimates are within 50 m of the true location and 67% of the indoor location estimates are within 80 m of their their true location. Experiments also showed that the modified indoor modeling improves location accuracy in both indoor and outdoor areas.

The New York trial represents a favorable scenario for E911 position: a dense urban network with high base station density. The 100 m and 300 m cumulative location error distributions reach 85.1% and 100.0%, which surpass the requirements of E911 Phase II set forth by the FCC.

The performance of the RSS method has been compared with the assisted GPS plus cell ID solution. The results showned that the RSS method outperformed the assisted GPS plus cell ID solution in this ultra-dense urban environment.

The results suggest that a hybridization of handset-based GPS methods and the RSS signature method may prove to be the most effective solution for locating handsets across a range of environments, including rural, suburban, dense urban, and indoors. The hybrid system will combine the high performance of GPS systems in rural areas and the high performance of RSS systems in urban and indoor environments.

The modified octant penetration model produces valuable improvements for ultra-dense urban environments. But there is still additional room for improvement. The following suggestions for improvement should lead to better performance for RSS location technology:

- Collect more measurements to tune the octant model penetration parameters
- Consider other dominant propagation paths beyond the over-rooftop diffraction for outdoor

PSD prediction. And pass the dominant path information to the indoor model. This will improve the accuracy of the PSDs for both outdoor and indoor areas.

- Test indoor and outdoor user discrimination algorithms based on received signal strength aggregate (RSSA) in the commercial location engine (LE).

CHAPTER VI

CONCLUSIONS

6.1 Thesis Contributions

The RSS signature location method has shown promising results in achieving accuracy with the great advantages of legacy handset coverage and low-cost implementation, which make it an ideal solution as part of a location system for cellular networks. The work performed in this thesis focuses on analyzing, validating, and improving the performance of the RSS signature location method. Our specific contributions include

- experimental validation that the RSS signature location method is accurate enough to be used as a stand-alone location technique for achieving the FCC's E911 requirements in urban and semi-urban environments;
- an algorithm to distinguish indoor and outdoor cellular users;
- location algorithms to improve the accuracy of RSS signature methods;
- an indoor model that improves location performance for indoor areas in a dense urban environment

First, we answered the debate of whether the RSS signature method is a valid solution for radiolocation by experimental results and showed that the RSS signature method meets the FCC's mandate in general cellular networks with *average base station-to-base station separation distance* (ABBSD) of at least 500 m. The RSS signature method can locate 66.7% of the handsets within a range that is $1/8$ to $1/3$ of the ABBSD in different environments. Three field experiments in different environments were conducted to support this conclusion, which included the semi-urban environment on the Georgia Tech campus (ABBSD of 500 m), the small town environment at Greenville, SC (ABBSD of 2000 m), and the dense-urban environment at Manhattan, NY (ABBSD of 200m). All three experiments showed great improvements in location accuracy compared with that from the

cell ID solution [36], which reports the serving base station location as handset location. We also showed that the indoor performance for the RSS signature method does not degrade much when an indoor PSD is properly modeled and calibrated. The ability to locate users in indoor environments and dense urban environments makes the RSS signature method stand out from other location methods. Though our implementation of the RSS signature algorithm is not satisfactory to meet FCC's requirements in rural areas where base stations are far from each other, the RSS signature method complements the GPS solution very well in areas where multi-path and NLOS are dominant. We foresee that the next step of location technology will be a combination of GPS and RSS signature solutions.

Next, we developed an algorithm to distinguish indoor users from outdoor users as a unique feature that the RSS signature method can provide. Received signal strength aggregate was calculated and used as the decision input. This method can reach up to 92% of the correct decision rate in a consistent environment like the Georgia Tech campus, where most of the buildings are similar to each other from building material to building style. The correct decision rate drop to 76% when the environment loses its consistency, as in the Greenville campaign. The environment in Greenville is a combination of urban and rural with buildings that vary in all possible ways. Further research is needed to conquer this environment-related issue.

We improved the basic location algorithms by applying more pieces of information in the cellular system. These algorithms are described in Chapter 4. In the Greenville campaign, we faced a major difficulty of large cell size in achieving required location accuracy. Instead of just performing the same set of Georgia Tech experiments in Greenville, we further proposed and tested several location algorithms to improve location accuracy. Though the proposed algorithms cannot provide sufficient improvement to make the RSS signature method reach the FCC's mandate in all areas of Greenville, these algorithms can be used in other environments with shorter ABBSDs to provide some enhancement for RSS signature location. Besides, the location performance campaign in Greenville demonstrates that our implementation of RSS signature method is not effective in areas with large cell size. Combined with the analysis from Chapter 2, the results form Greenville campaign suggest that our implementation of RSS signature methods are good for cellular networks with ABBSD less than 1000 m in order to meet the FCC's mandate.

Finally, to improved the indoor location performance and reduce the indoor calibration workload, we proposed and tested an indoor model in the dense urban environment of Manhattan. The indoor model improved indoor location performance by being able to locate 12.5% more indoor users within 50 m from its groundtruth. The ambiguity of a PSD is reduced after applying indoor modeling and as a result, outdoor user location accuracy is also improved up to 2.8% for different statistics.

6.2 Uniqueness

This dissertation discusses a number of unique and novel research topics in radiolocation. A novel outdoor-to-indoor signal strength propagation model and its dense urban revised version are proposed and tested to improve the location accuracy for indoor environments. An algorithm to distinguish indoor users from outdoor users is proposed. A elevation-related received signal strength model is also presented. Furthermore, this research is the first academic experiment to validate the performance of RSS signature location with emphasis on locating *indoor* users.

6.3 List of publications

Our research results are published or presented on 1 journal and 3 conferences. These publications are listed below:

- Jian Zhu and Gregory D. Durgin, “Indoor/Outdoor Location of Cellular Handsets Based on Received Signal Strength”, IEE Electronics Letters, 6 January 2005
- Jian Zhu and Gregory D. Durgin, “How to Locate an Indoor Cellular User with Received Signal Strength Information”, IWCT 2005, Oulu FINLAND, 6 June 2005
- Jian Zhu and Gregory D. Durgin, “Indoor/Outdoor Location of Cellular Handsets Based on Received Signal Strength”, IEEE 2005 Spring Vehicular Technology Conference, Stockholm SWEDEN, 31 May 2005
- Jian Zhu, Steve Spain, Tarun Bhattacharya, Gregory D. Durgin, “Performance of an Indoor/Outdoor RSS Signature Cellular Handset Location Method in Manhattan ”, 2006 IEEE Int’l Symposium on Antennas and Propagation, Albuquerque NM, July 2006

6.4 Future Area of Research

The RSS signature location method is a promising solution to locate a handset in the cellular environment. It has already shown advantages over other location technologies, especially for indoor areas. There are still many challenging issues to be solved in order to locate a handset with better accuracy.

- The outdoor propagation model: The propagation model is used to generate the PSD before the driving calibration is preformed. The outdoor driving calibration is necessary to reduce prediction error in PSD. A more accurate outdoor propagation model could minimize the requirement for driving calibration. Nowadays, more GIS information is available from commercial vendors, such as digital elevation maps and digital canopy maps. This information shall be combined with outdoor propagation models to further improve outdoor modeling accuracy.

- Stationary caller behavior: When the handset user makes a call without moving around, the handset measurements have greater differences from the PSD because the head/handset distortion and small scale fading effect are not averaged out over space. This stationary caller behavior increases the difficulty of locating a handset in a cellular network. The problems needing further investigation are how to distinguish a stationary call from other moving calls and how to modify the location engine to locate a stationary call with higher accuracy.

- The combination of GPS and RSS signature solutions: The future location system will be a combination of the GPS-based solution for the area with accurate GPS signals and the RSS-based solution for the area where GPS signals cannot reach or are too degraded by the multipath propagation environment. In most conditions, both GPS and RSS signature solutions provide location estimates. The problem needing further research is how to combine these two estimates for a better overall estimate.

REFERENCES

[1] Aguirre, S., Loew, L., and Yeh, L., "Radio Propagation into Buildings at 912, 1920, and 5990 MHz Using Microcells," in *Proceedings of 3rd IEEE ICUPC*, pp. 129–134, Oct 1994.

[2] Ahonen, S. and Laitinen, H., "Database correlation method for umts location," vol. vol.4 of *57th IEEE Semiannual Vehicular Technology Conference. VTC 2003 (Cat. No.03CH37431)*, (Jeju, South Korea), p. 2696, IEEE, 2003.

[3] Aso, M., Kawabata, M., and Hattori, T., "A New Location Estimation Method Based on Maximum Likelihood Function in Cellular Systems," in *Vehicular Technology Conference 2001 Fall. IEEE VTS 54th*, vol. 1, pp. 106 – 110, 2001.

[4] Bertoni, H. L., *Radio Propagation for Modern Wireless Systems*. Prentice Hall, Inc., 2000.

[5] Bertoni, H., Honcharenko, W., Maciel, L., and Xia, H. H., "UHF Propagation Prediction for Wireless Personal Communications," *Proceedings of the IEEE*, vol. 82, pp. 1333–1359, Sep 1994.

[6] Caffery, J. J., "A New Approach to The Geometry of TOA Location," *Vehicular Technology Conference, 2000*, vol. 4, pp. 1943 – 1949, 2000.

[7] Caffery, J. J. and Stuber, G., "Subscriber Location in CDMA Cellular Networks," *IEEE Transactions on Vehicular Technology*, vol. 47, no. 2, pp. 406 – 416, 1998.

[8] Catovic, A. and Sahinoglu, Z., "The Cramer-Rao Bunds of Hbrid TOA/RSS and TDOA/RSS location estimation schemes," *IEEE Communications Letters*, vol. 8, pp. 626 – 8, Oct 2004.

[9] Chen, Y. and Kobayashi, H., "Signal Strength Based Indoor Geolocation," in *Communications, 2002. ICC 2002. IEEE International Conference on*, vol. 1, pp. 436 – 439, May 2002.

[10] Christ, R. and Lavigne, R., "Radio Frequency-based Personnel lLocation Systems," in *Security Technology, 2000. Proceedings. IEEE 34th Annual 2000 International Carnahan Conference on*, pp. 141 – 150, Oct 2000.

[11] Deng, P., Liu, L., and Fan, P., "An Enhanced Data Fusion Model for Mobile Position Estimation and Its Simulation Study," *Journal of China Institute of Communications*, vol. 24, no. 11, p. 166, 2003.

[12] Durgin, G. D., "Compendium of Polaris Wireless Inc. Technical Reports for Cellular Radiolocation," tech. rep., Georgia Institute of Technology, March 2003.

[13] Durgin, G., "Location Estimation of Wireless Terminals Using Indoor Radio Freqency Models.," *Patent filed on*, December 2003.

[14] Durgin, G., *Space-Time Wireless Channels*. Prentice Hall Inc., 2003.

[15] Durgin, G., Rappaport, T., and Xu, H., "Partition-Based Path Loss Analysis for In-Home and Residential Areas at 5.85 GHz," in *IEEE GLOBECOM 98*, (Sydney, Australia), Nov 1998.

[16] Federal Communication Commission, "Enhanced 911 - Wireless Services." Online at http://www.fcc.gov/911/enhanced/, 1999.

[17] Feng, S. and Law, C. L., "Assisted gps and its impact on navigation in intelligent transportation systems," *IEEE 5th International Conference on Intelligent Transportation Systems (Cat. No.02TH8613)*, pp. 926 – 31, 2002.

[18] Gardner, W.A. Chen, C.-K., "Signal-selective time-difference-of-arrival estimation for passive location of man-made signal sources in highly corruptive environments. i. theory and method," *IEEE Transactions on Signal Processing*, vol. 40, pp. 1168 – 1184, May 1992.

[19] Heine, G., *GSM Netwroks: Protocols, Terminology, and Implementation*. Artech House Publishers, 1999.

[20] Hero, A. I., Fessler, J., and Usman, M., "Exploring estimator bias-variance tradeoffs using the uniform cr bound," *IEEE Transactions on Signal Processing*, vol. 44, pp. 2026 – 41, Aug 1996.

[21] Kelly, I. Y., Hai, D., and Hao, L., "On the Feasibility of the Multipath Fingerprint Method for Location Finding in Urban Environments," *Applied Computational Electromagnetics Society Journal*, vol. 15, no. 3, p. 232, 2000.

[22] Klukas, R. and Fattouche, M., "Line-of-sight Angle of Arrival Estimation in The Outdoor Multipath Environment," *Vehicular Technology, IEEE Transactions on*, vol. 47, pp. 342 – 351, Feb 1998.

[23] Koorapaty, H., Grubeck, H., and Cedervall, M., "Effect of Biased Measurement Errors on Accuracy of Position Location Methods," *Conference Record / IEEE Global Telecommunications Conference*, vol. 3, p. 1497, 1998.

[24] Koshima, H. and Hoshen, J., "Personal Locator Services Emerge," *Spectrum, IEEE*, vol. 37, pp. 41 – 48, Feb 2000.

[25] Liu, S., Wan, Q., and Peng, Y., "A Non-line-of-sight High-resolution Location Algorithm Based on TDD for Mobile Station," *Acta Electronica Sinica*, vol. 30, no. 9, p. 1288, 2002.

[26] Mehrotra, A., *GSM System Engineering*. Artech House Publishers, 1997.

[27] Nerguizian, C., Despins, C., and Affes, S., "Indoor Geolocation with Received Signal Strength Fingerprinting Technique and Neural Networks," in *""*, Telecommunications and Networking - ICT 2004. 11th International Conference on Telecommunications. Proceedings (Lecture Notes in Comput. Sci. Vol.3124), (Fortaleza, Brazil), p. 866, Springer-Verlag, 2004.

[28] Pahlavan, K. and X. Li, J. M., "Indoor Geolocation Science and Technology," *IEEE Communications Magazine*, vol. 40, pp. 112–118, Feb 2002.

[29] Patwari, N., Hero, A.O., I., Perkins, M., Correal, N., and O'Dea, R., "Relative location estimation in wireless sensor networks," *IEEE Transactions on Signal Processing*, vol. 51, pp. 2137 – 48, Aug 2003.

[30] Perez-Breva, L., Chong, C.-Y., Dressler, R. M., Rao, P. R., Siccardo, P., and Spain, D. S., "Location and Determination Using RF Fingerprinting," *U.S. Patent No. 6,393,294, 22 Issued to Polaris Wireless Inc.*, March 2000.

[31] Raja, K., Buchanan, W. J., and Munoz, J., "We know where you are [cellular location tracking]," *Communications Engineer*, vol. 2, no. 3, p. 34, 2004.

[32] Rao, P. R., "Multiple Location Estimates in a Cellular Communication System," *U.S.Patent No. 6,449,486 Issued to Polaris Wireless Inc.*, May 1999.

[33] Rappaport, T., *Wireless Communications: Principles and Practice*. New Jersey: Prentice-Hall Inc., 2nd ed., 2002.

[34] Redl, S. M., Weber, M. K., and Oliphant, M. W., *GSM and Personal Communications Handbook*. Artech House Publishers, 1998.

[35] Sakagami, S., Aoyama, S., Kuboi, K., Shirota, S., and Akeyama, A., "Vehicle Position Estimates by Multibeam Antennas in Multipath Environments," *IEEE Transactions on Vehicular Technology*, vol. 41, pp. 63 – 68, Feb 1992.

[36] Trevisani, E. and Vitaletti, A., "Cell-id location technique, limits and benefits: an experimental study," *Proceedings. Sixth IEEE Workshop on Mobile Computing Systems and Applications*, pp. 51 – 60, 2004.

[37] Valenzuela, R., Landron, O., and Jacobs, D., "Estimating local mean signal strength of indoor multipath propagation," *IEEE Transactions on Vehicular Technology*, vol. 46, pp. 203 – 12, Feb 1997.

[38] Warrior, J., McHenry, E., and McGee, K., "They Know Where You Are [location detection]," *IEEE Spectrum*, vol. 40, no. 7, p. 20, 2003.

[39] Weiss, A., "On The Accuracy of A Cellular Location System Based on RSS Measurements," *IEEE Transactions on Vehicular Technology*, vol. 52, pp. 1508 – 1518, Nov 2003.

[40] Whalen, A. D., *Detection of Signals in Noise*. Academic Press, INC., 1971.

[41] Yamamoto, R., Matsutani, H., Matsuki, H., Oono, T., and Ohtsuka, H., "Position location technologies using signal strength in cellular systems," *IEEE VTS 53rd Vehicular Technology Conference, Spring 2001. Proceedings (Cat. No.01CH37202)*, vol. vol.4, pp. 2570 – 4, 2001.

[42] Zhao, Y., "Standardization of Mobile Phone Positioning for 3G Systems," *IEEE Communications Magazine*, vol. 40, pp. 108–116, July 2002.

[43] Zhu, J. J. and Durgin, G. D., "Indoor/Outdoor Location of Cellular Handsets Based on Received Signal Strength," Tech. Rep. PG-TR–JZ040618, Georgia Institute of Technology, http://www.propagation.gatech.edu, June 2004.

VITA

Jian Zhu was born in Beijing, P.R. China. He received the B.S.E.E. degree from Beijing University of Technology, Beijing, China in 2000 and the M.S. degree from Georgia Tech in 2003. He has currently working toward the Ph.D. degree at the Propagation Group at Georgia Institute of Technology.

From August 2001 to December 2003, He was with Information Transmission and Processing Laboratory at the Georgia Institute of Technology as Graduate Research Assistant. Since 2003, he has been a Graduate Research Assistant in the propagation Group at the Georgia Institute of Technology. His research focuses on radiolocation, radio wave propagation, and channel modeling.